SAND2007-4202P

Overview of Diagnostics on Z

Mini-Course on Diagnostics for High Energy Density Plasmas and Pulsed Power Systems

2007 IEEE Int'l Conference on Plasma Science

Albuquerque, New Mexico

June 23, 2007

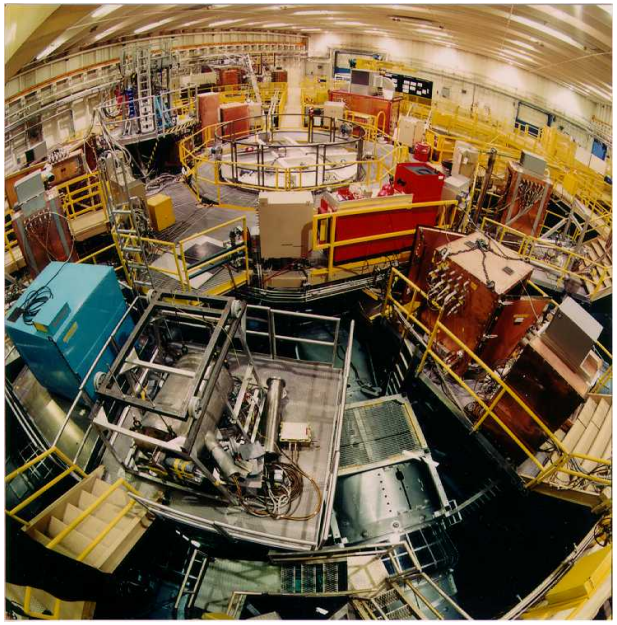

Ramon J. Leeper, 505-845-7185, rjleepe@sandia.gov

Sandia is a multiprogram laboratory operated by Sandia Corporation, a Lockheed Martin Company, for the United States Department of Energy under contract DE-AC04-94AL85000.

Sandia National Laboratories

Outline of presentation

- Introduction to High Energy Density Physics Research
- X-ray fluence and flux diagnostics
- X-ray imaging diagnostics
- Z-Beamlet laser and backlighter diagnostic systems
- Time-integrated and time resolved spectroscopy diagnostics
- Shock physics based diagnostics
- Neutron diagnostic systems
- Summary

Pulsed-power accelerators with a variety of loads provide efficient time compression and power amplification

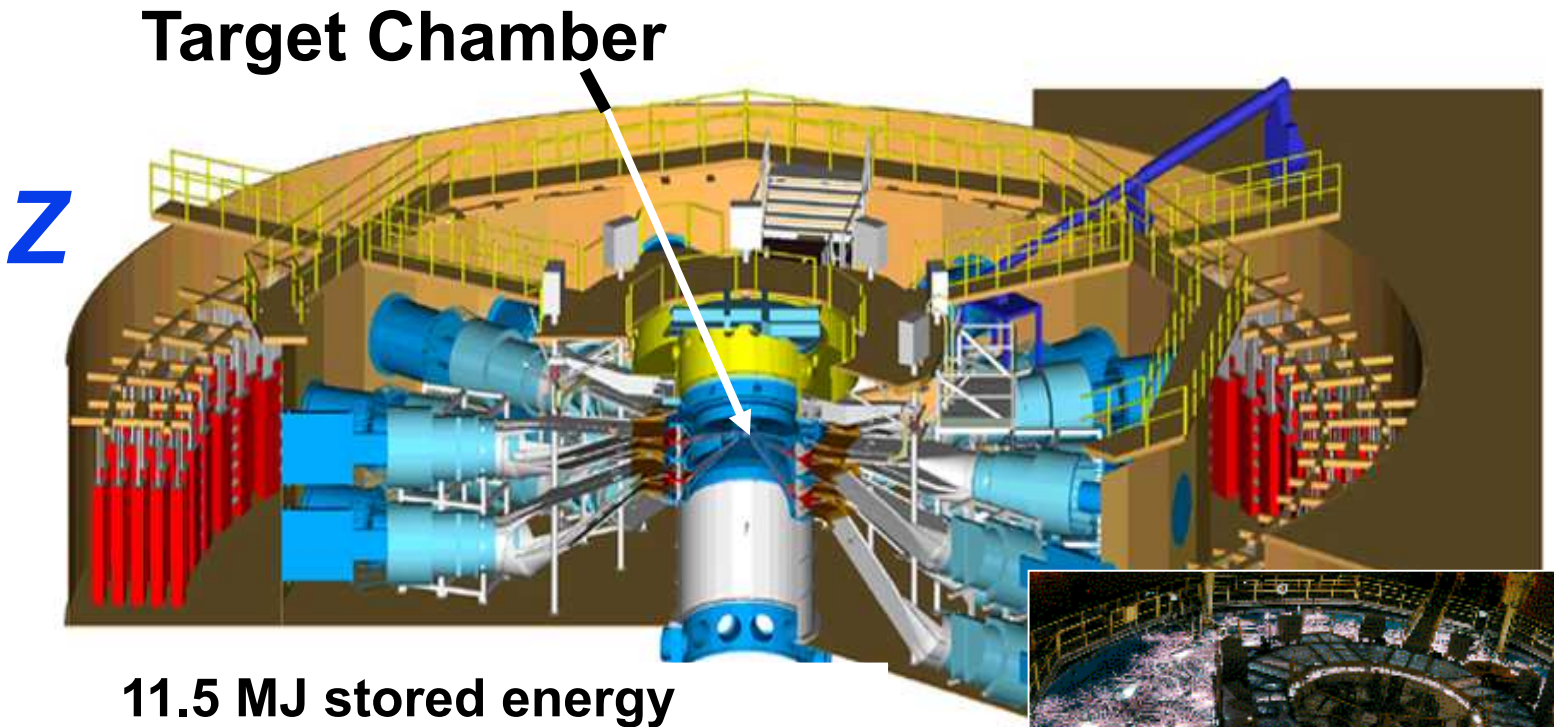

- 11.5 MJ stored energy
- 19-20 MA peak load current
- 40 TW electrical power to load
- 100-250 TW x-ray power
- 1-1.8 MJ x-ray energy

Two complementary approaches to Z-pinch-driven fusion are being studied at Sandia

Double-ended hohlraum

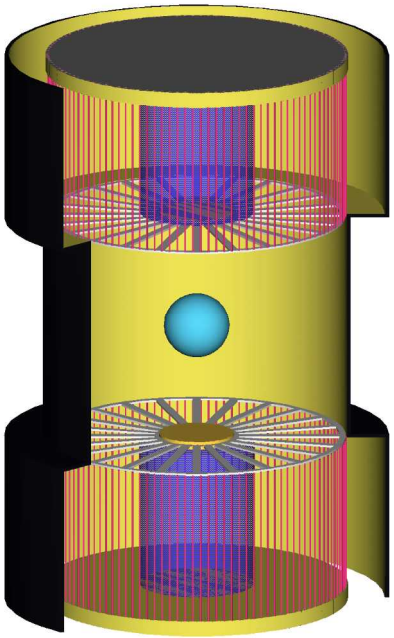

- Two 60 MA pinches
- 380 MJ yield

Key issues

- hohlraum energetics
- radiation symmetry
- pulseshaping
- preheat
- capsule implosions

Dynamic hohlraum

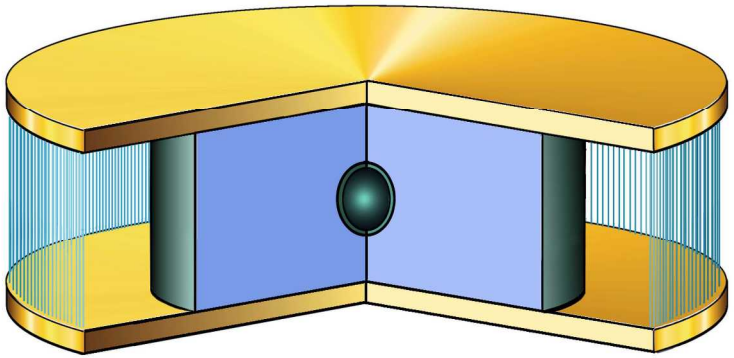

- 54 MA pinch
- 530 MJ yield

The Z facility is a challenging environment for developing and fielding x-ray, γ-ray, and nuclear diagnostics

Debris field	Large amounts of debris of various sizes requires extensive baffle arrangements and fast closure valves
EMP background	Electric fields of ~ 1 MV/m
X-rays: 100 eV to 3 keV	1.6 MJ and 200 TW
X-rays: 1 keV to 10 keV	50-150 kJ and 10-30 TW
γ-rays: 30 keV to ~ 5 MeV	75 rads at 1 m in 5 ns pulse yielding 1.5×10^{10} rads/s
Neutrons: ~ 2.45 MeV	2.6×10^{11} neutrons/4π produced in dynamic hohlraum capsule experiments
Neutrons: ~ 2.45 MeV	3.7×10^{13} neutrons/4π for D_2 gas puff z-pinch on Z at 18 MA

High energy density physics measurements require extensive diagnostic suites

- X-ray fluence and flux diagnostics
- X-ray imaging diagnostics
- X-ray backlighting diagnostics
- Time-integrated and time resolved spectroscopy diagnostics
- Shock physics based diagnostics
- Neutron detector systems

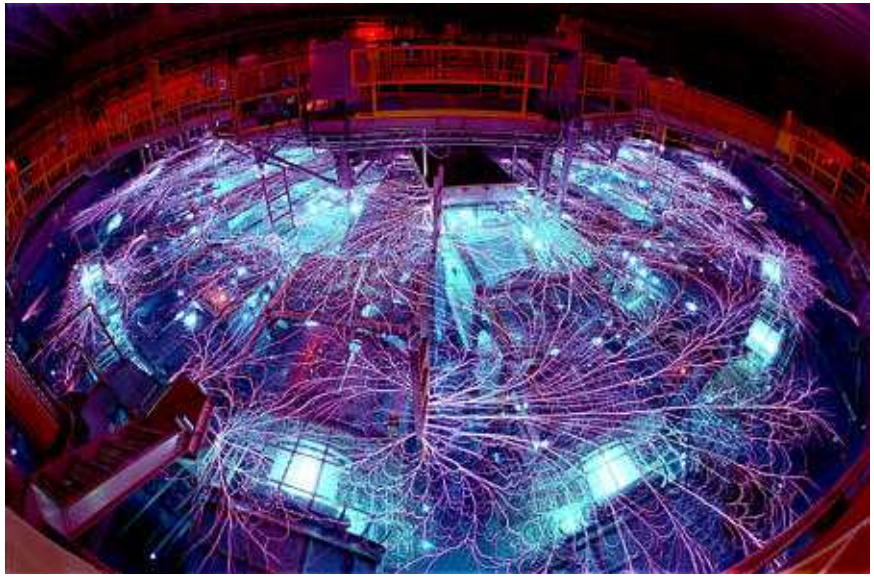

The arrangement of diagnostics on Z take advantage of the available solid angle

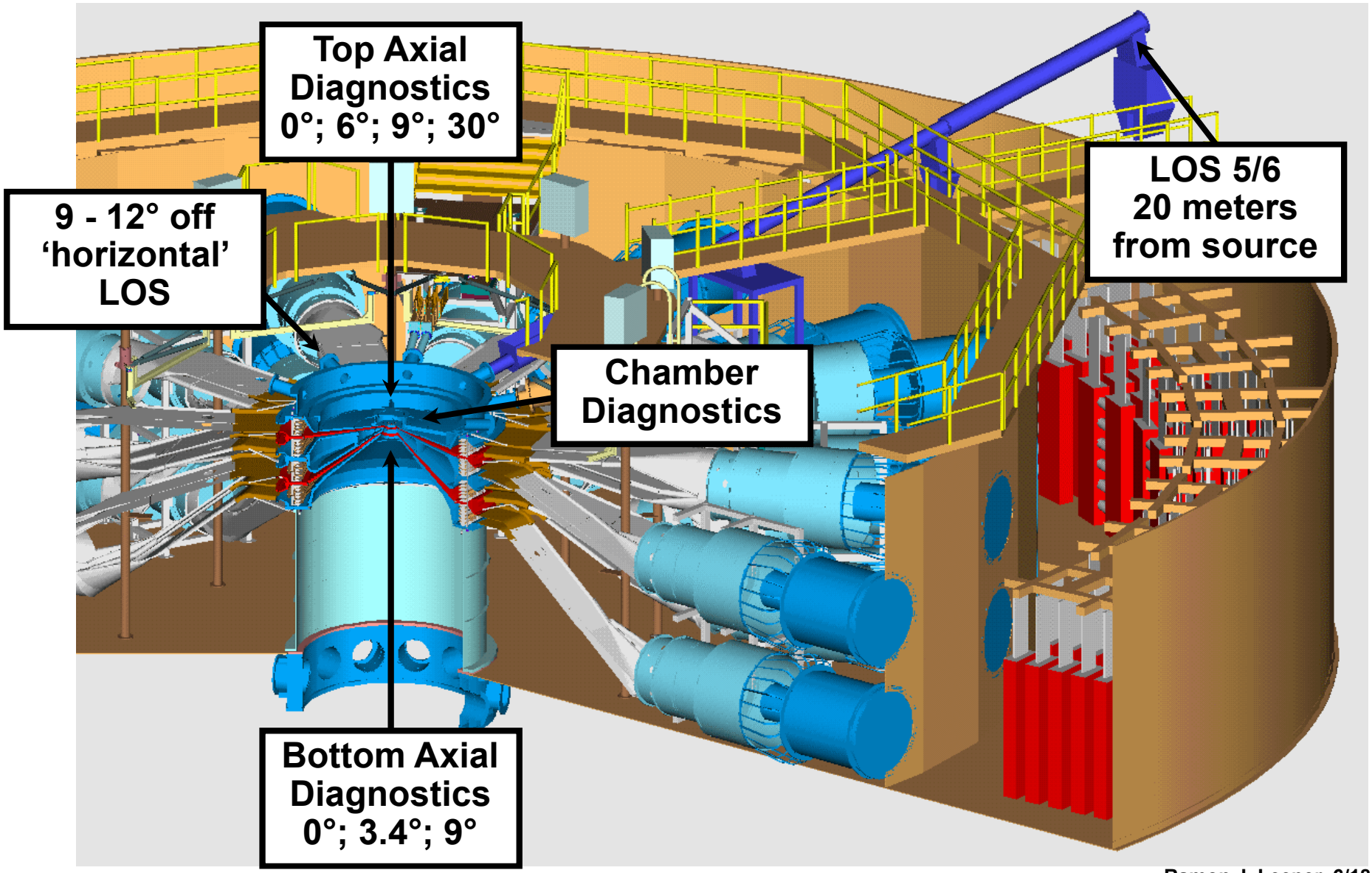

Axial measurements on Z make use of the the Z axial diagnostic package

Coaxial cable runs on Z are located in a high EMP environment

- Digitizers are located in screen boxes arranged azimuthally around Z's central vacuum chamber
- The cables used are typically 6.7 m of Andrew LDF4-50A 1.3 cm Heliax cables using "N" Type connectors
- Inside the screen box is a 2.4 m run of RG9914
- Special care is taken to minimize noise on the cable runs by installing an outer steel braid to the Heliax cable runs and securing one end to the "N" connector at the diagnostic and attaching the opposite end to the screen box feedthrough
- The connector at the screen box feedthrough is isolated electrically by wraps of electrical tape
- The braid is then mechanically attached to the feedthrough housing and thus creates a triaxial cable run
- The combination of Heliax and RG9914 cables creates a cable run to allow signals recording in excess of 4 GHz, which exceeds the digitizer recording capability
- Fast signals are primarily recorded using the TDS684 and TVS645 with a sample rate of 200 ps/sample

Noise on Z cable runs is minimized by installing an outer steel braid on Heliax cables and securing one end to the "N" connector at the diagnostic and the other end to the screen box feedthrough

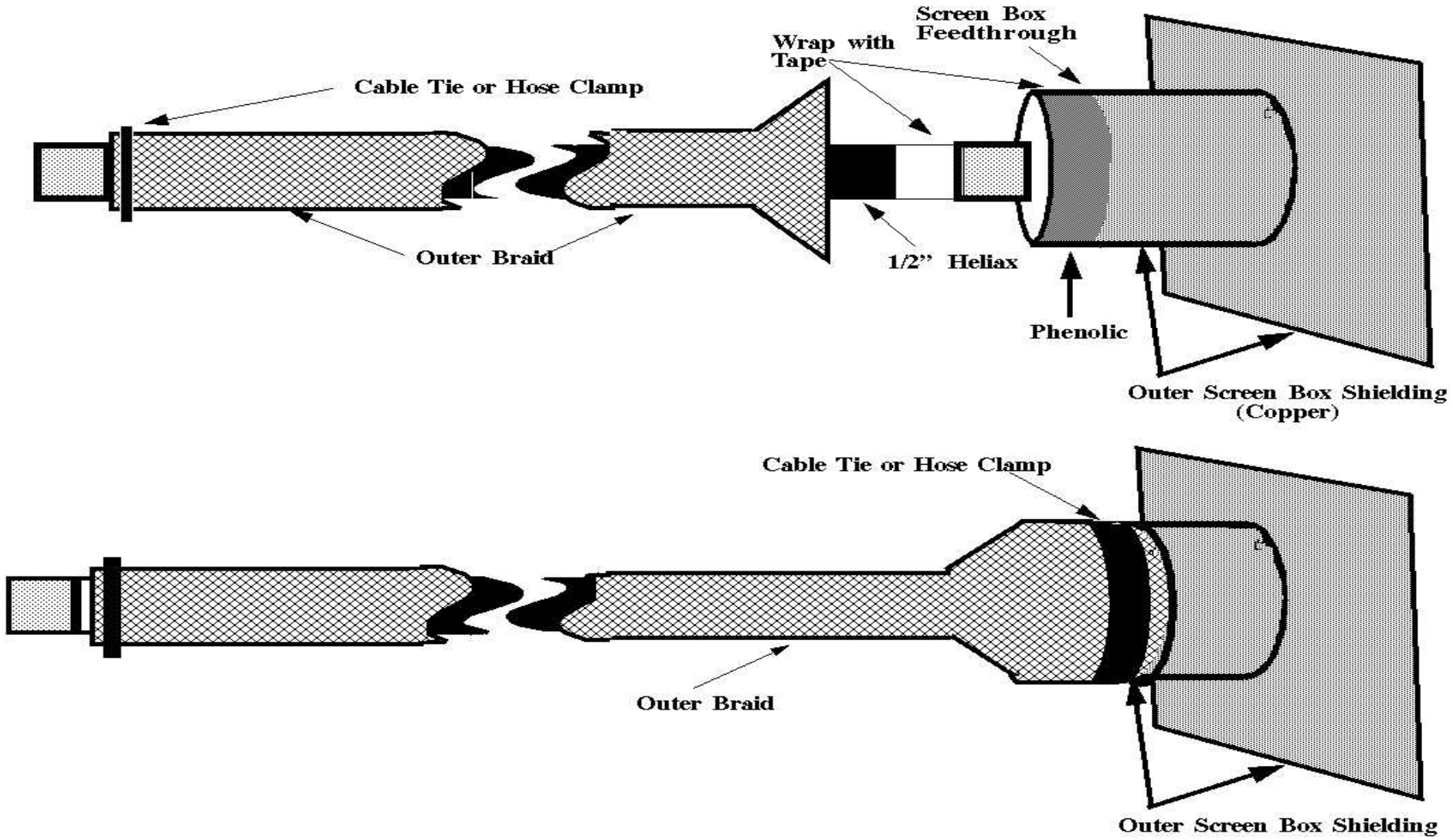

X-ray fluence and flux diagnostics are used to characterize the z-pinch source and hohlraum temperature

DIAGNOSTIC	QUANTITY OBSERVED	USED TO OBTAIN
XRD Array	145 eV To 2.5 keV X-rays	Source Temperature
Bolometer	Few eV To 2 keV X-rays	Total X-ray Yield
Soft X-ray Calorimeter	Few eV To 2 keV X-rays	Total X-ray Yield
Transmission Grating Spectrograph (Time-Resolved)	50 eV To 2 keV X-rays	Continuum Measurement of Source Temperature

Filtered x-ray diodes (XRDs) are used to primarily measure the soft x-ray flux from the source

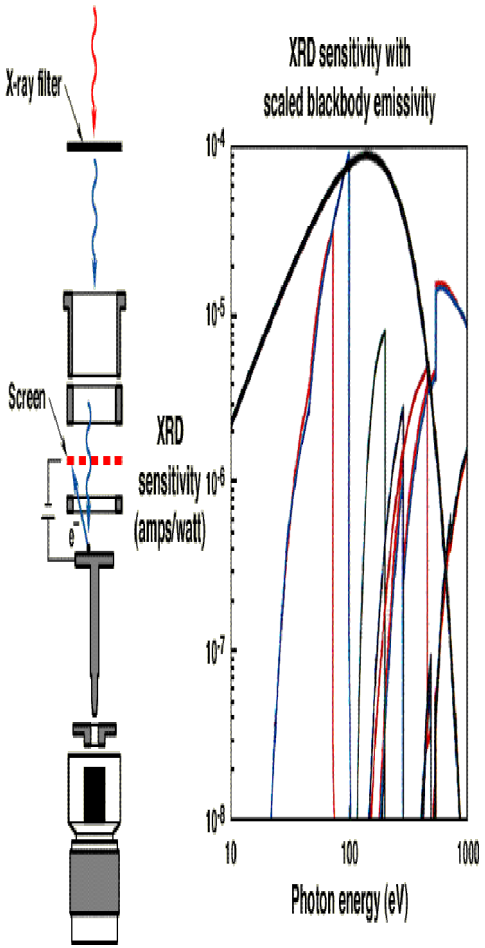

- XRD Photocathodes: Vitreous carbon
- Time resolution: ~ 500 ps fwhm
- Bias voltage: -1000 volts
- Spectral coverage: 140 eV - 2.5 keV

Predicted XRD Responses with carbon photocathodes

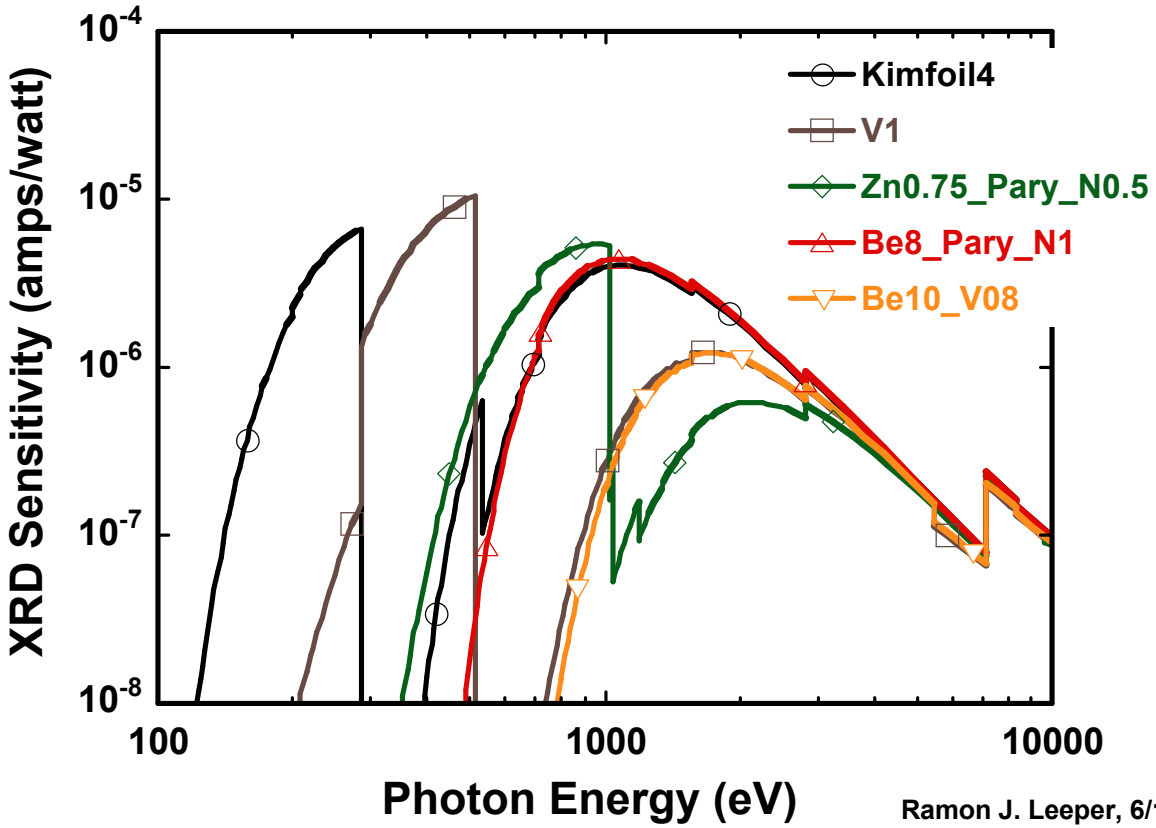

Ramon J. Leeper, 6/18/07

Fast closure valves are used to protect diagnostics from target debris on Z

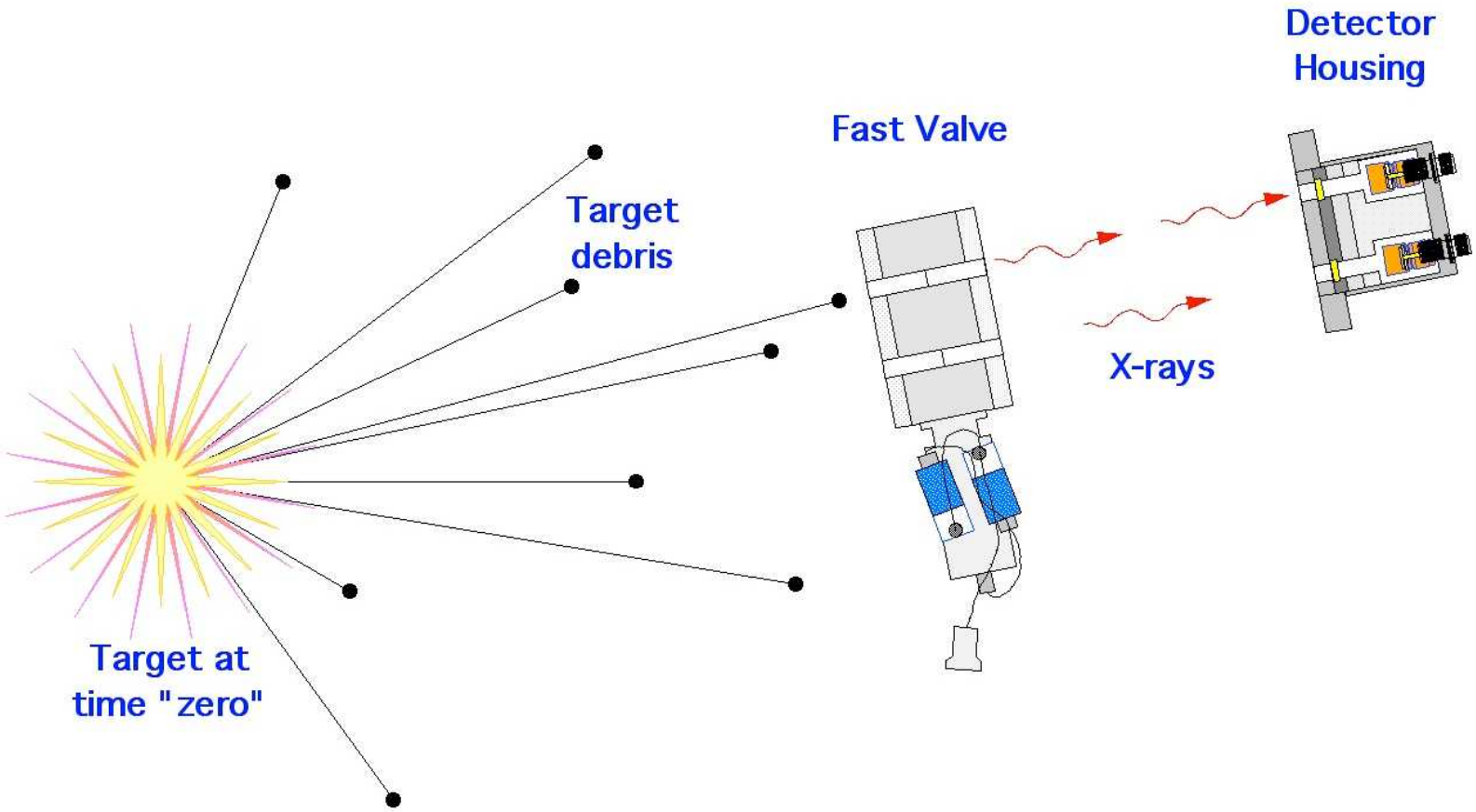

An eleven-port Z fast valve is shown in this photograph

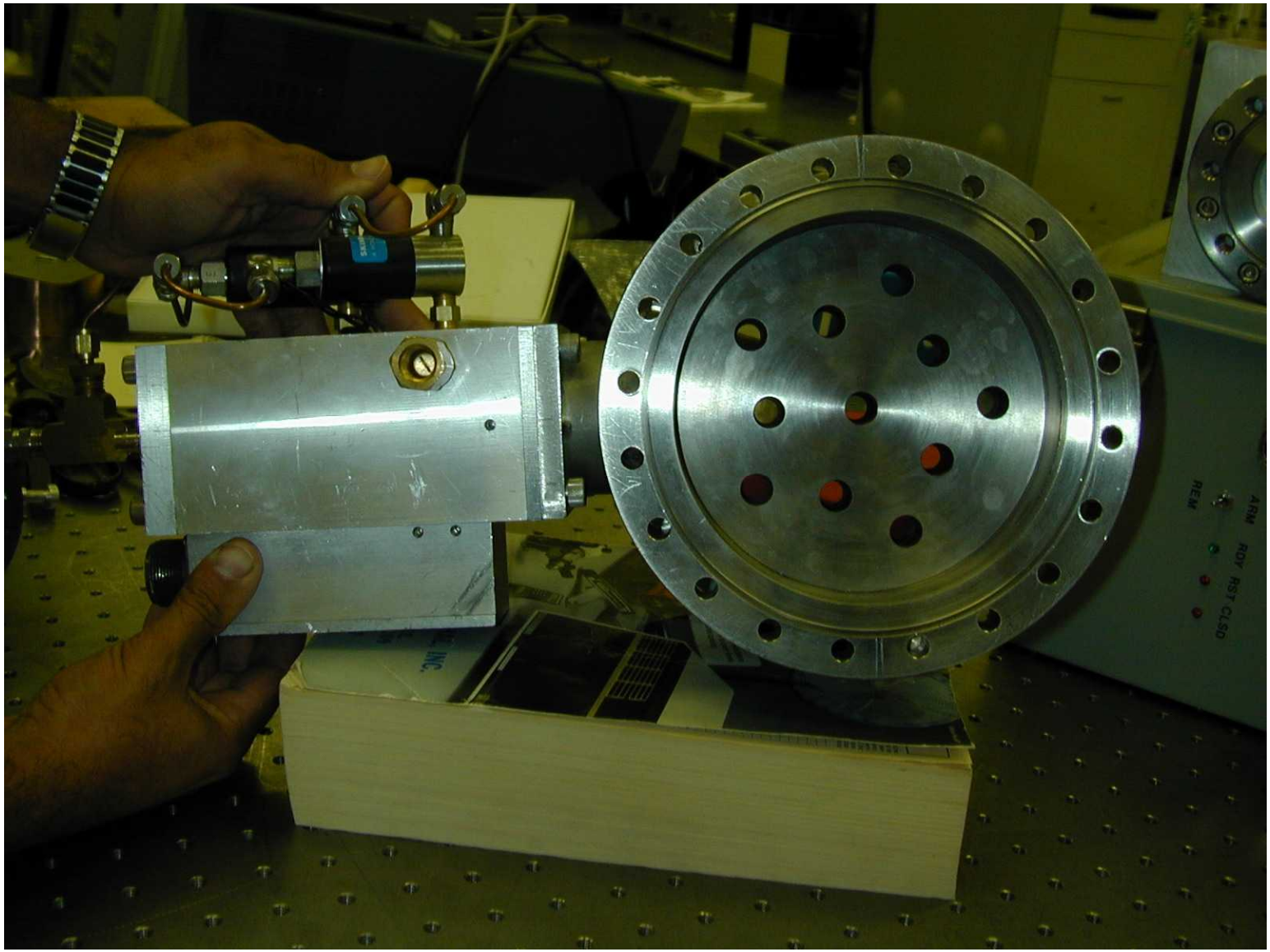

Ramon J. Leeper, 6/18/07

A five-port Z fast closure valve is shown in this photograph

Ramon J. Leeper, 6/18/07

Schematic of eleven port fast valve showing open and closed positions

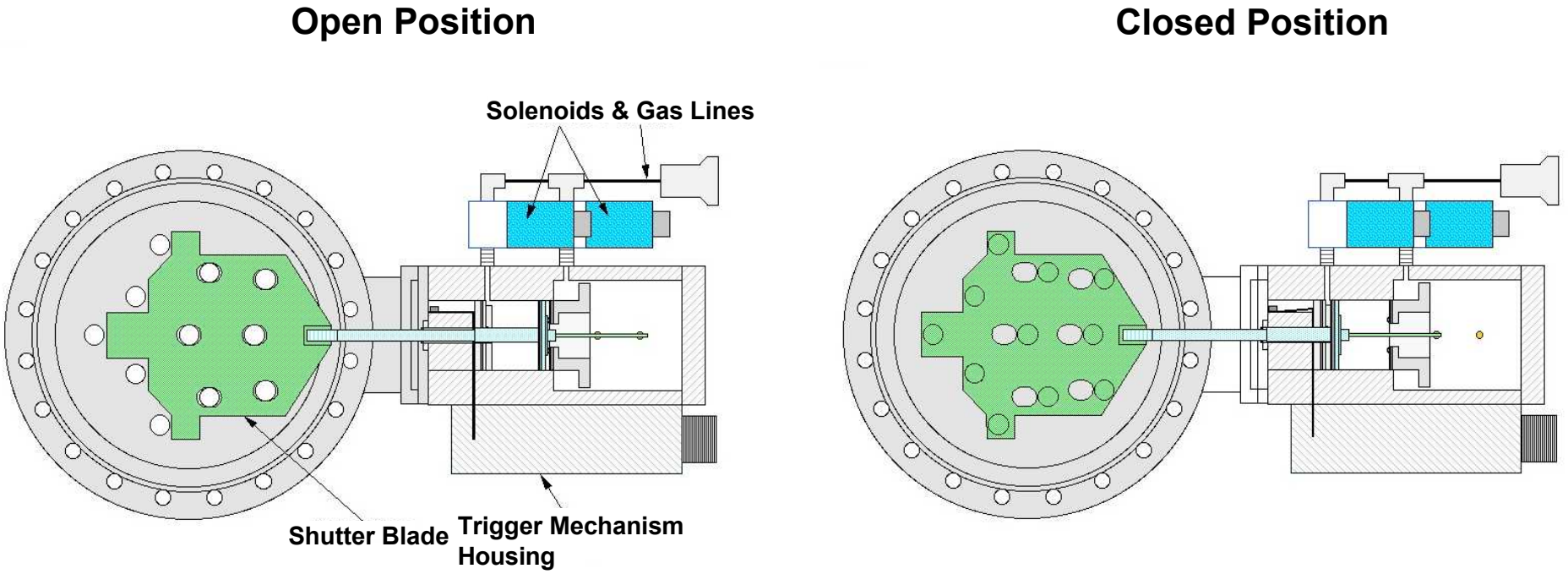

- The Z fast valves operate at typical nitrogen pressures of 160 psi
- The valves can be operated in Close-Open-Close (C-O-C) and Open-Close Modes (O-C)
- In the C-O-C mode, the time to close a 3 mm x 28.2 mm slit is ~ 0.10 ms and a 11-port set 12.7 mm diameter apertures in ~0.2 ms
- In the O-C mode, the time to close a 11-port set of 12.7 mm diameter apertures is ~ 0.8 ms

Ramon J. Leeper, 6/18/07

Filtered-XRD array for x-ray power

- Typical set of response functions $R_k(E)$ for the 5-channel, filtered-XRD diagnostic:

  - Spectral Cuts determined by x-ray absorption coefficients

  - R_{4A} and R_{5A} approximate the high energy tails of R_{1A} and R_{2A}.

- The flux estimate F_{unfold} is obtained from

$$F_{unfold} \equiv \sum_{j=1}^{N} S_j \Delta E_j$$

where the bin-widths ΔE_j largely coincide with the spectral cuts and the coefficients S_j represent a histogram solution to the Fredholm equation:

$$D_i = \int R_i(E) S(E) dE \equiv \sum_{j=1}^{N=5} R_{ij} S_j$$

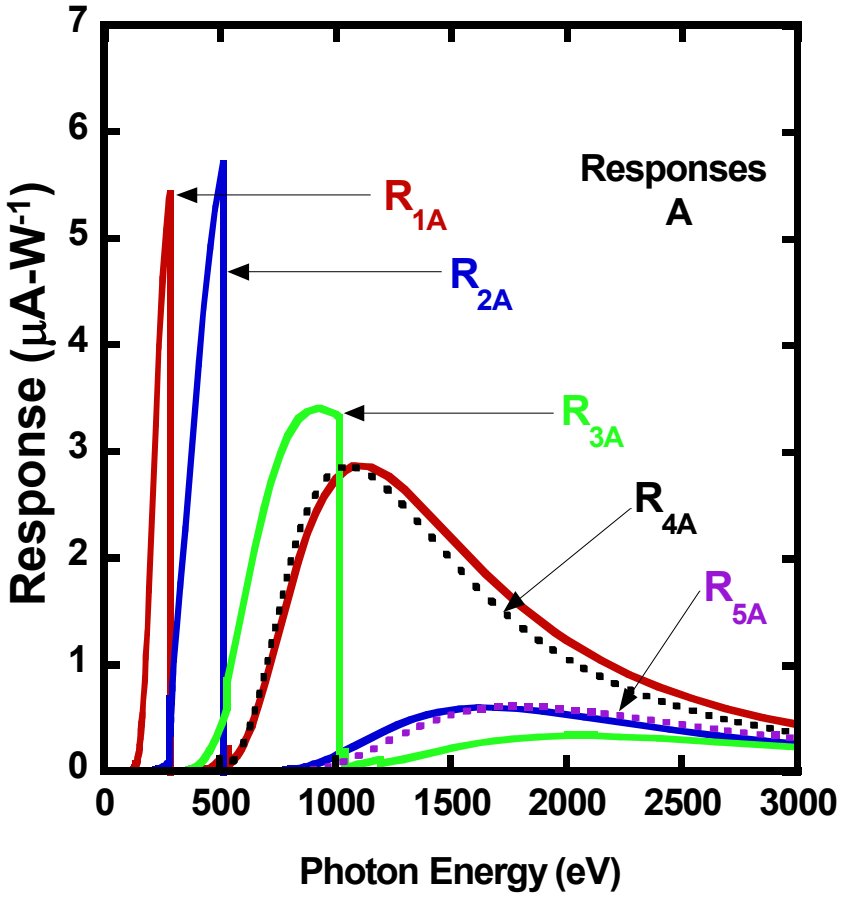

Unfold approximation for data simulated from a 250 eV Planckian spectrum

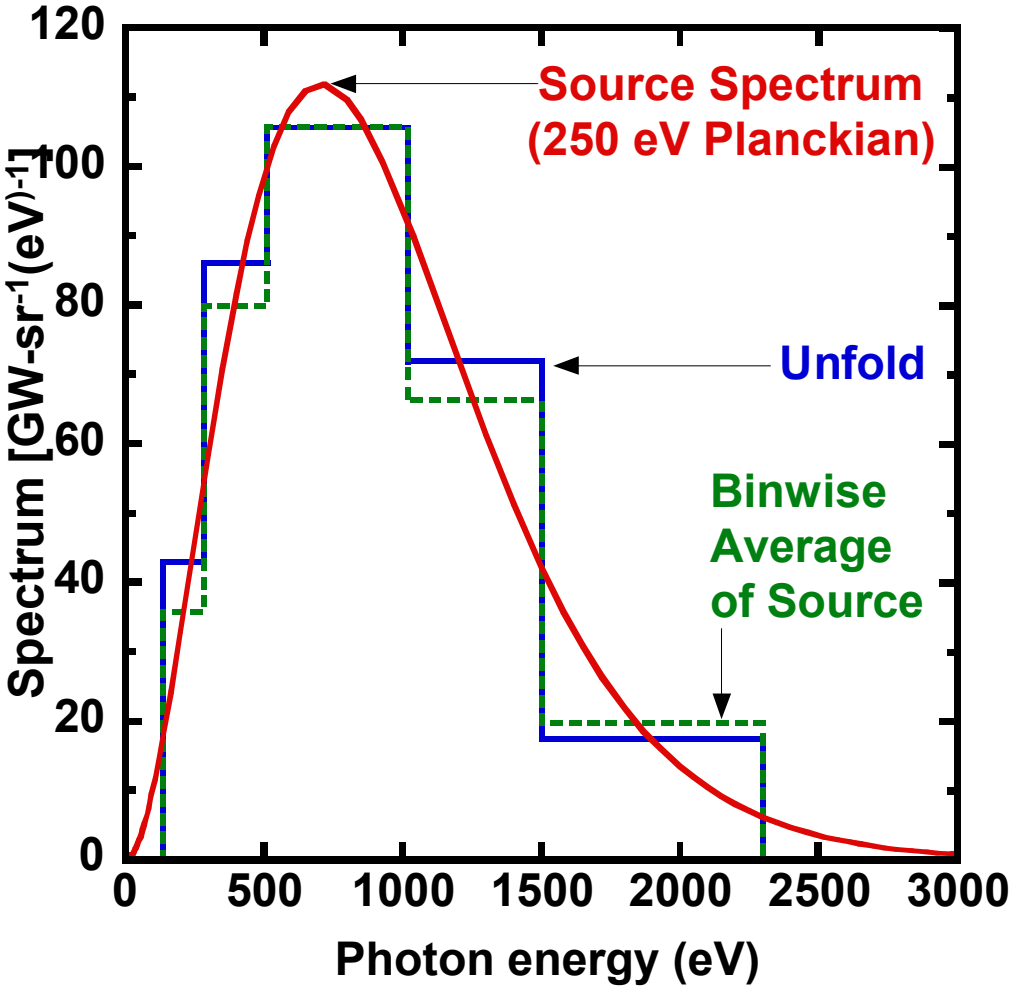

Comparison of a 250-eV black-body spectrum (1-cm^2 source area) with

(1) a 5-bin *unfold* (137eV—2300 eV);

(2) the source average in the unfold bins.

No normalizations are used in this comparison.

Time history of source radiation temperature can be measured by a transmission grating spectrograph

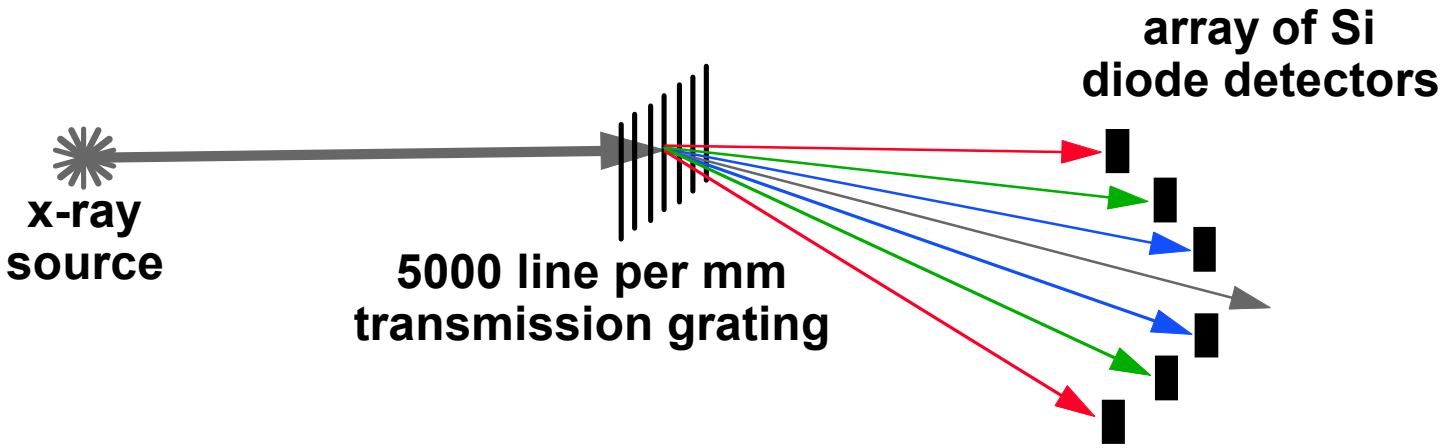

L. E. Ruggles, M. E. Cuneo, J. L. Porter, D. F. Wenger, and W. W. Simpson, Rev. Sci. Instrum. 72, 1218 (2001)

Spectra obtained with the transmission grating spectrograph are in good agreement with XRD measurements

x-ray spectrum at time of peak emission

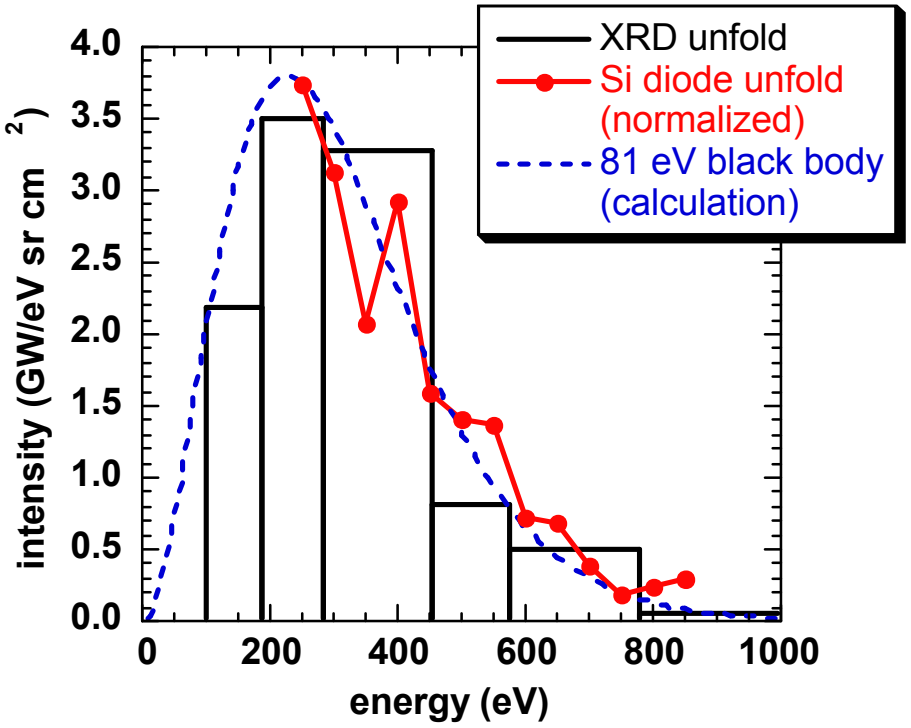

time history of radiation temperature

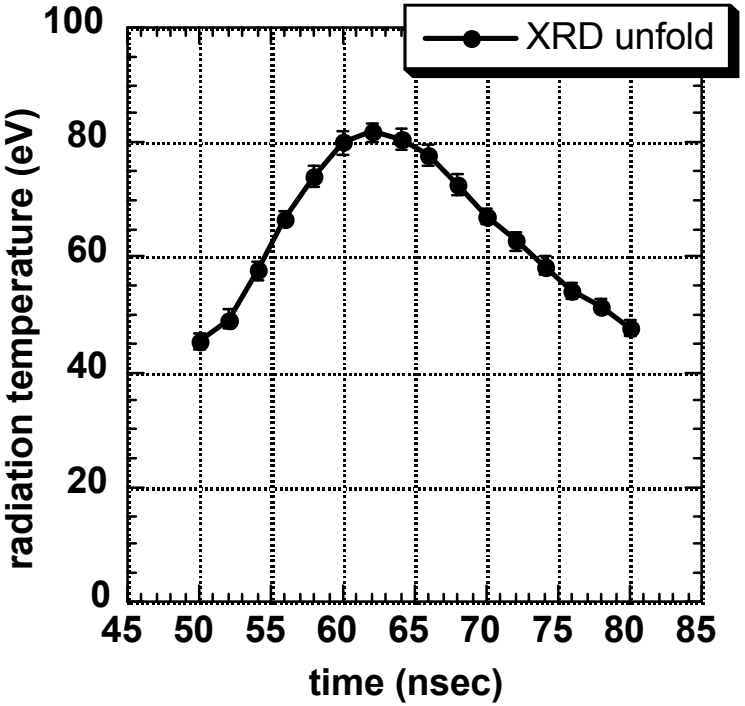

Ramon J. Leeper, 5/2/00

Bolometer diagnostic measures total x-ray fluence

- Bolometer elements:
  - 1 μm Nickel - Total x-ray yields < 2 keV
  - 1 μm Gold - x-ray yields 1 - 10 keV
- Time resolution ~ 2 ns
- Sensitivity w/40 amps drive current (V/mJ/cm^2): Ni: ~0.2 and Au: ~0.07

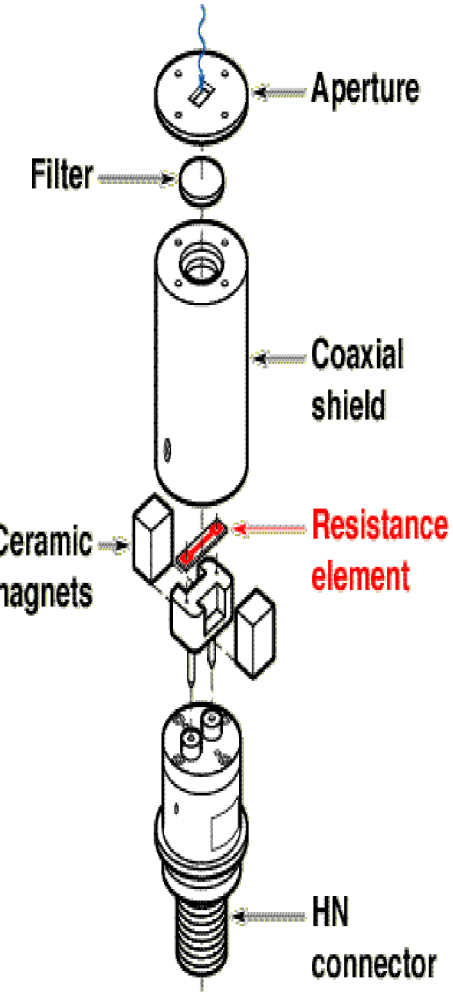

- Primarly sensitive < 1 keV
- Bolometer element 1μ Ni
- Time resolution is a few ns

Bolometer relative response vs photon energy

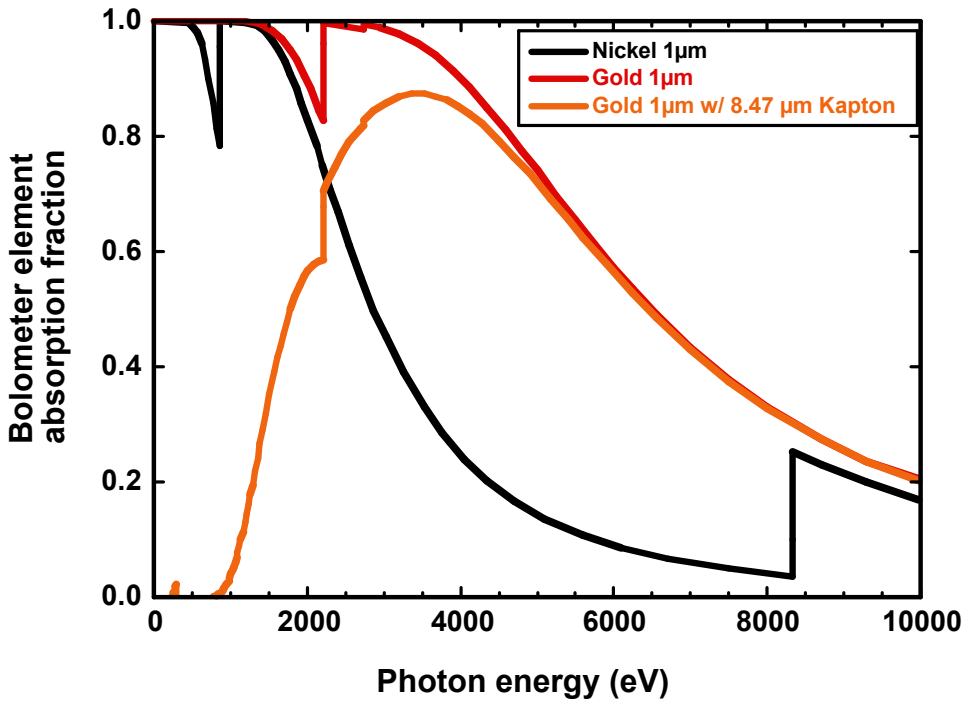

The soft x-ray calorimeter enables absolute fluence measurements to be made

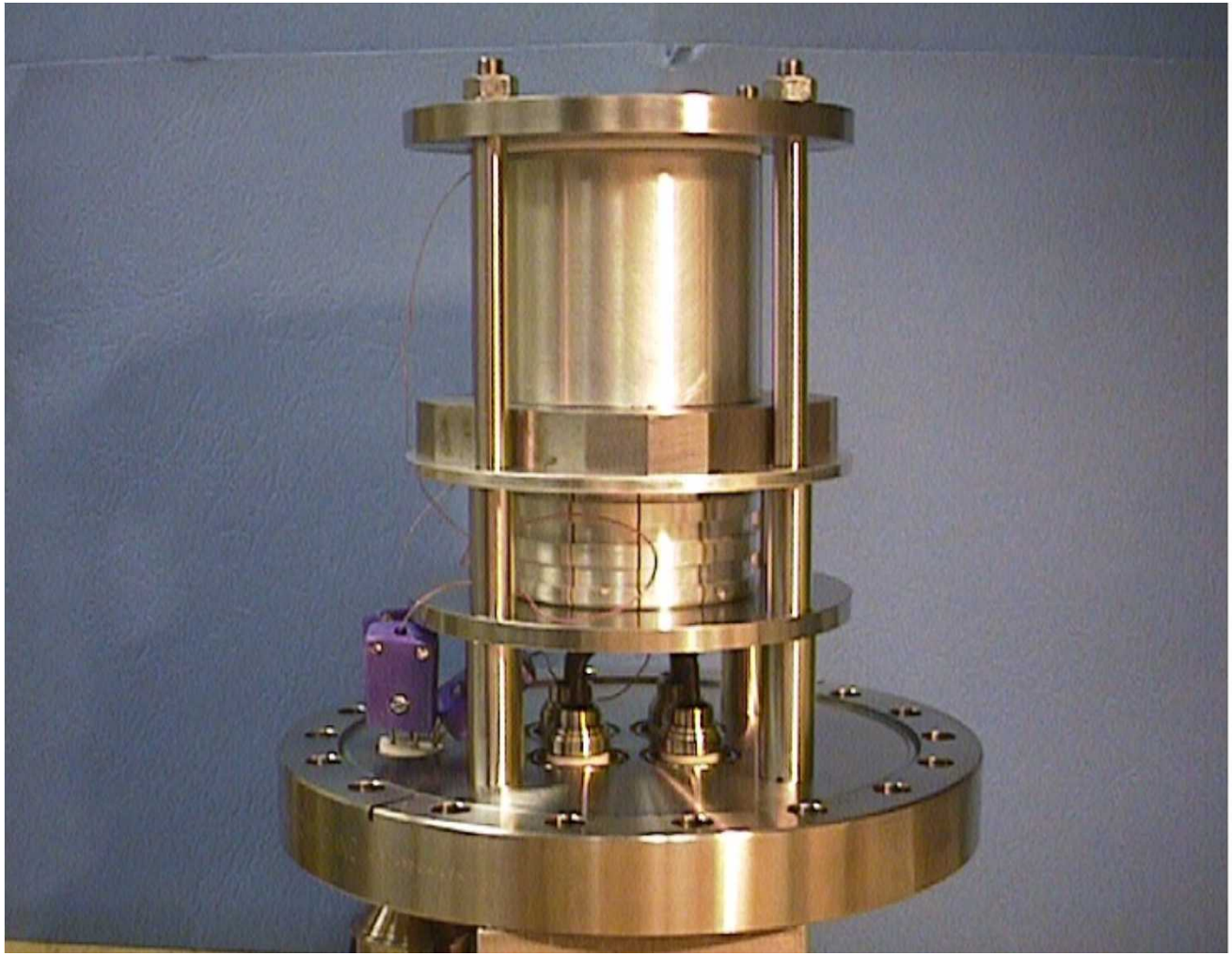

D. L. Fehl, D. J. Muron, R. J. Leeper, G. A. Chandler, C. Deeney, W. A. Stygar, and R. B. Spielman, Rev. Sci. Instrum. 70, 270 (1999).

The diamond photoconducting detectors (PCD's) typically measure x-ray flux from 1 - 10 keV

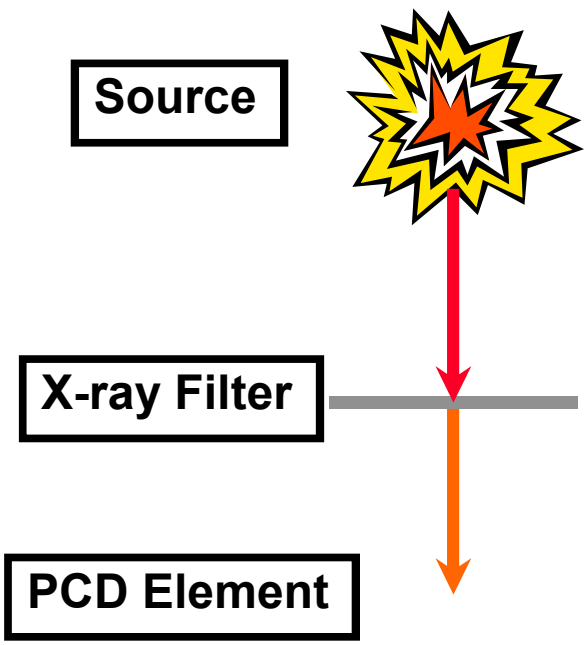

- Diamond PCD sizes (mm):
  - 1W x (1 or 3)L x 0.5T
- Time resolution: ~ 100 ps fwhm
- Sensitivity @ 100 volt bias (A / W): ~4×10^{-4}

Relative Response for 0.5 mm Thick Diamond PCDs with the specified filters

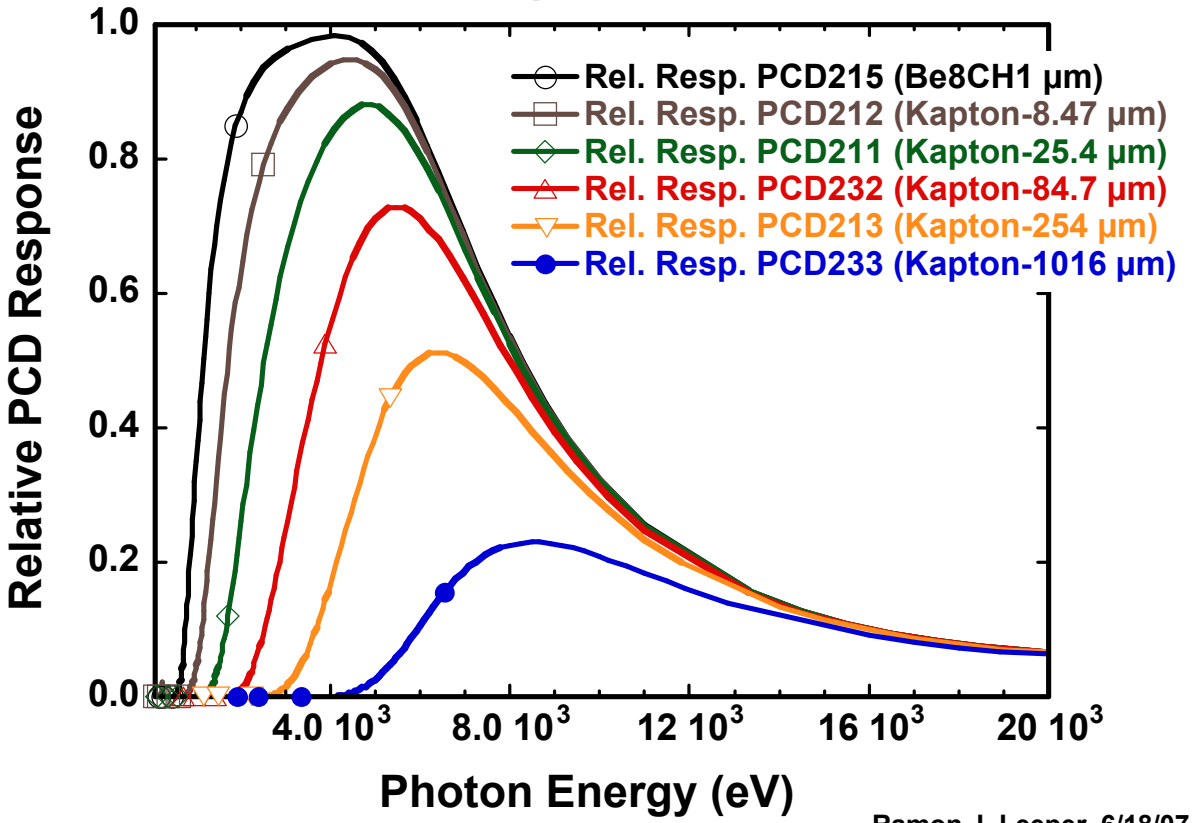

QuickTime™ and
Photo - JPEG decompr
'e needed to see this pi

Ramon J. Leeper, 6/18/07

Imaging diagnostic techniques are core to quality measurements in high energy density physics

DIAGNOSTIC	QUANTITY OBSERVED	USED TO OBTAIN
X-ray Pinhole Camera (Time-Integrated)	30 eV To 10 keV X-rays	Source Image
X-ray Pinhole Camera (Time-Resolved)	30 eV To 10 keV X-rays	Source Image
Streaked Fiber Arrays (Time-Resolved)	100 eV To 3 keV X-rays	1-D Filtered Source Image
Z/Beamlet Laser Backlighter	1.865 keV To 10 keV X-rays	Absorption Image

The fundamental concept of pinhole imaging is shown here

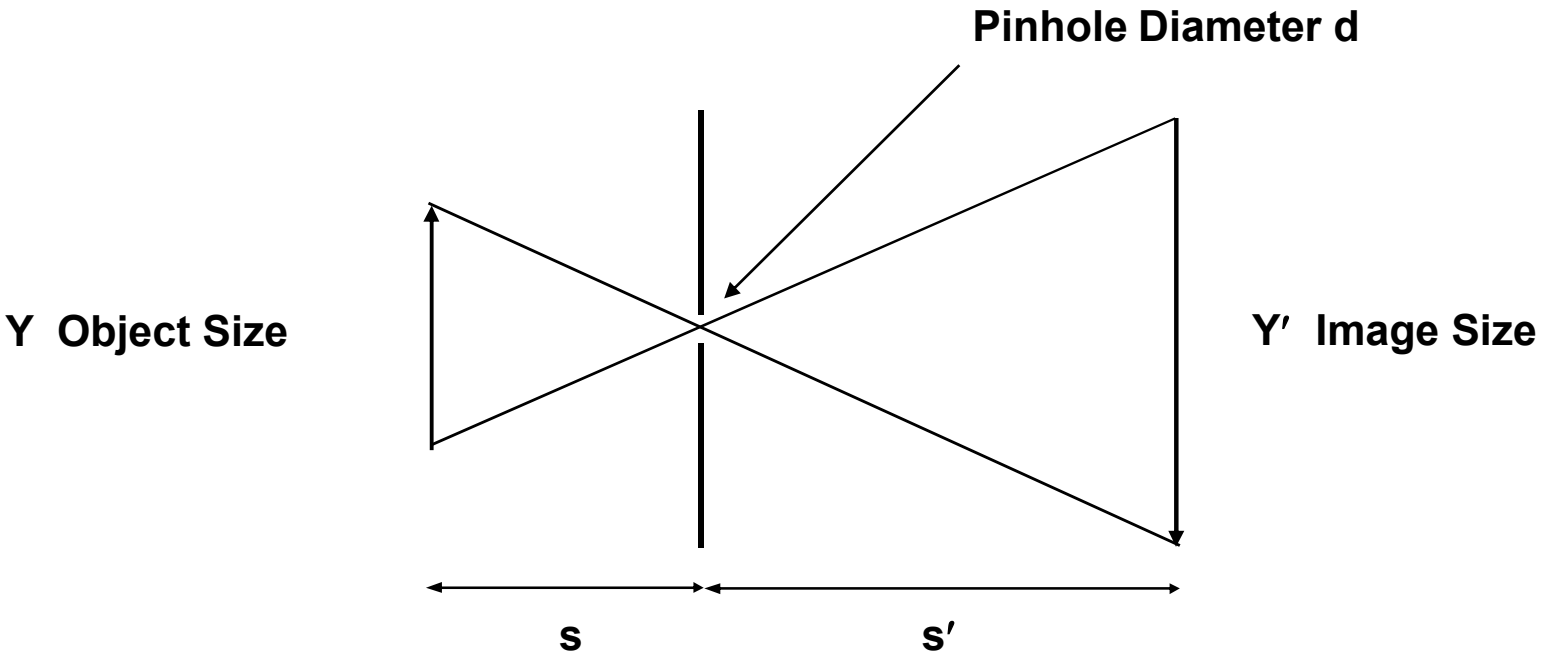

$$\text{Magnification} = M = \frac{s'}{s} = \frac{y'}{y}$$

$$\text{Resolution} = R = d\left(\frac{s+s'}{s'}\right) = d\left(1+\frac{1}{M}\right)$$

$$\text{Image Fluence} = F = \frac{Nd^2}{4\pi s^2 (y')^2} = \frac{Nd^2}{4\pi s^2 y^2 M^2}$$

Ramon J. Leeper, 6/18/07

Time-resolved x-ray pinhole camera (TRXPHC) measures space and time-dependent soft x-ray emission

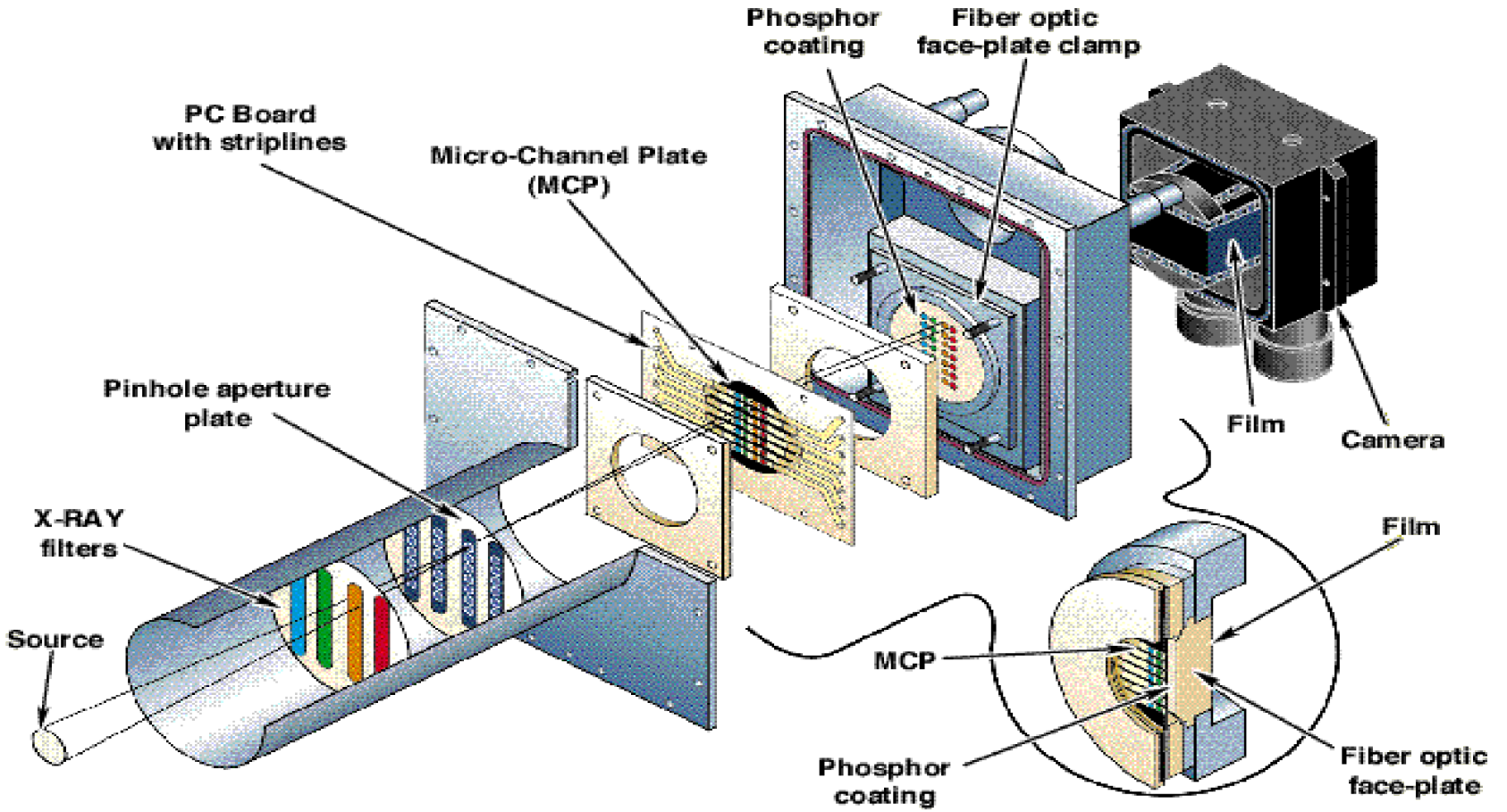

Ramon J. Leeper, 8/18/07

The fundamental operation of the micro-channel plate detector is shown here

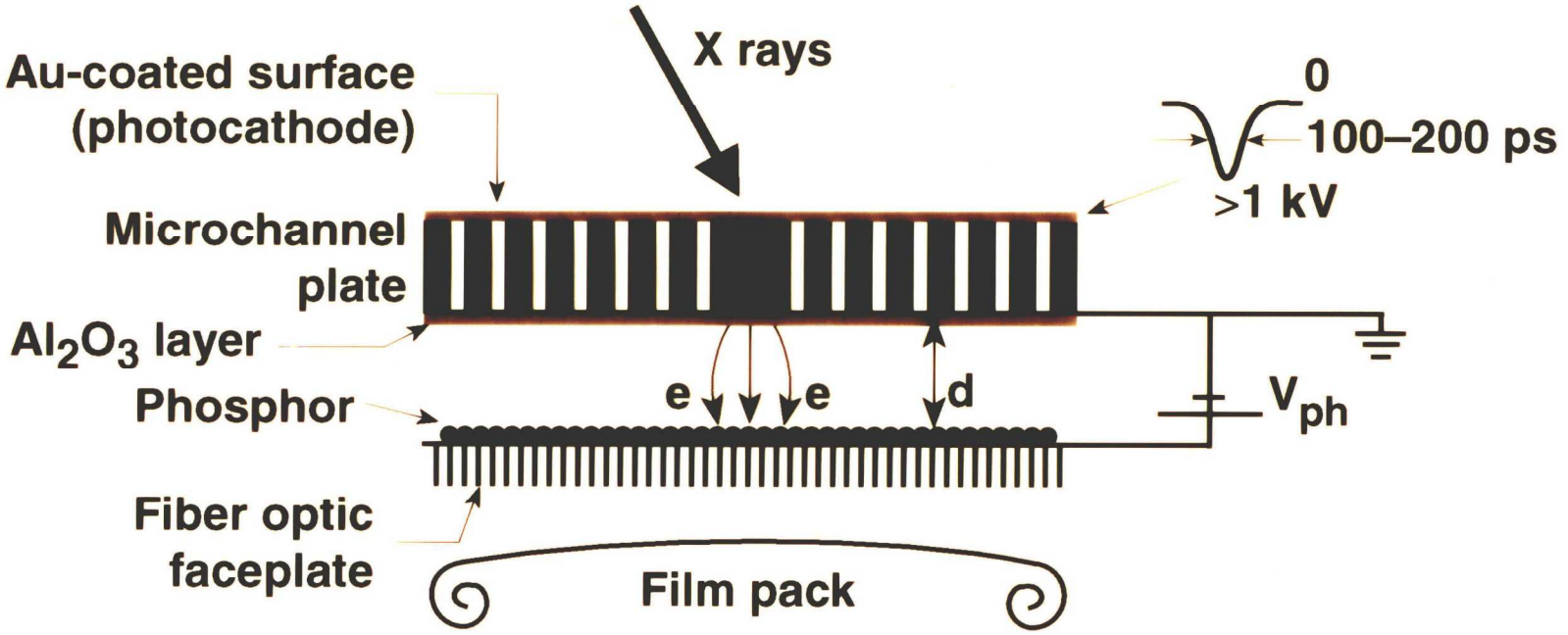

- Electrons are multiplied through MCP by voltage V_c.
- Images are recorded on film behind phosphor.
- Insulating Al_2O_3 layer allows V_{ph} to be increased, thus improving spatial resolution of phosphor.

On-axis framing camera observes detailed interior features of a dynamic hohlraum

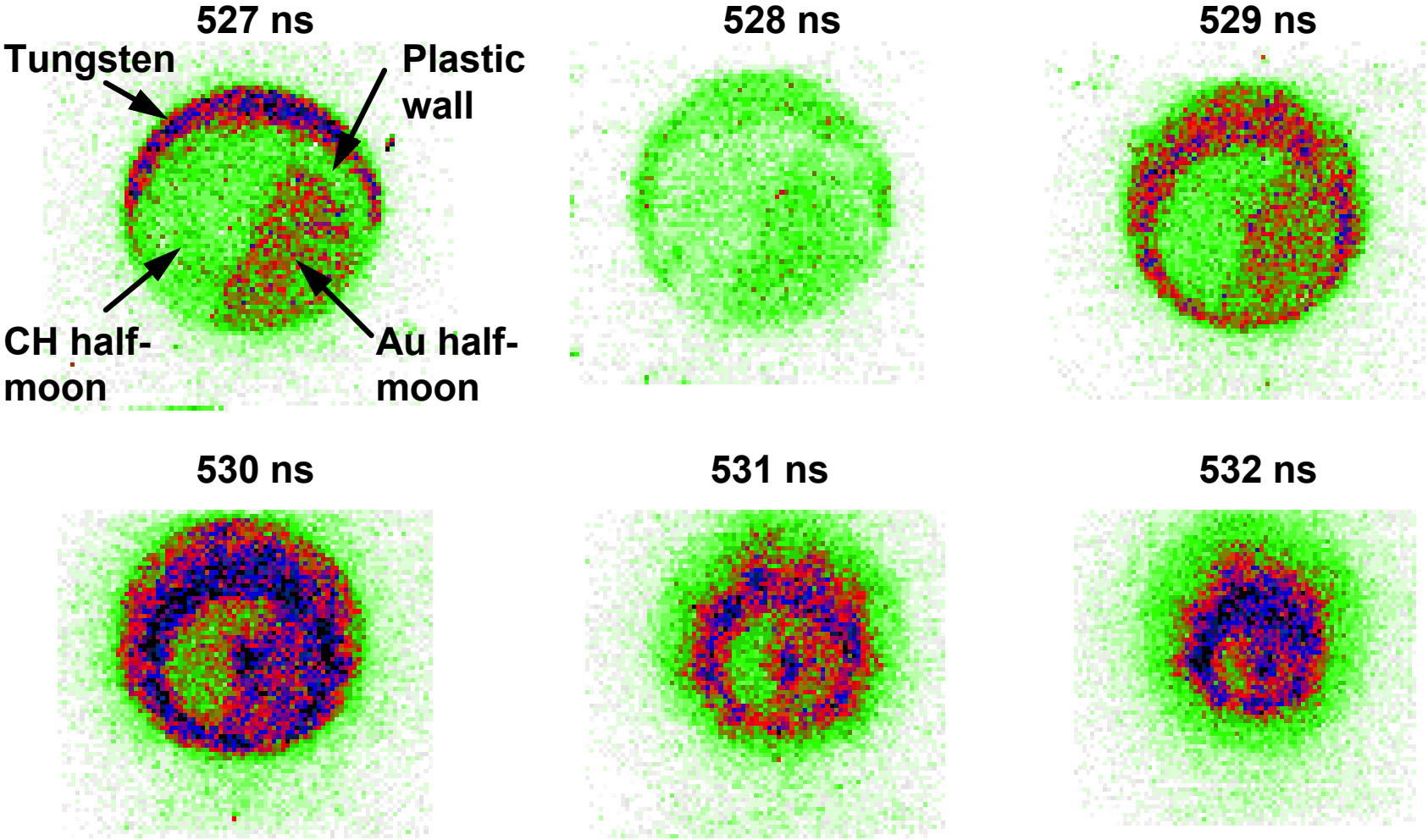

(1 ns time-resolved, 250 eV x-ray images)

Ramon J. Leeper, 6/18/07

The actual microchannel plate detector systems used for imaging and spectroscopy are shown here

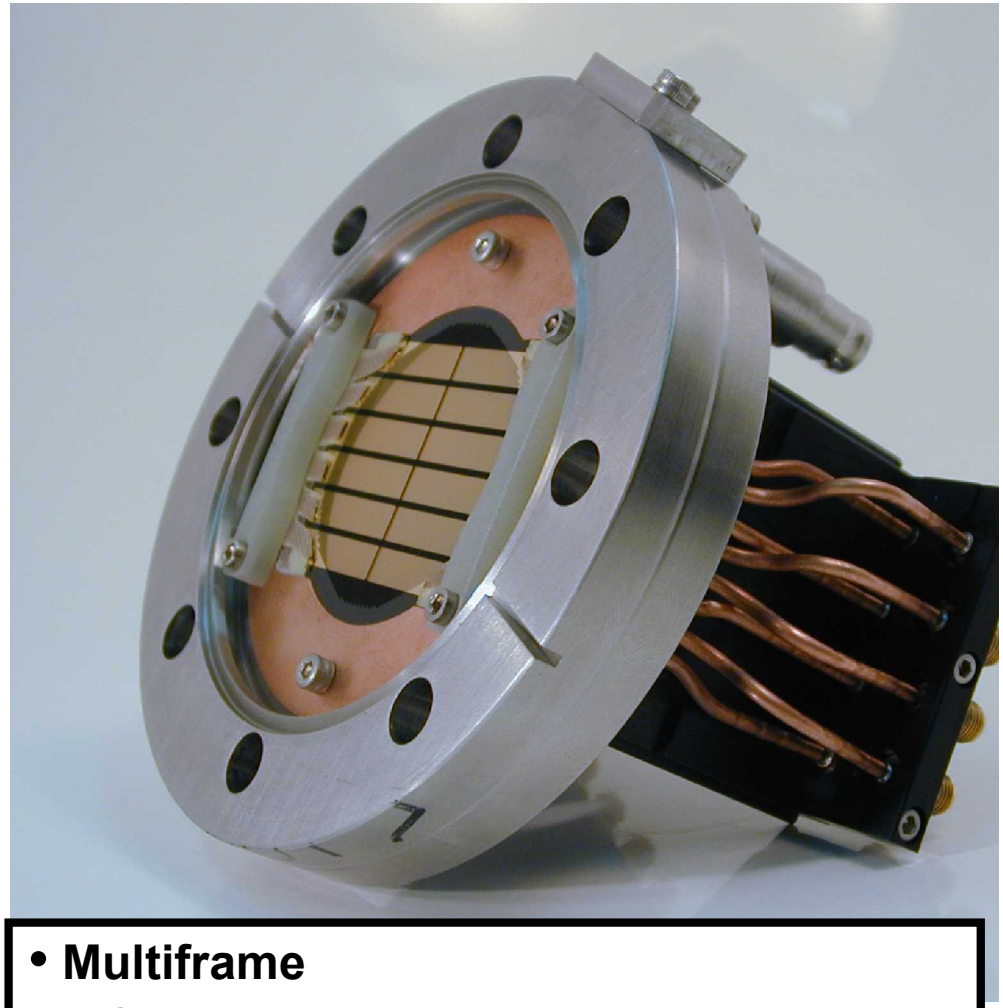

- Multiframe
- MCP's: 50 mm diameter
- MCP Gate times: ~0.8 - 5 ns

A fast large format pinhole camera (LFPHC) was developed for viewing pinch dynamics

QuickTime™ and a TIFF (LZW) decompressor are needed to see this picture.

- Nine frames
- MCP's: 20 mm wide x 60 mm tall
- Magnification: 1.72x with 5x mag. option
- Field of view: 11 mm wide x 35 mm high
- MCP Gate time: ~100 ps
- Spatial Resolution: ~100 μm
- Stripline impedance: 5.5 ohms

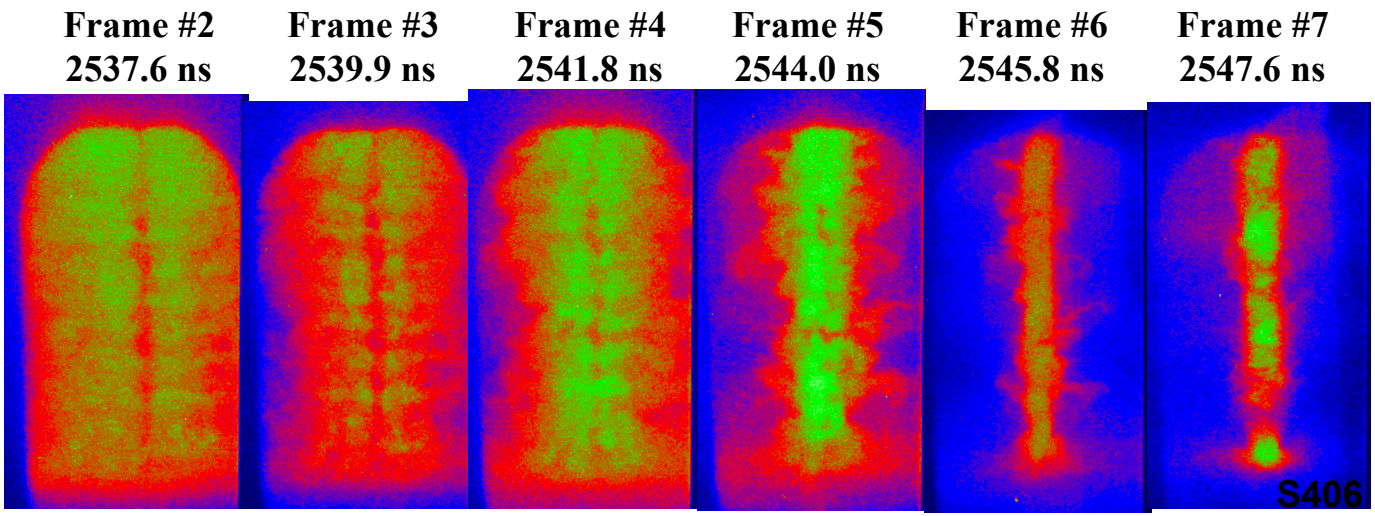

Ramon J. Leeper, 6/18/07

Multilayer mirror (MLM) pinhole camera produces monochromatic images

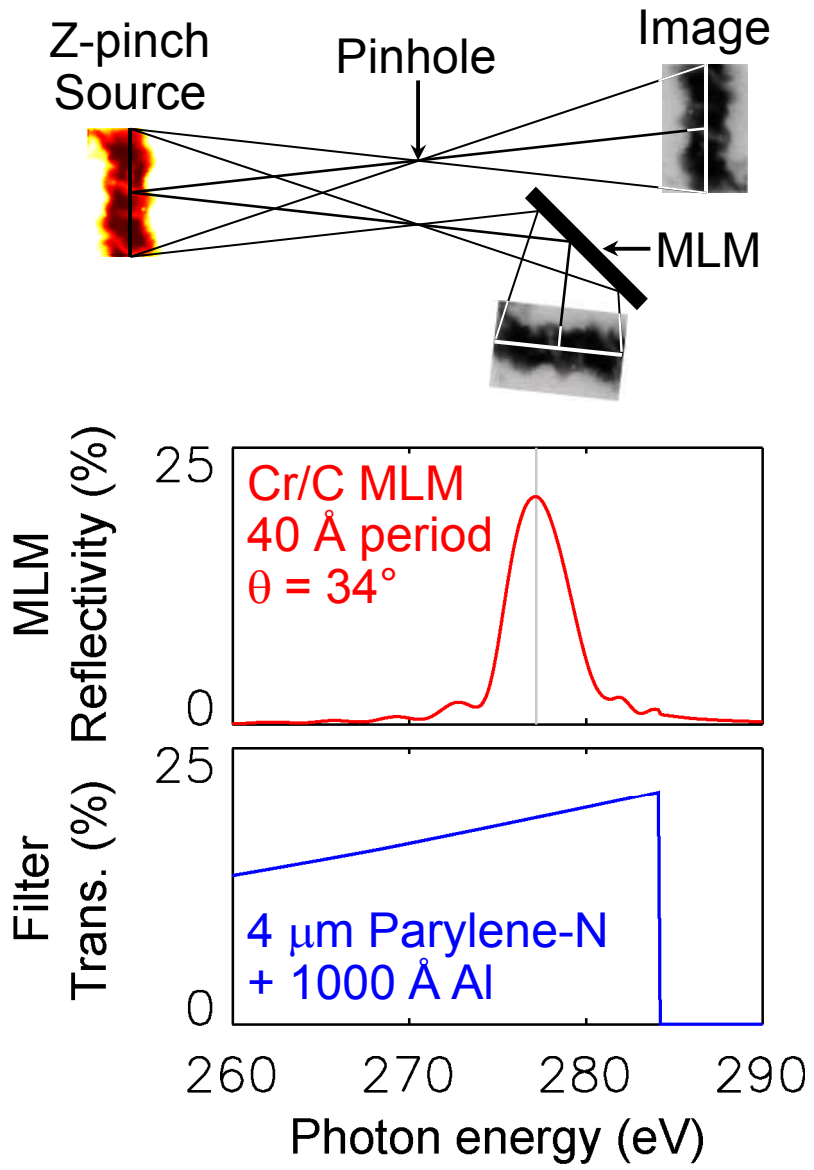

- **Pinhole images are reflected from planar Cr/C multilayer mirror (MLM)**
  - **Calculated 20% peak reflectivity, ~5 eV photon energy bandwidth**
  - **34° grazing angle allows shielding of detector from hard x-rays**
- **Thin filter blocks UV/visible light, suppresses second harmonic MLM reflection**
- **Instrument on the Z machine combines MLM-reflected and standard pinhole cameras (PHC)**

Ramon J. Leeper, 6/18/07

MLM PHC is currently fielded on the Z accelerator

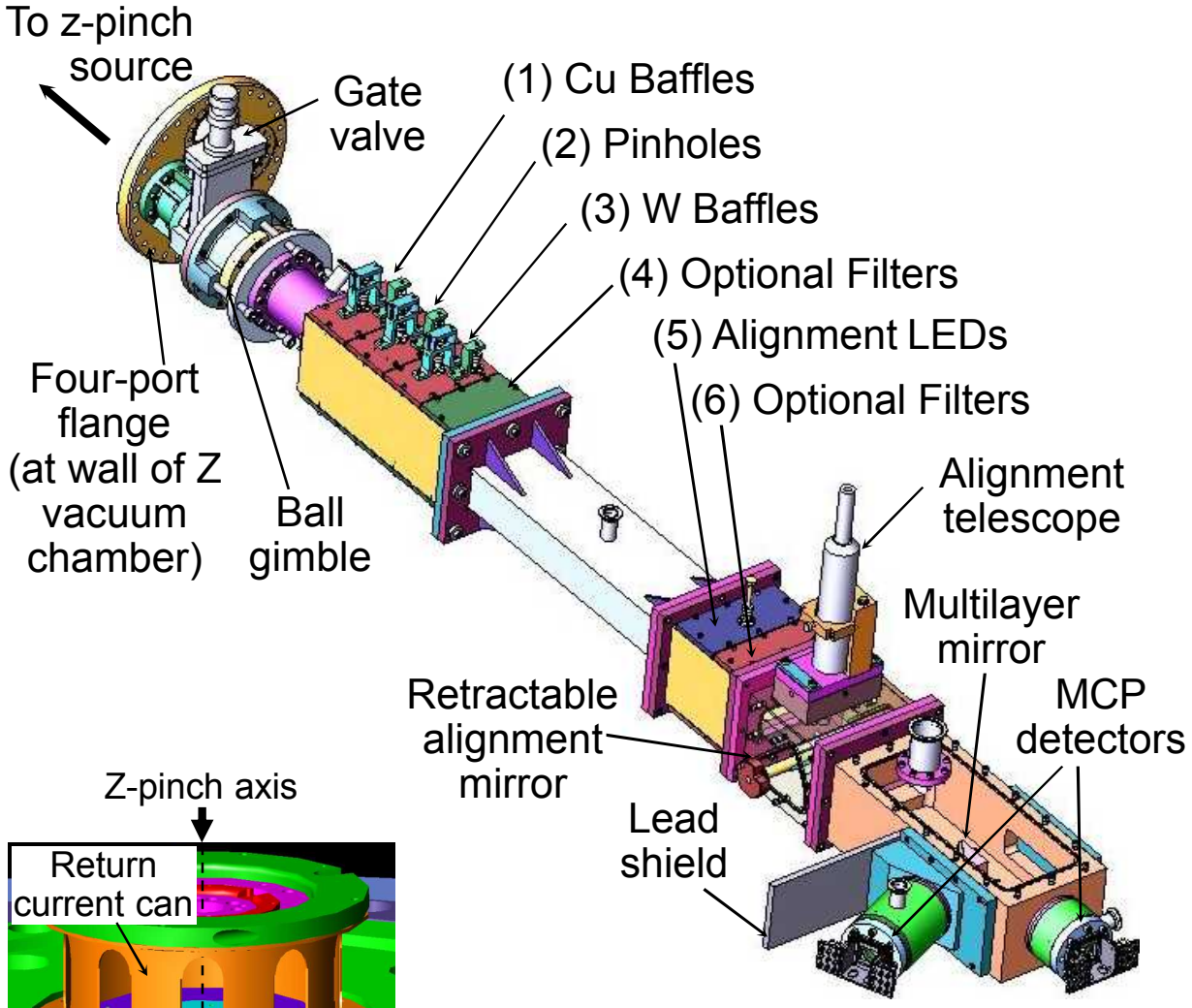

View of load region from 12° Line-of-sight

- **Instrument mounts on 12° side-on LOS**
- **3 PHCs can be fielded (two shown)**
- **Ball gimble pivots to align with source**
- **Alignment under vacuum corrects for pipe sag and movement in Z load region**
- **Instrument is differentially pumped behind gate valve**

B. Jones, C. Deeney, A. Pirela, C. Meyer, D. Petmecky, P. Gard, R. Clark, and J. Davis, Rev. Sci. Instrum. 75, 4029 (2004).

Detector box can accommodate two MLMs and standard PHC

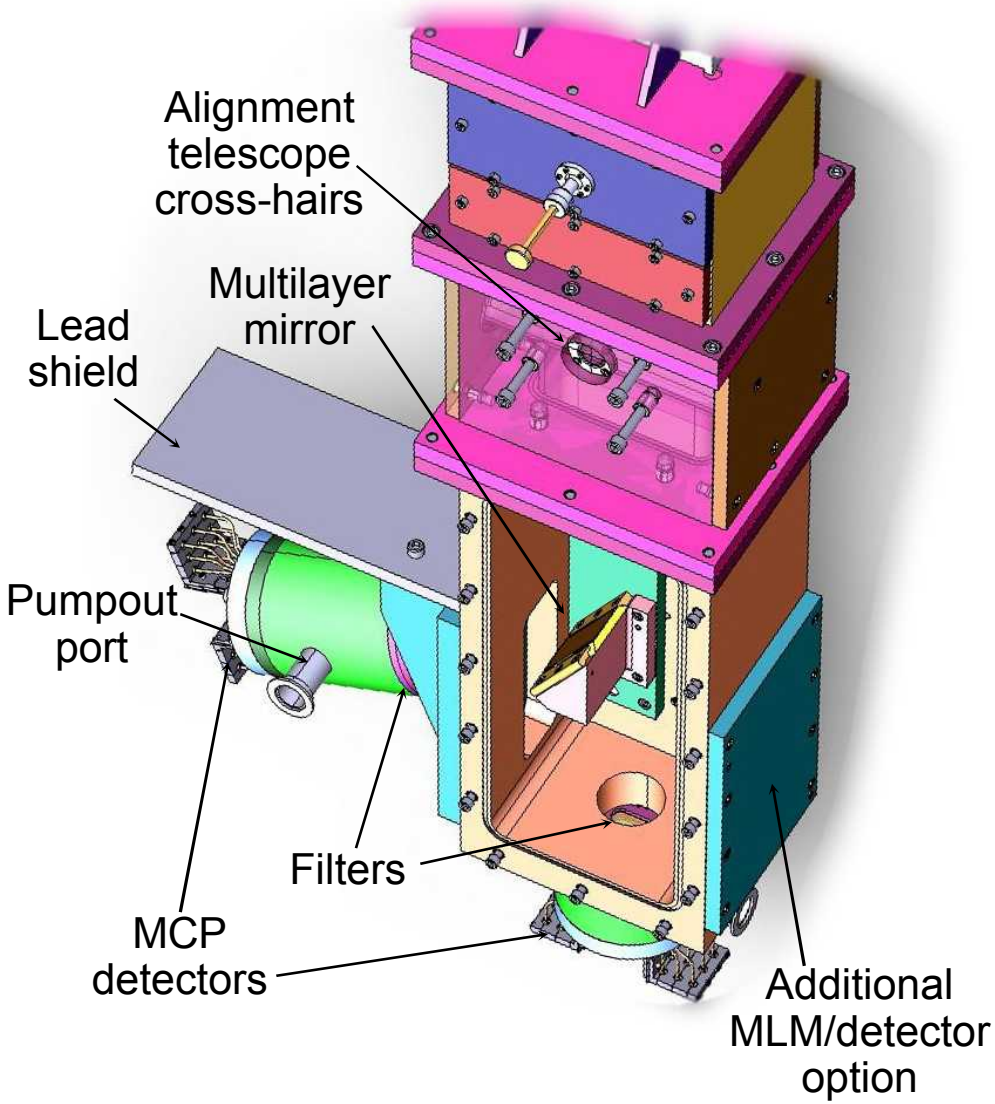

- Large 34° grazing angle allows detector shielding from hard x-rays generated in the Z load region
- Aluminized filters in front of MCP eliminate < 100 eV photons from reflection or fluorescence at MLM
- Standard pinhole camera on instrument axis can be filtered to look at K-shell emission from the z-pinch
- Space is available for a second MLM PHC

MLM PHC has excellent signal-to-noise during final implosion

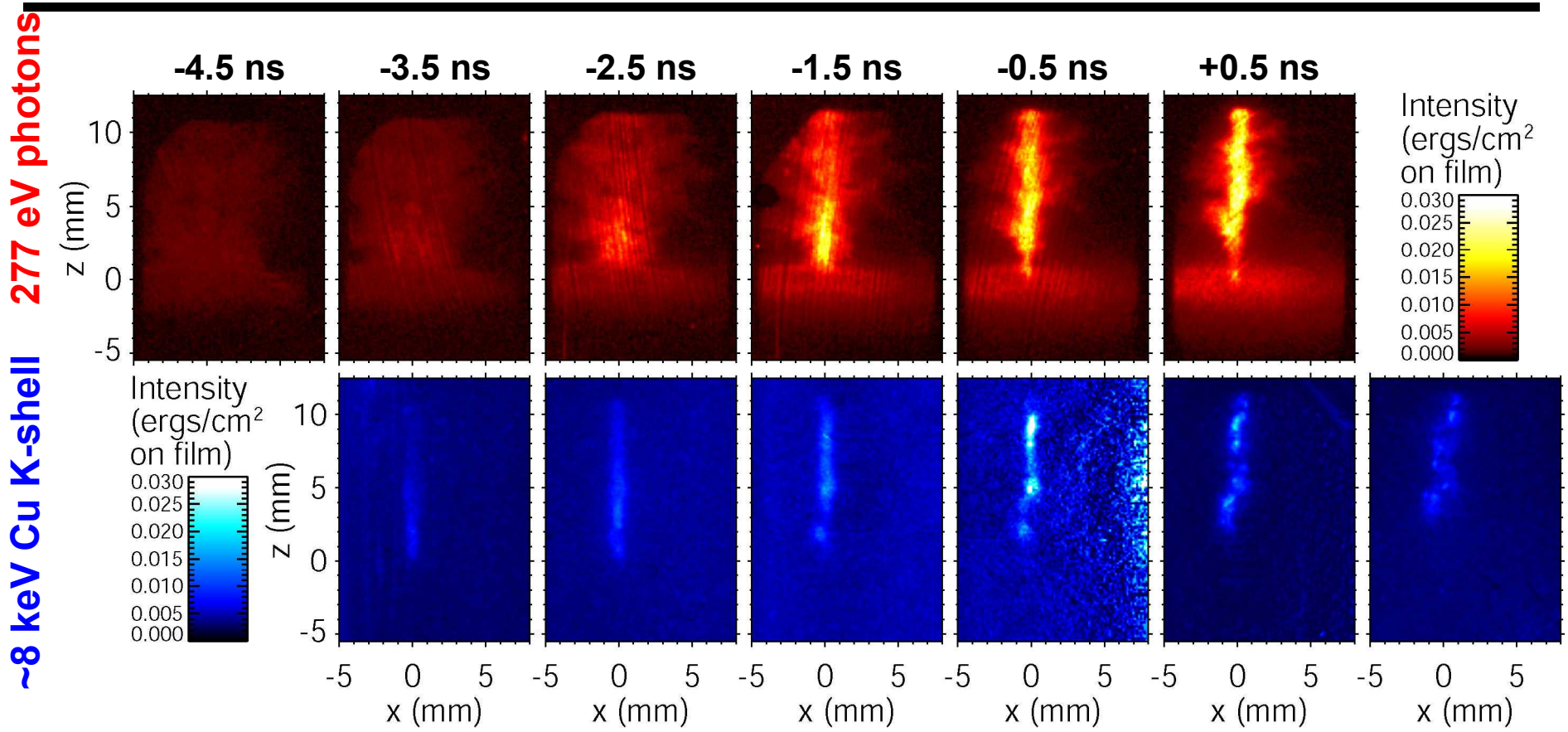

- **No hard x-ray background on MLM-reflected images**
- **Gradual accretion of mass on axis during ~5 ns x-ray pulse rise**
- **3D structure: zipper at stagnation, trailing mass at large radius**
- **Imaging at 2-3 energies can determine n,T profiles**

Ramon J. Leeper, 6/18/07

Streaked scintillator fiber array diagnostic measures energy-,1-D spatial-, and time-resolved soft x-ray target emission

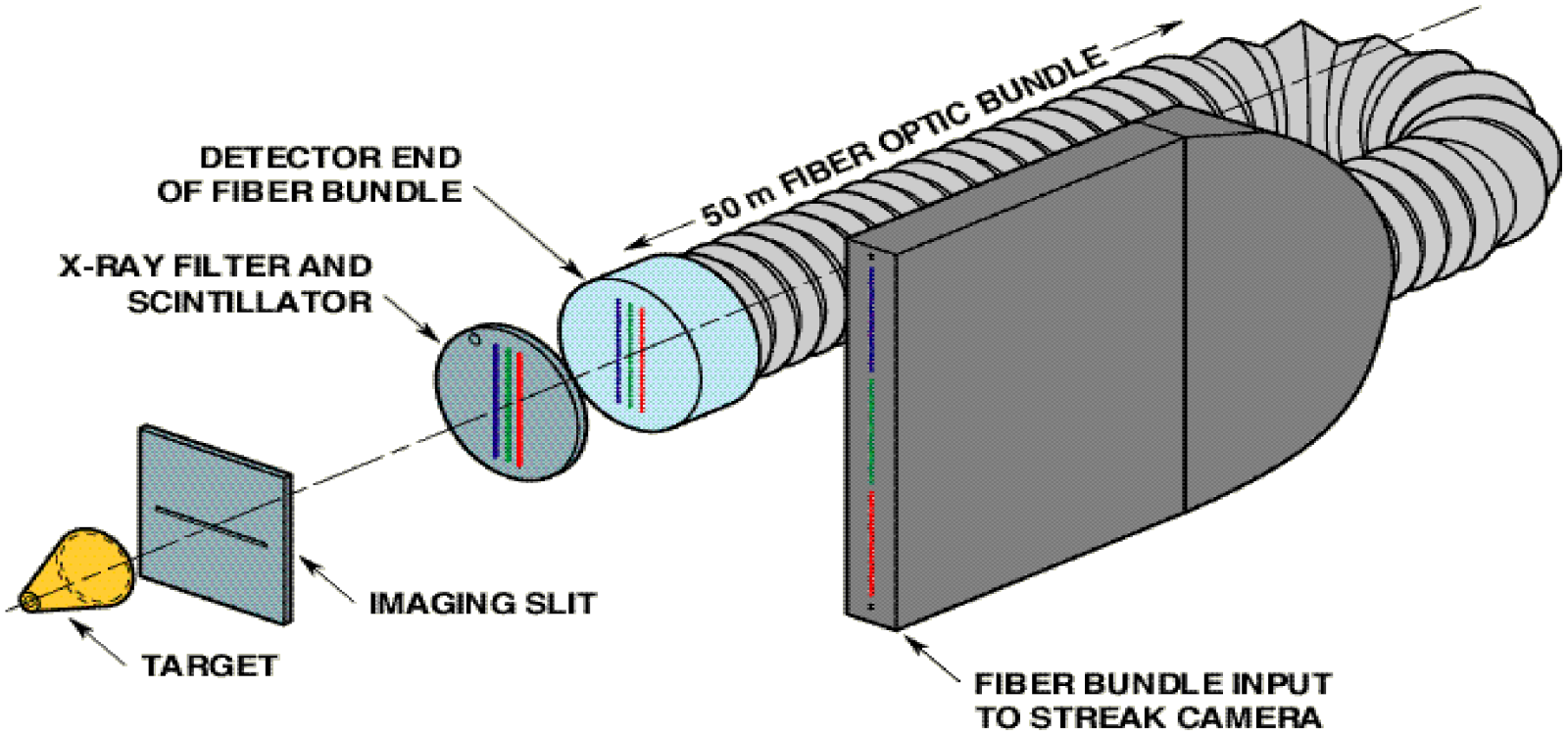

R. J. Leeper, J. E. Bailey, A. L. Carlson, G. A. Chandler, M. S. Derzon, R. J. Dukart, D. E. Hebron, J. A. Hunter, L. P. Mix, A. R. Moats, T. J. Nash, W. R. Olson, P. D. Rockett, C. L. Ruiz, J. A. Torres, D. F. Wenger, R. W. Olsen, T. L. Barber, P. W. Lake, and F. A. Schmidlapp, Rev. Sci. Instrum. 66, 511 (1995)

Ramon J. Leeper, 8/18/07

The Z/Beamlet laser provides a versatile x-ray source on Z for absorption imaging

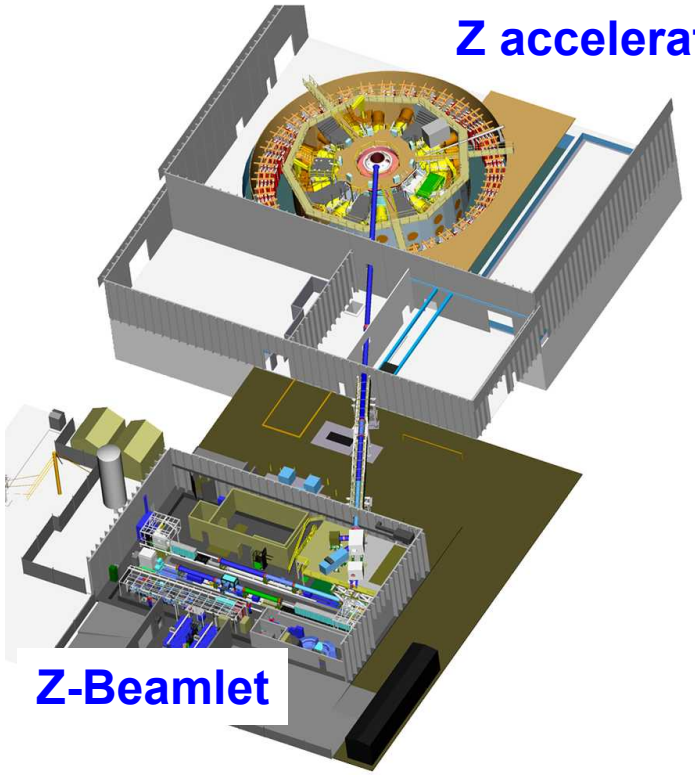

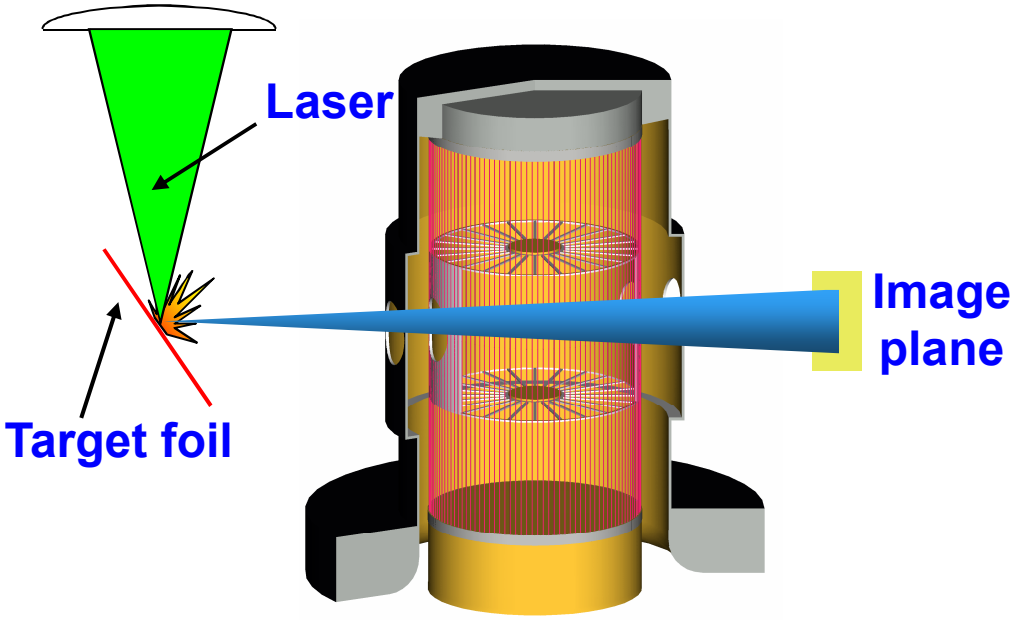

Capsule Radiographs with Fe He$_\alpha$ (6.7 keV) backlighter

- 2 kJ of 526.5 nm light in 1 ns pulse
- Point projection and bent crystal imaging backlighting capabilities

The Z-Beamlet laser is integrated into the Z-machine using on-axis final optics

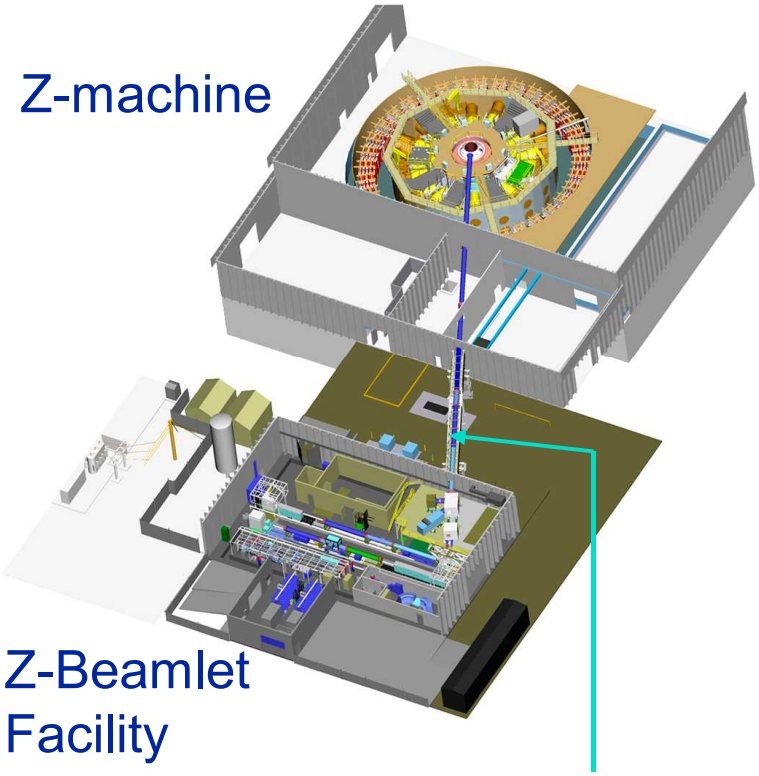

A ~ 75-m-length relay telescope brings the beam to the top of the Z chamber

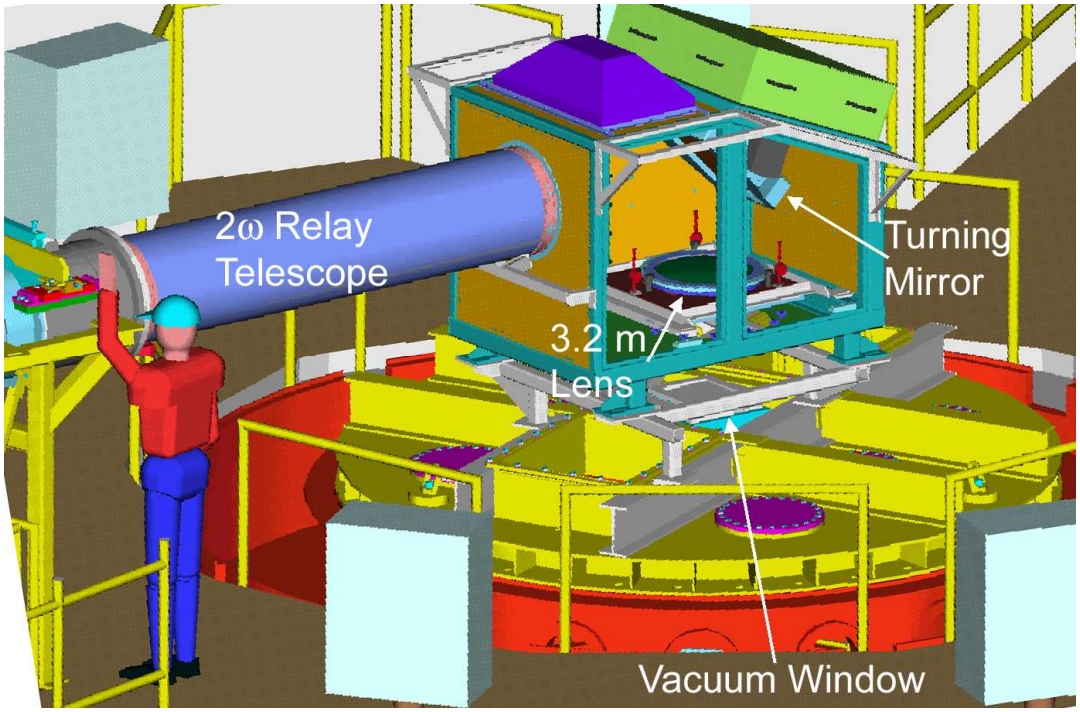

At the Z-machine a turning mirror and lens are used to make 50-150 μm diameter x-ray spots 100-200 mm from the axis (>10^{15} W/cm^2 on target→ 0.1-1 J x rays)

Point projection x-radiography on Z has advantages and disadvantages compared to using this imaging technique on a laser ICF facility

Advantages:

(1) ZBL 50-μm-diam spot (when fully optimized) suggests that pinhole assistance may not be necessary

(2) With up to 100 cm foil-to-capsule distances possible on Z, it is easy to attain low M for high spatial resolution

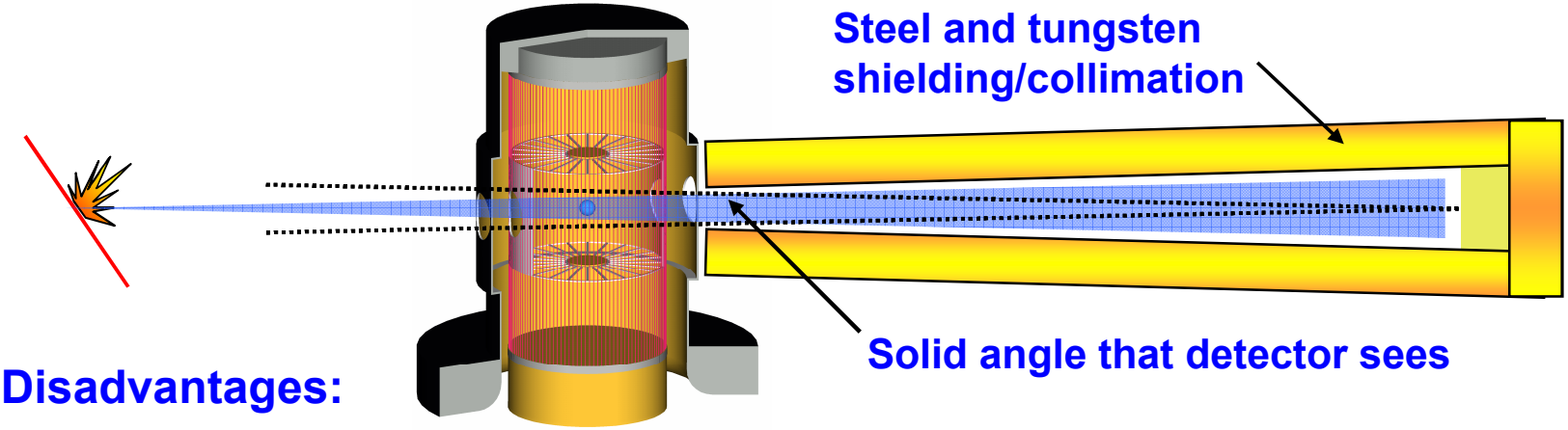

Disadvantages:

In contrast to a laser ICF facility the fragile x-ray filter/film package is susceptible to:

(1) Severe Z debris issues

(2) Intense high-energy Bremmstrahlung background radiation

Monochromatic x-ray backlighting using bent crystals an elegant solution

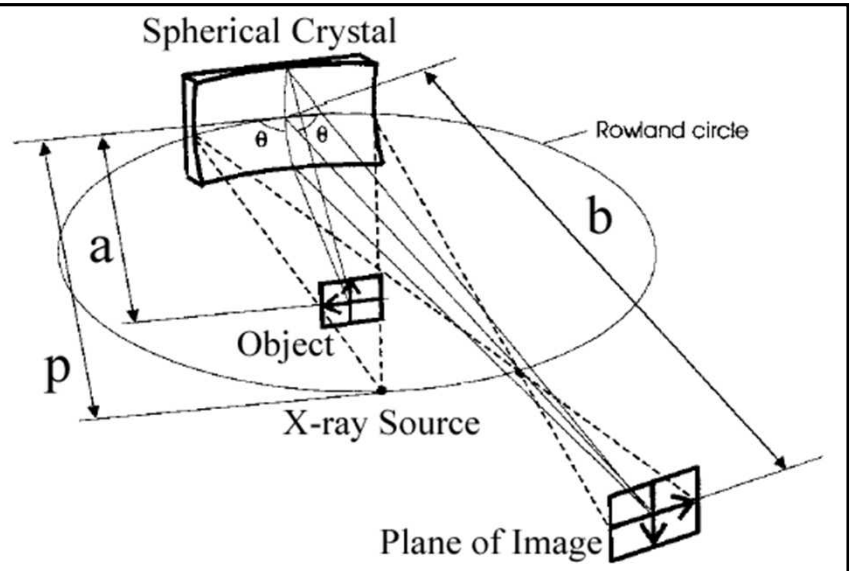

Bent-crystal Imaging

- **Monochromatic (~0.5 eV bandpass)**
- **10 micron resolution**
- **Large field of view (e.g. 20 mm x 4 mm)**
- **Debris mitigation**

- **S.A. Pikuz *et al.* proposed the concept in mid-1990s.**
  - S.A. Pikuz *et al.*, Rev. Sci. Instrum. **68**, 740 (1997).
- **Y. Aglitskiy *et al.* implemented a 1.865 keV backlighter at NRL**
  - Y. Aglitskiy *et al.*, Rev. Sci. Instrum. **70**, 530 (1999).
- **J.A. Koch *et al.* proposed crystal imaging techniques for microscopy/backlighting on NIF**
  - J.A. Koch *et al.*, Rev. Sci. Instrum. **70**, 525 (1999).

Monochromatic backlighting and point-projection backlighting comparison

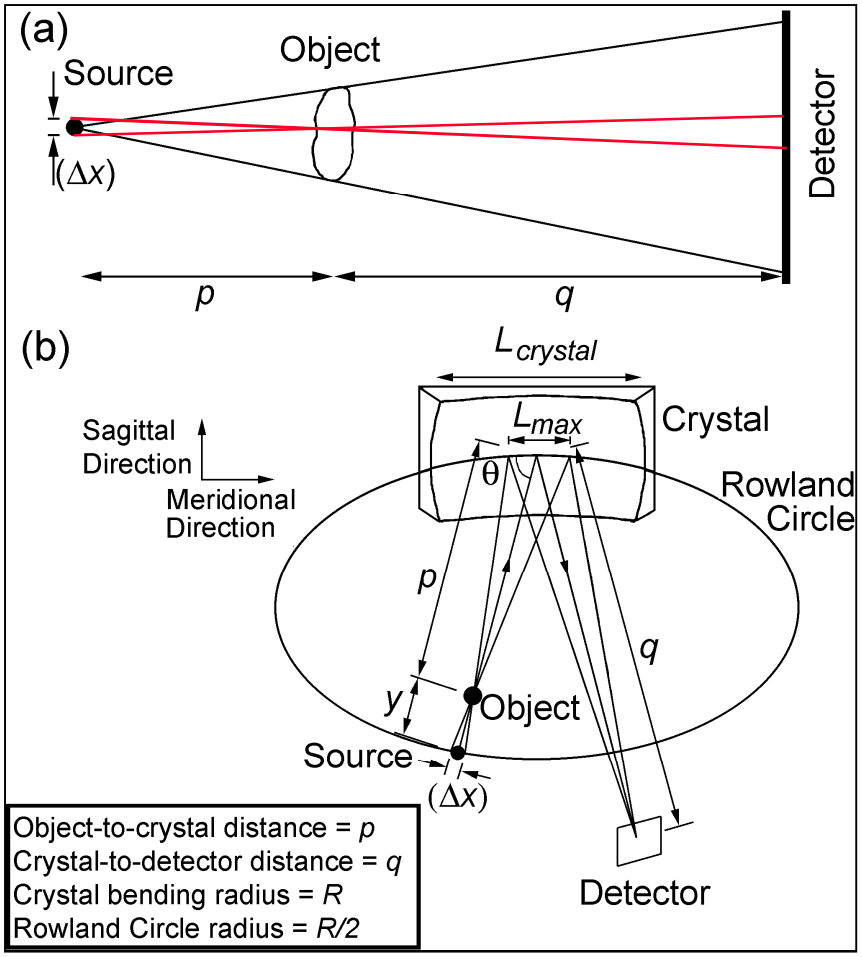

Backlighting Geometries

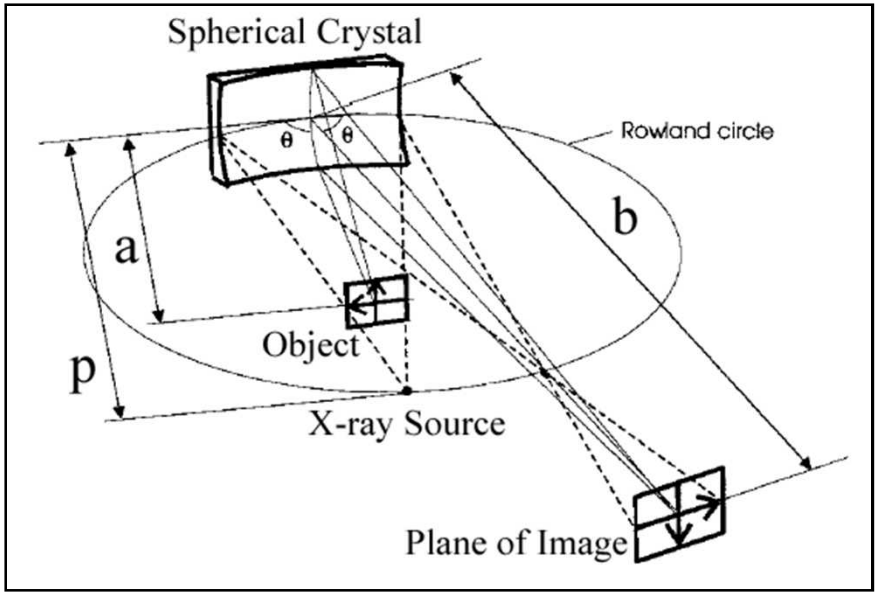

Bent-crystal Imaging

- **Monochromatic (~0.5 eV bandpass)**
- **10 micron resolution**
- **Large field of view (e.g. 20 mm x 4 mm)**
- **Debris mitigation**
- **Source 0.1-1 J; Object ~1 MJ**

Two versions are in use on Z: 1.865 keV or 6.151 keV radiography diagnostics*

1.865 keV Radiography†

- X-ray source: He-like Si 2*p* $^1P_1$ line at 1.865 keV
- Crystal: R=250 mm Quartz 10-11 (2d=6.685 Å)
- Bragg Angle: 83.9°
- Magnification: 6.0
- Field of view: 4 mm tall by 20 mm wide
- Spectral bandpass: <0.5 eV
- Spatial resolution: 9-10 microns
- Detector: Kodak RAR 2497 film

6.151 keV Radiography††

- X-ray source: He-like Mn 2*p* $^3P_1$ line at 6.151 keV
- Crystal: R=250 mm Quartz 22-43 (2d=2.030 Å)
- Bragg Angle: 83.15°
- Magnification: 6.0
- Field of view: 4 mm tall by 20 mm wide
- Spectral bandpass: <0.5 eV
- Spatial resolution: 10-11 microns
- Detector: Kodak DEF film

† This diagnostic based on previous work by Y. Aglitskiy *et al.*, Rev. Sci. Instrum. 70 (1999)

†† This diagnostic based on proposal in J. A. Koch *et al.*, Rev. Sci. Instrum. 70 (1999)

* Z radiography diagnostics described in D.B. Sinars *et al.*, Rev. Sci. Instrum. 75, 3672 (2004)

The power of the curved-crystal imaging technique in suppressing Z's hard x-ray bremmsstrahlung background and debris is clearly shown in these radiographs*

3.4-mm diameter plastic ICF capsule

Capsules had 100s of known defects on surface that apparently produced a myriad of small jets

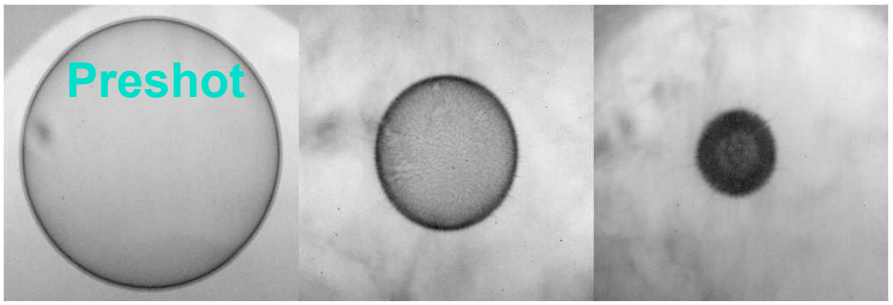

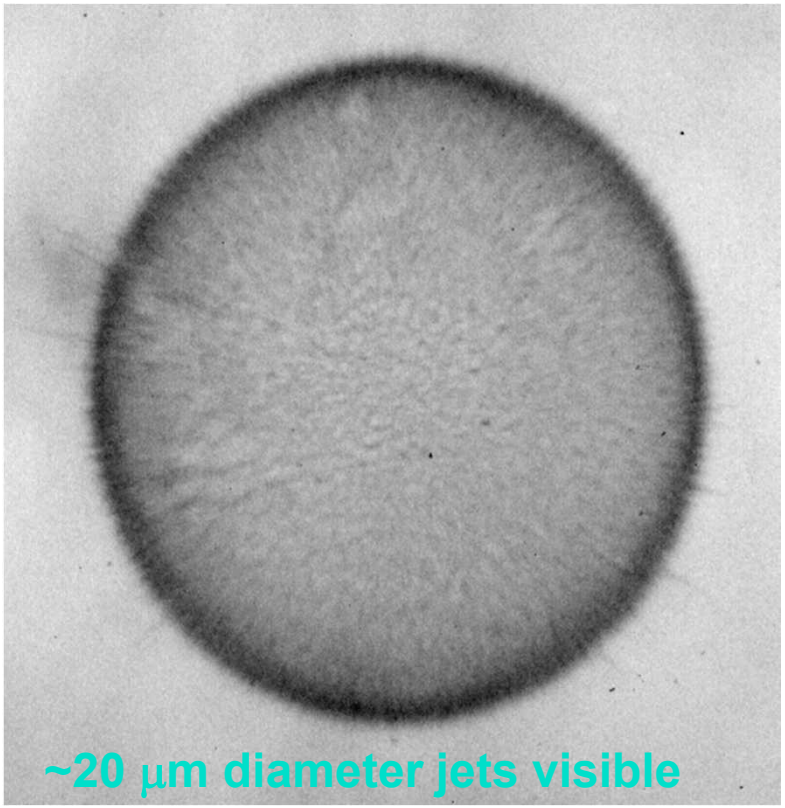

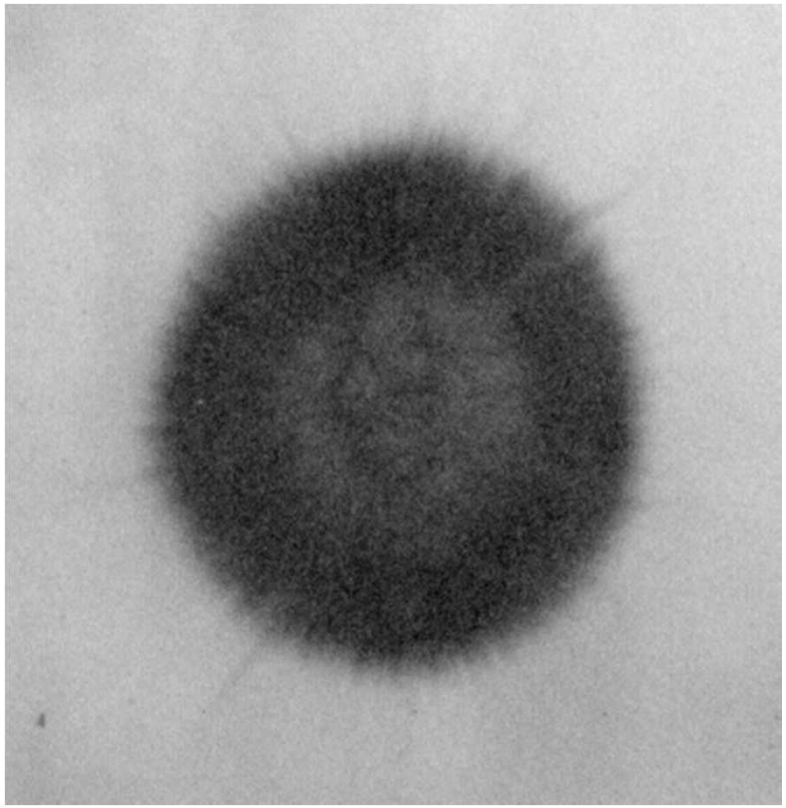

* M.E. Cuneo, G.R. Bennett

X-ray backlighting is being used to measure the mass profile and instability growth during wire-array implosions

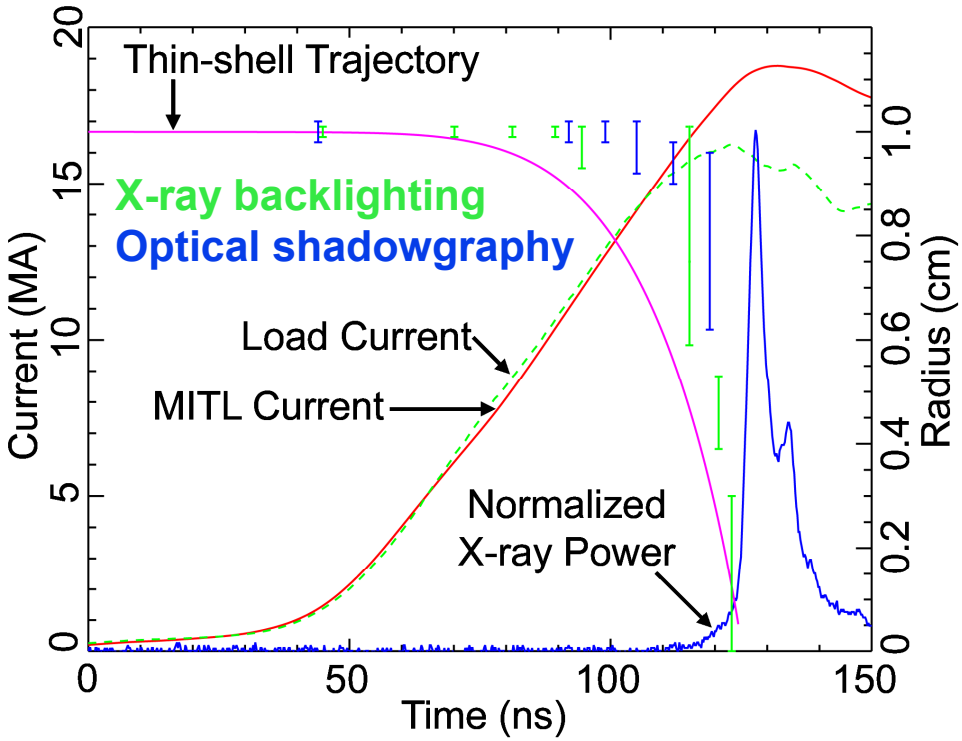

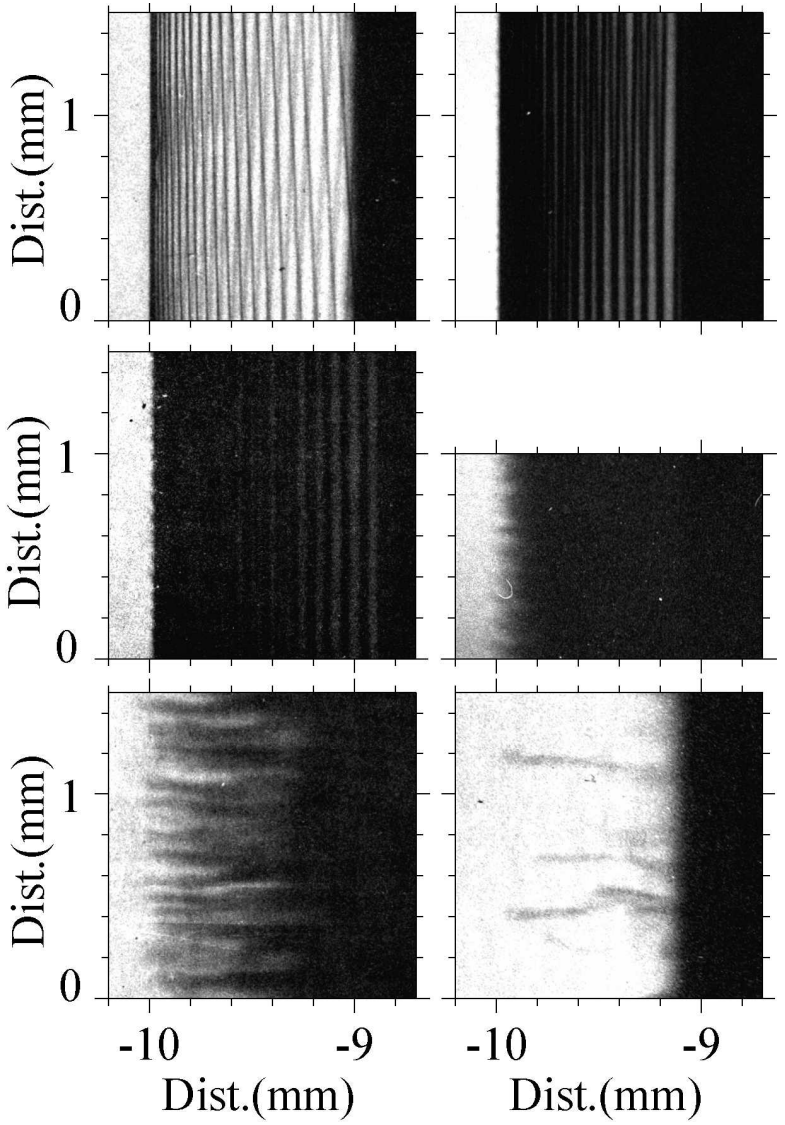

Correlated instabilities and axially non-uniform breakup of wires contribute to the creation of trailing mass and limit peak radiation powers

D.B. Sinars *et al.*, Phys. Rev. Lett. 93, 145002 (2004).

Spectroscopy characterizes the z-pinch source, radiation matter interaction, and shocked matter

DIAGNOSTIC	QUANTITY OBSERVED	USED TO OBTAIN
Optical Spectrograph	1.7 eV To 6.2 eV Photons	Plasma Temperature And Density
McPig Spectrograph (Time-Resolved and 1-D Spatial)	15 eV To 1 keV X-rays	Continuum and Line Ratio Measurement of Source Temperature
Elliptical and Convex Crystal Spectrographs	500 eV To 10 keV X-rays	Plasma Temperature And Density
Filtered Diamond Photoconducting Detector Array	1 keV To 10 keV X-rays	Broadband Kilovolt X-ray Spectrum And Yield

Time-integrated and time-resolved convex crystal spectrometers are used routinely on Z

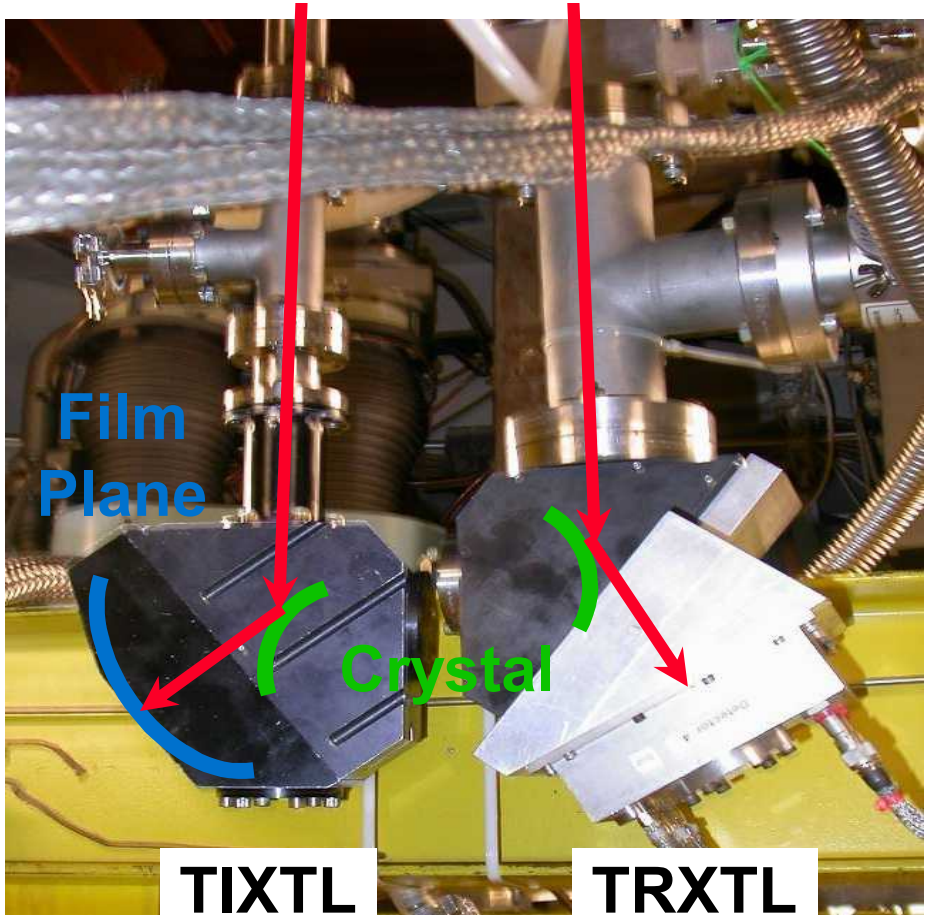

- Wavelength coverage: 500 eV to 10 keV
- Spectral resolution: ~1000
- TIXTL Magnification: 1
- TRXTL Gate widths: ~1 - 4 ns
- TRXTL Number of Gates: 7

Stainless Steel Wire Array
TIXTL: Axial resolved

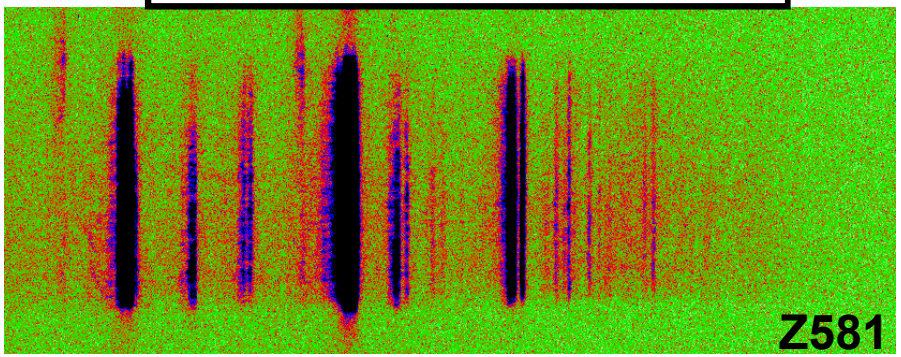

Cr He_α Fe He_α Ni He_α

Elliptical crystal spectrographs provide higher sensitivity, lower noise spectral measurements

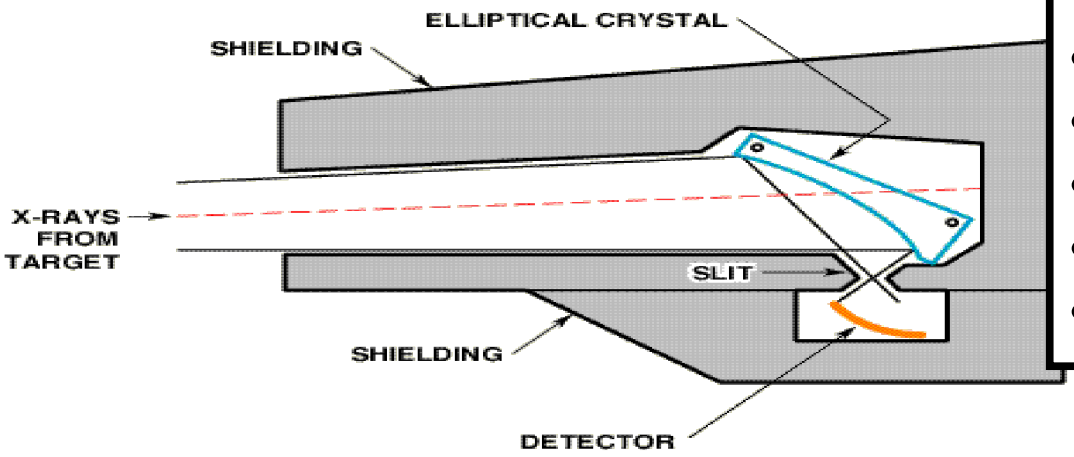

- Wavelength coverage:1 to 10 keV
- Spectral resolution: ~1000
- Magnifications: 0.5; 1; 2
- Fields of view (mm): 8; 4; 2
- Gate widths: ~1 - 4 ns
- Number of Gates: 6

Argon spectra from capsule implosion

QuickTime™ and a TIFF (LZW) decompressor are needed to see this picture.

Sectional view of the Z double time-resolved elliptical crystal spectrometer (TREX)

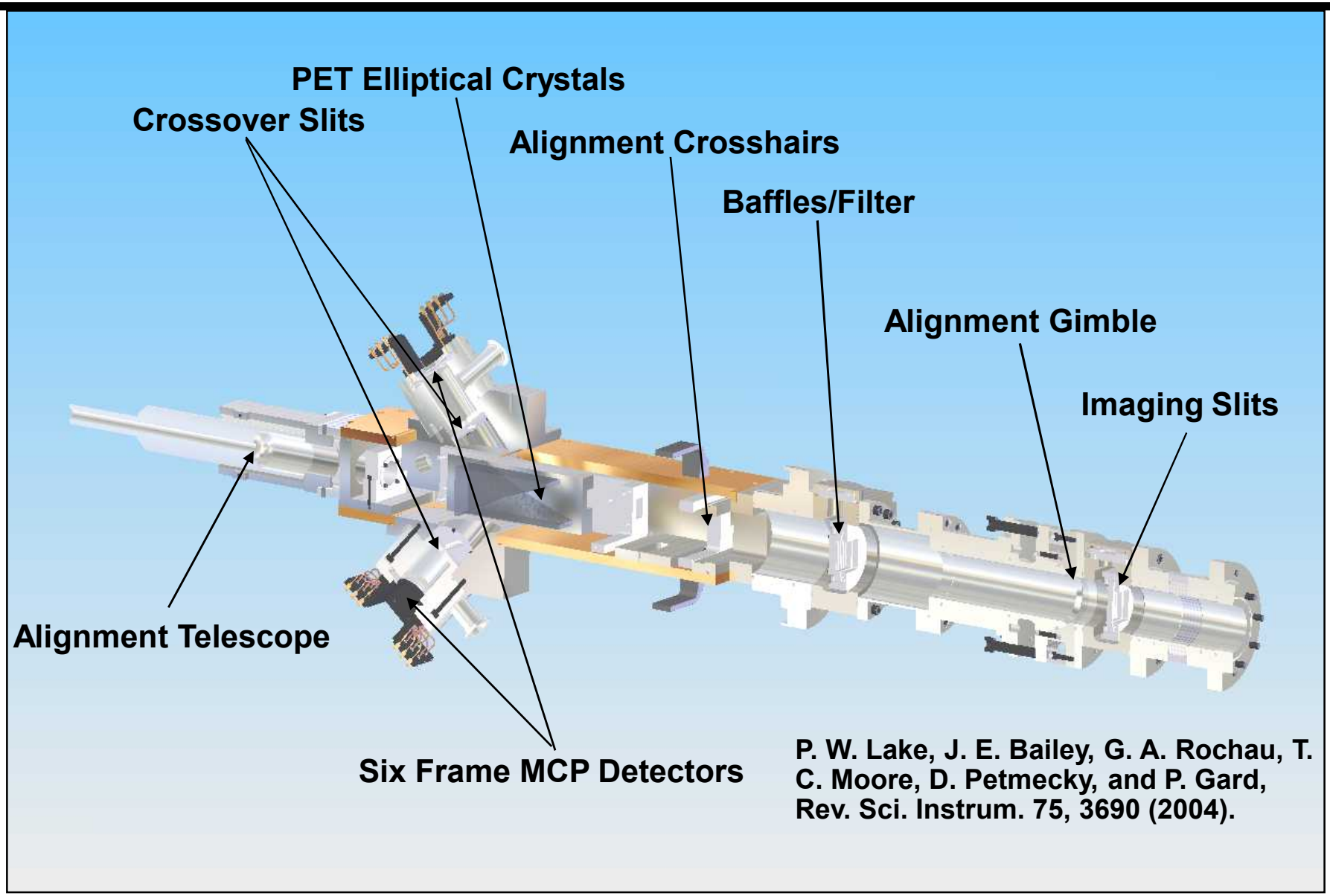

P. W. Lake, J. E. Bailey, G. A. Rochau, T. C. Moore, D. Petmecky, and P. Gard, Rev. Sci. Instrum. 75, 3690 (2004).

Initial time-resolved tomographic spectroscopy measurements have been performed

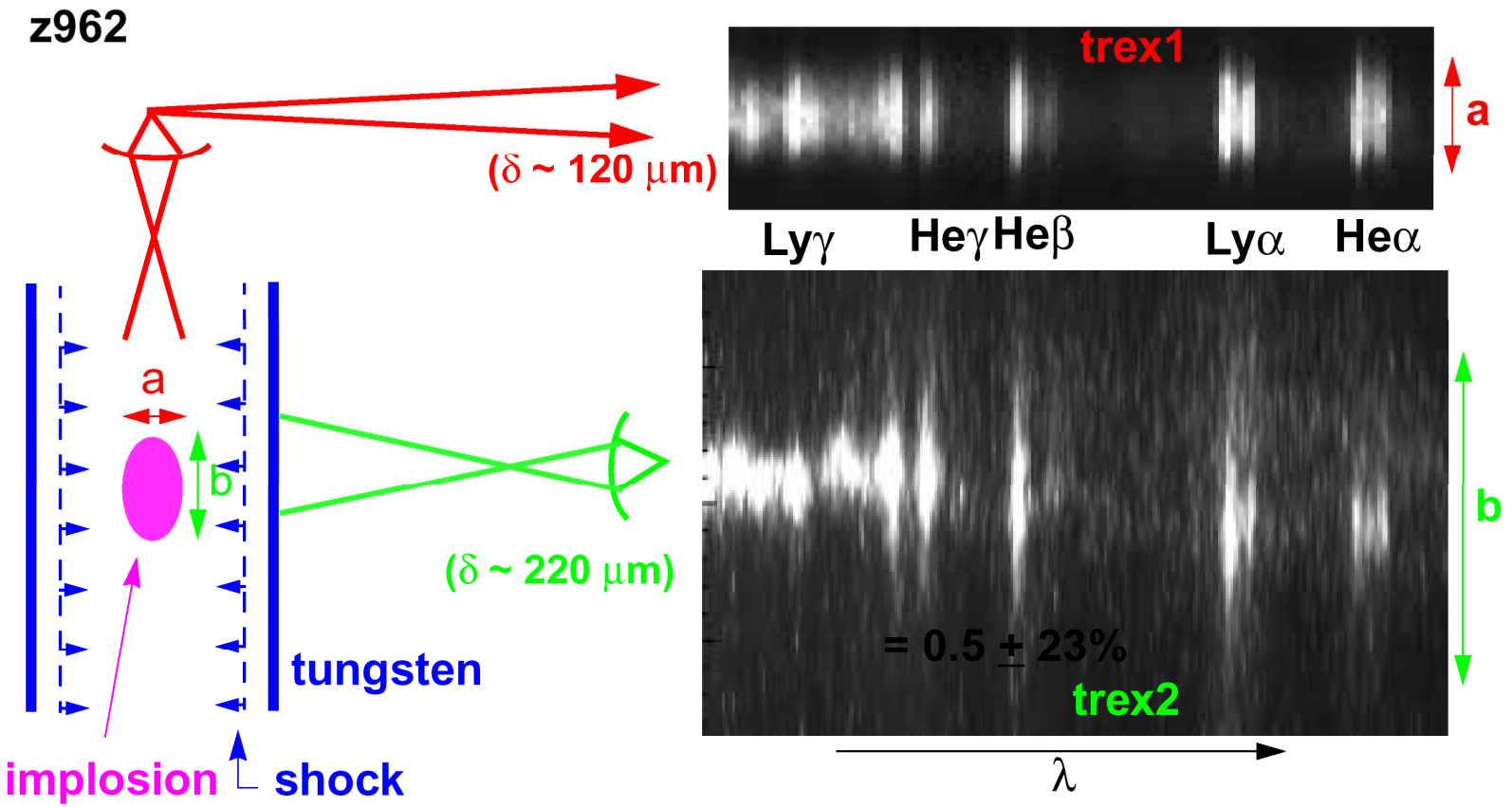

Spatial resolution was improved to 50 μm and 85 μm for the TREX1 and TREX2 spectrometers
A third TREX (side view, radial resolution) has been recently fabricated

J. E. Bailey, G. A. Chandler, S. A. Slutz, I. Golovkin, P. W. Lake, J. J. MacFarlane, R. C. Mancini, T. J. Burris-Mog, G. Cooper, R. J. Leeper, T. A. Mehlhorn, T. C. Moore, T. J. Nash, D. S. Nielsen, C. L. Ruiz, D. G. Schroen, and W. A. Varnum, Phys. Rev. Lett. 92, 085002 (2004)

A variety of shock diagnostic techniques have been developed for measurement of hohlraum temperature and material properties

DIAGNOSTIC	QUANTITY OBSERVED	USED TO OBTAIN
Active Shock Breakout	Radiation Driven Shock Velocity	Hohlraum Temperature
Fiber Optic Active Shock Breakout	Radiation Driven Shock Velocity	Hohlraum Temperature
Conventional VISAR	Shock and Particle Velocity	Hohlraum Temperature and Material Properties
Line VISAR	Shock and Particle Velocity	Spatially-Resolved Hohlraum Temperature and Material Properties

The active shock breakout diagnostic uses a laser probe to measure the arrival time of a shock

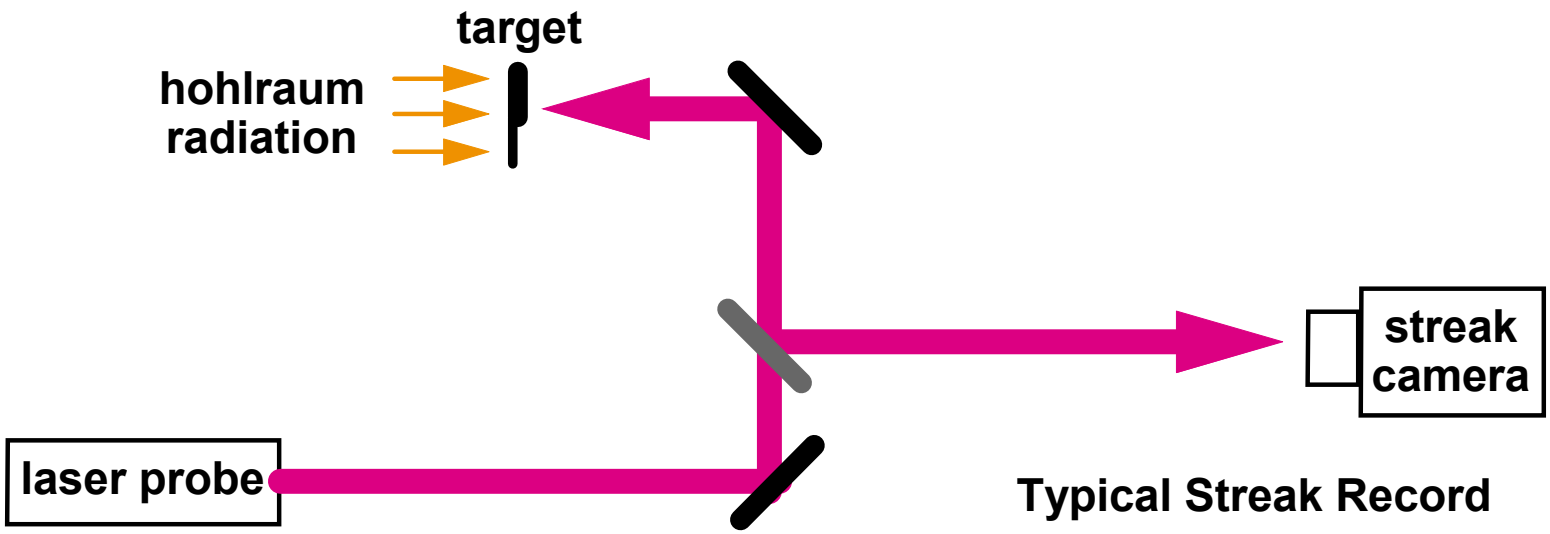

Typical Streak Record

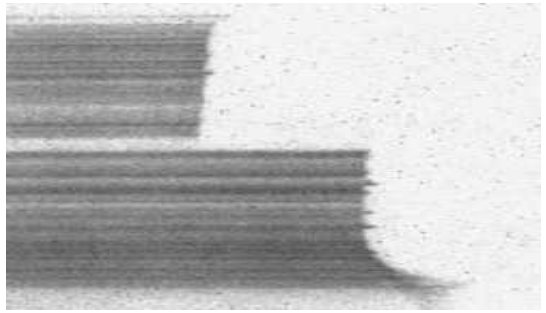

R. E. Olson, J. L. Porter, G. A. Chandler, D. L. Fehl, D. O. Jobe, R. J. Leeper, M. K. Matzen, J. S. McGurn, D. D. Noack, L. E. Ruggles, P. Sawyer, J. A. Torres, M. Vargas, D. M. Zagar, H. N. Kornblum, T. J. Orzechowski, D. W. Phillion, L. J. Suter, A. R. Thiessen, and R. J. Wallace, Phys. Plasmas 4, 1818 (1997)

The streak camera concept is illustrated in the following schematic

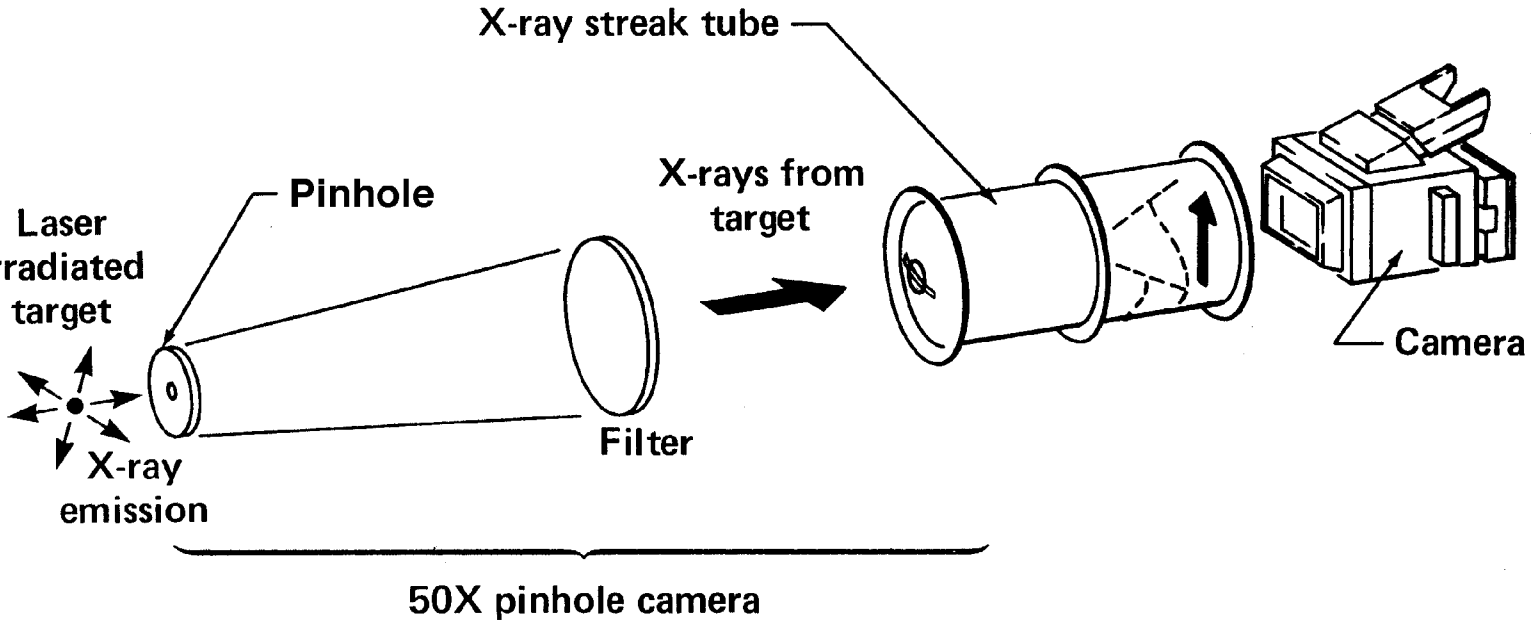

- Streak camera provides continuous temporal response
- Streak camera enable 1-D spatial imaging

Nuclear diagnostics that measure the parameters of the capsule core region are essential

Theoretical calculation of capsule core region

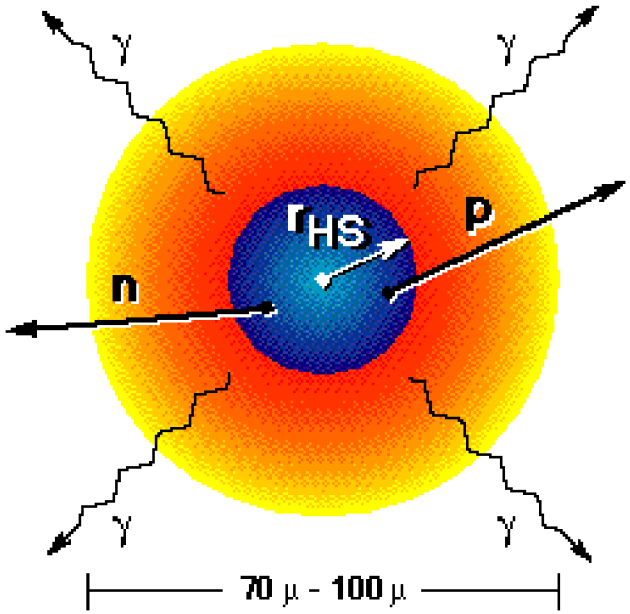

Capsule temperature and density versus fuel core radius

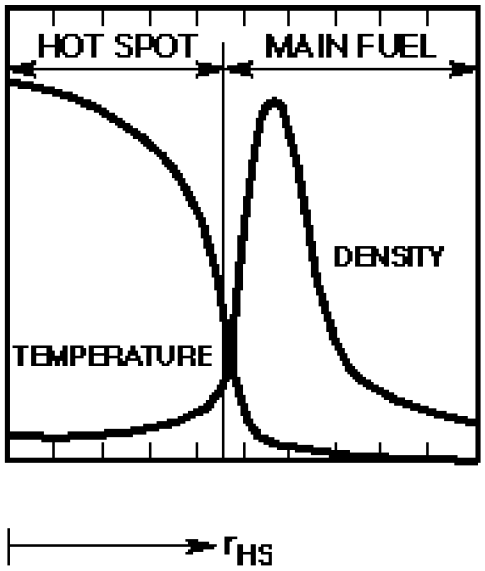

Experimental reality of capsule core region

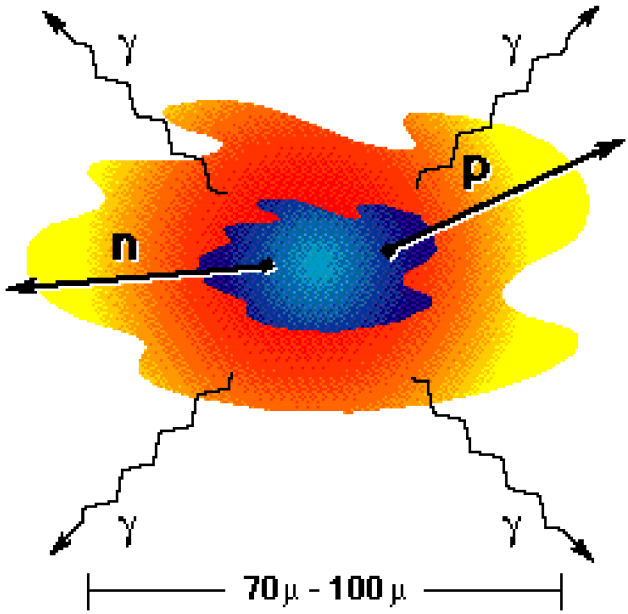

T301_LLCP7009.01

As we approach ignition conditions, only nuclear reaction products can penetrate the capsule core region

Ramon J. Leeper, 6/18/07

A suite of neutron diagnostics have been developed for capsule experiments

DIAGNOSTIC	QUANTITY OBSERVED	USED TO OBTAIN
Neutron TOF Detector	2.45 MeV or 14.1 MeV Neutrons	Neutron Yield and Ion Temperature
Pb Activation Detector	2.45 MeV or 14.1 MeV Neutrons	Total Neutron Yield
Indium or Beryllium Activation Detector	2.45 MeV Neutrons	Total Neutron Yield
Copper Activation Detector	14.1 MeV Neutrons	Total Neutron Yield

Neutron diagnostics typically fielded in high energy density experiments include neutron activation and neutron time-of-flight detectors

- Passive (activation) detectors:
  - Indium -- ^{115}In (n , n')^{115m}In (336.0 keV, $\tau_{1/2}$ = 4.49 hr.)
  - Copper -- ^{63}Cu(n , 2n)^{62}Cu ($\beta+$, $\tau_{1/2}$ = 9.74 min.)
  - Lead probe -- ^{207}Pb(n , n')^{207m}Pb (1064 keV, $\tau_{1/2}$ = .8 sec.)

- Active (neutron-time-flight) detectors:
  - Conventional scintillator/photomultipler detector
  - Scintillator/microchannel plate detector

- The ^{115}In (n , n')^{115m}In and ^{207}Pb(n , n')^{207m}Pb reactions may also be activated by a large flux of hard x-rays via the reactions ^{115}In (γ , γ')^{115m}In and ^{207}Pb(γ , γ')^{207m}Pb and so these hard x-ray backgrounds must be characterized to determine their contribution to the activation signals

In activation counting system: Germanium detector with associated electronics

A Pb activation detector has been adapted for the measurement of DD total neutron yield on Z

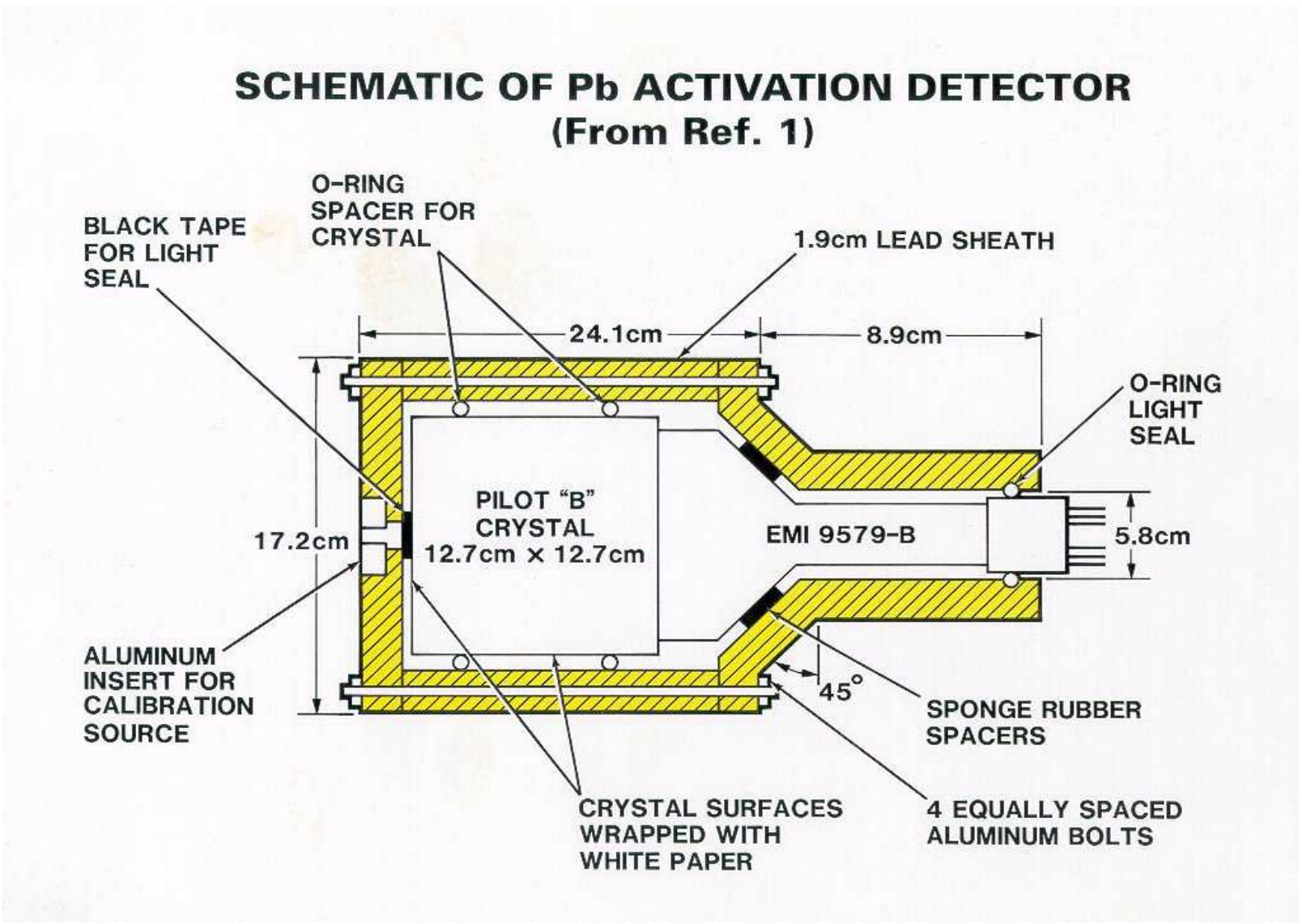

The absolutely calibrated SNL Pb activation detector is shown in this photograph

The relevant cross sections for operation of the Pb activation detector are shown here

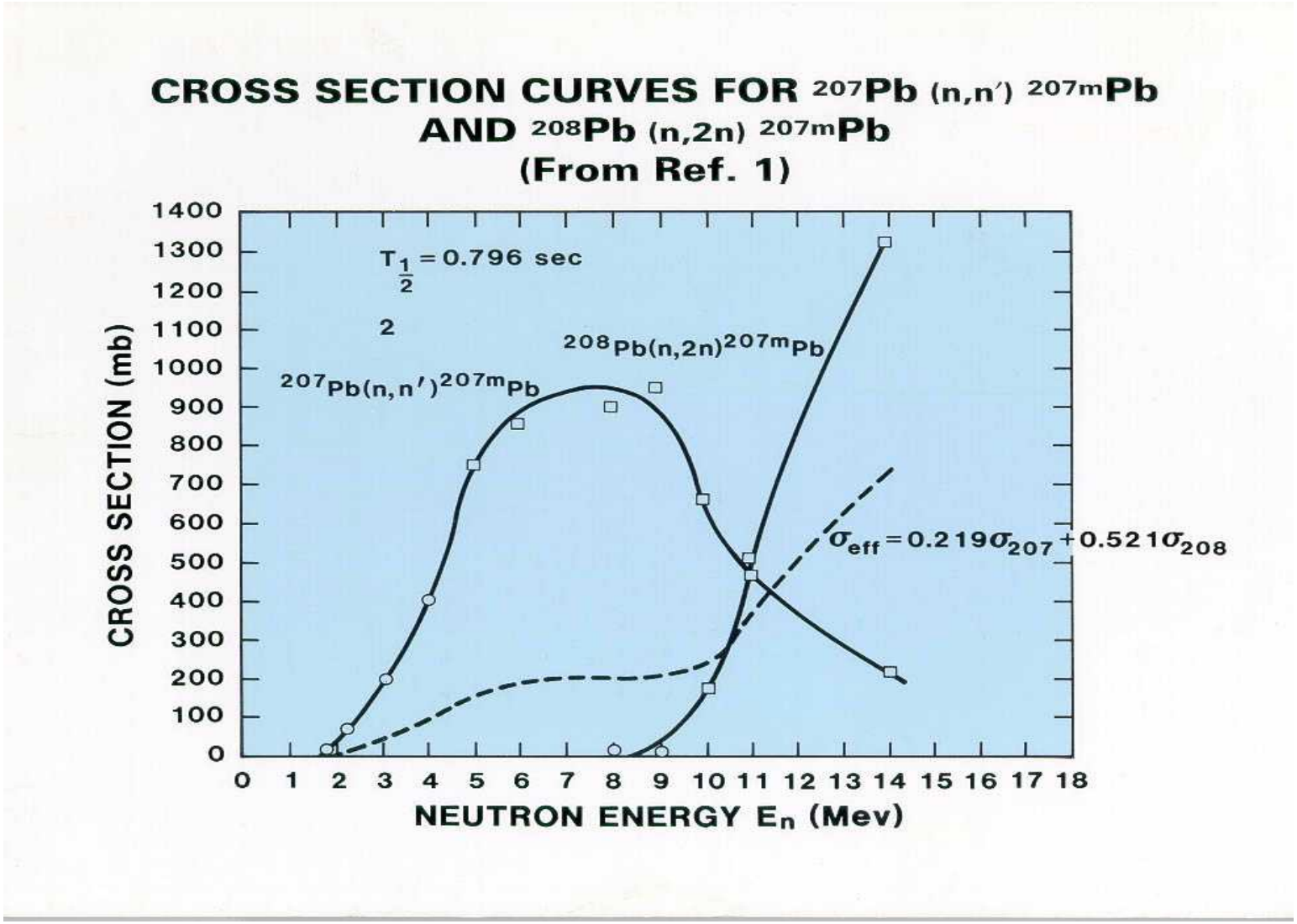

Ramon J. Leeper, 6/18/07

Total yield of 14.1 MeV neutrons is measured with the $^{63}Cu(n,2n)^{62}Cu$ reaction

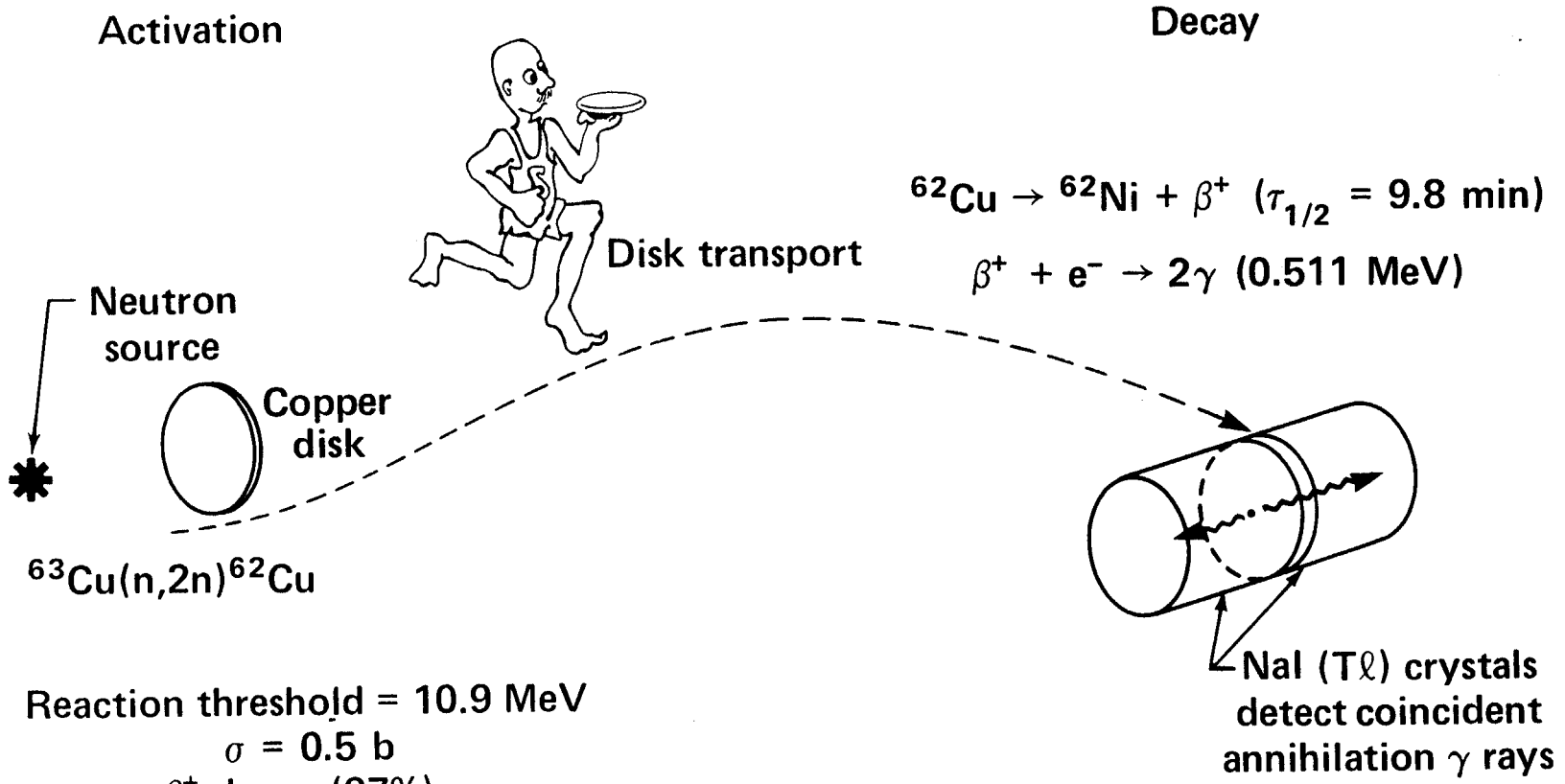

Reaction threshold = 10.9 MeV
σ = 0.5 b
β^+ decay (97%)

Present system

- Disk size = 76 mm dia × 9.5 mm
- Source to target distance = 41 cm
- Present detectability ≈ 10^8 neutrons

Ramon J. Leeper, 6/18/07

Coincidence counting arrangement used with activation detectors is shown here

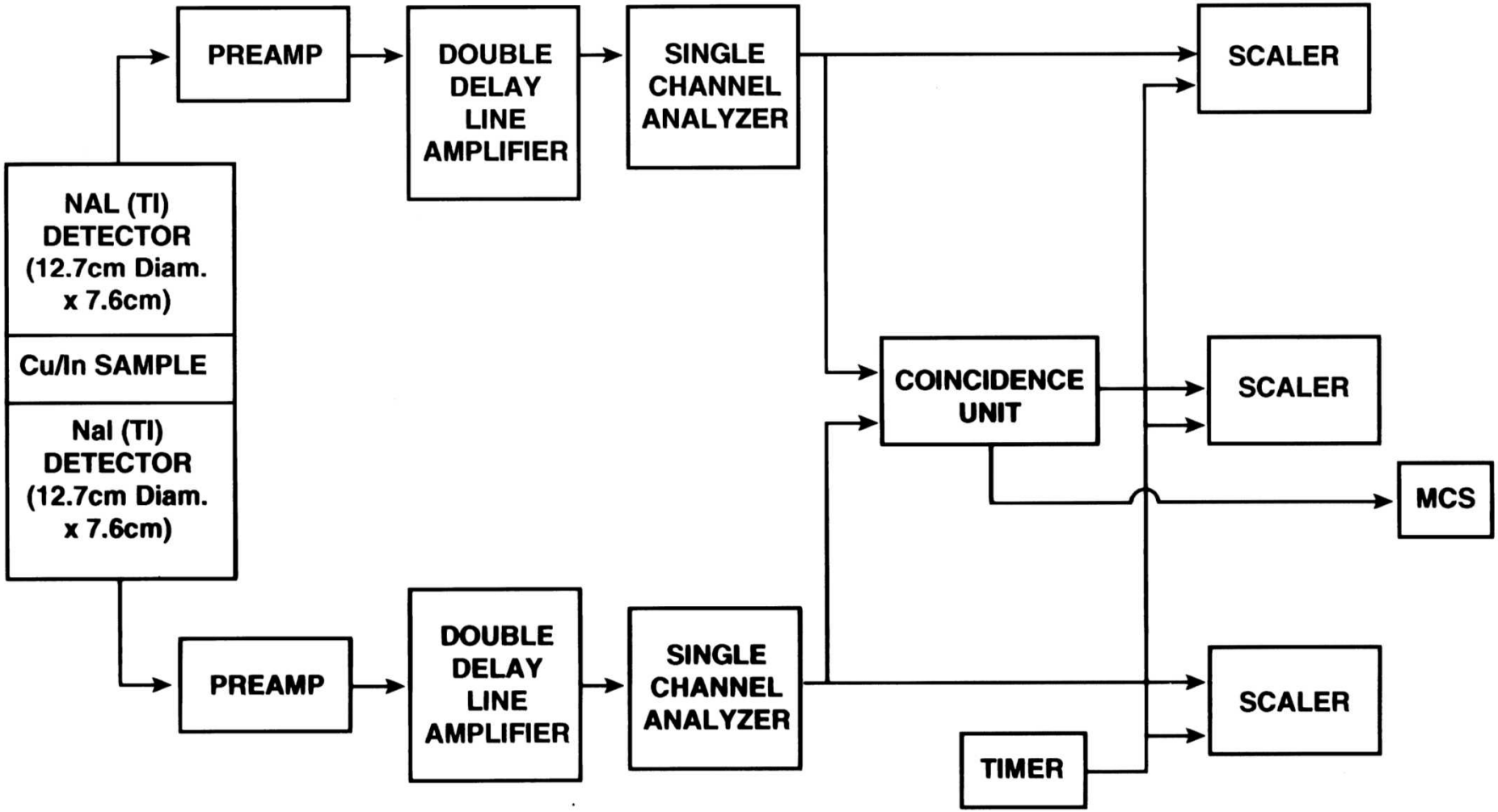

Ramon J. Leeper, 6/18/07

Cu activation coincidence counting system: NaI detectors and Pb shield

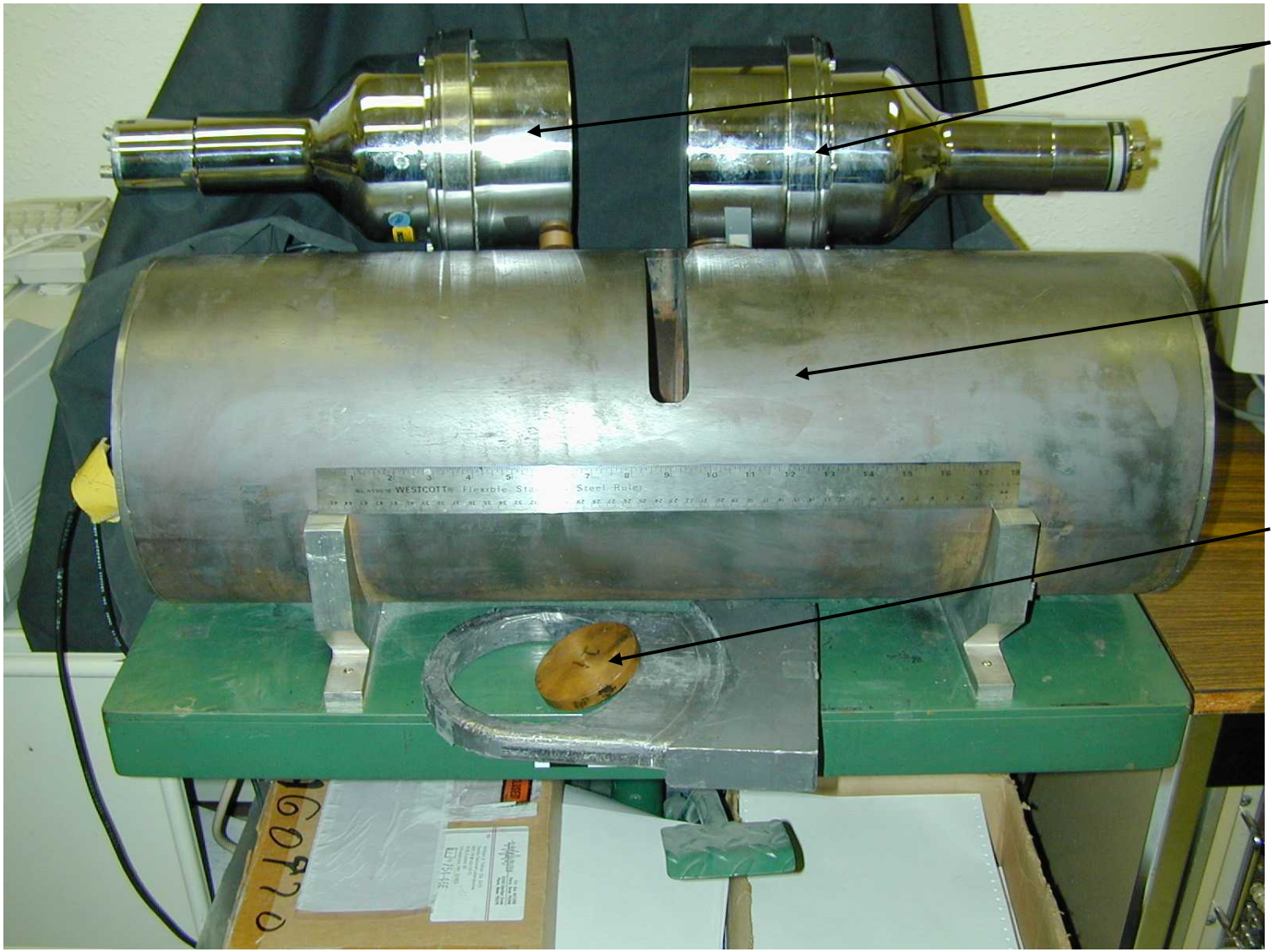

Schematic of a typical neutron diagnostic arrangement used in high energy density experiments

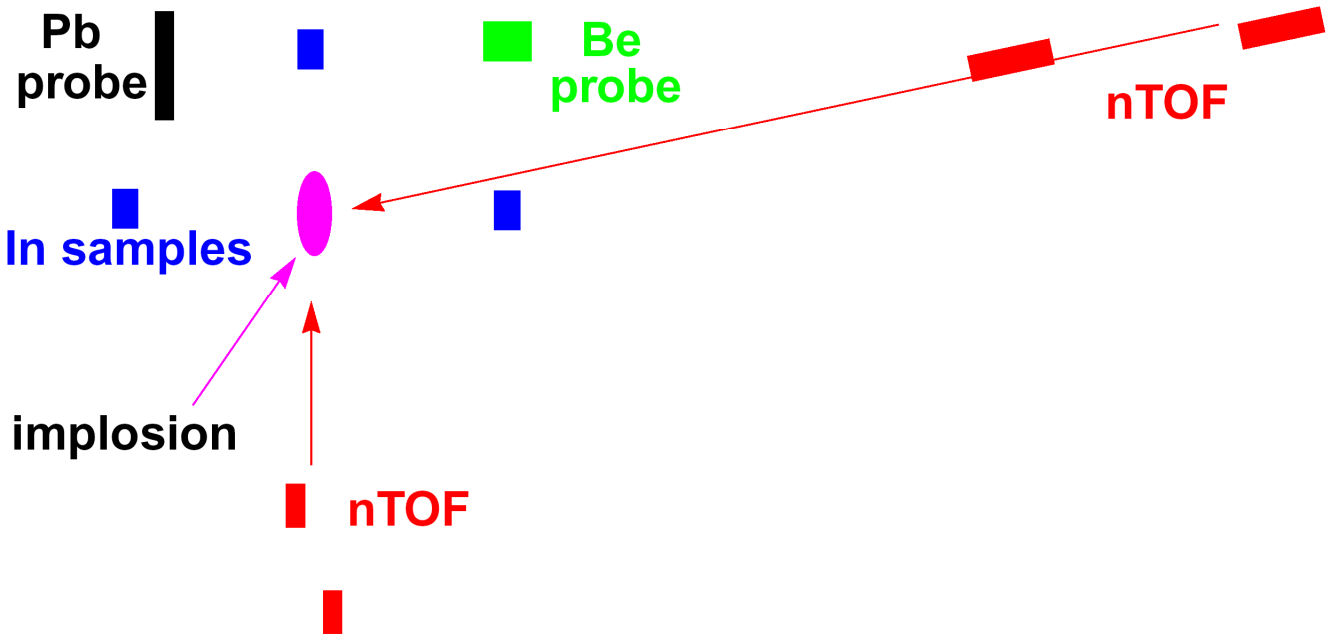

C. L. Ruiz, G. W. Cooper, S. A. Slutz, J. E. Bailey, G. A. Chandler, T. J. Nash, T. A. Mehlhorn, R. J. Leeper, D. Fehl, A. J. Nelson, J. Franklin, and L. Ziegler, Phys. Rev. Lett. 93, 015001 (2004).

The measured side and on-axis neutron energies restricts the possibility of a beam induced neutron mechanism

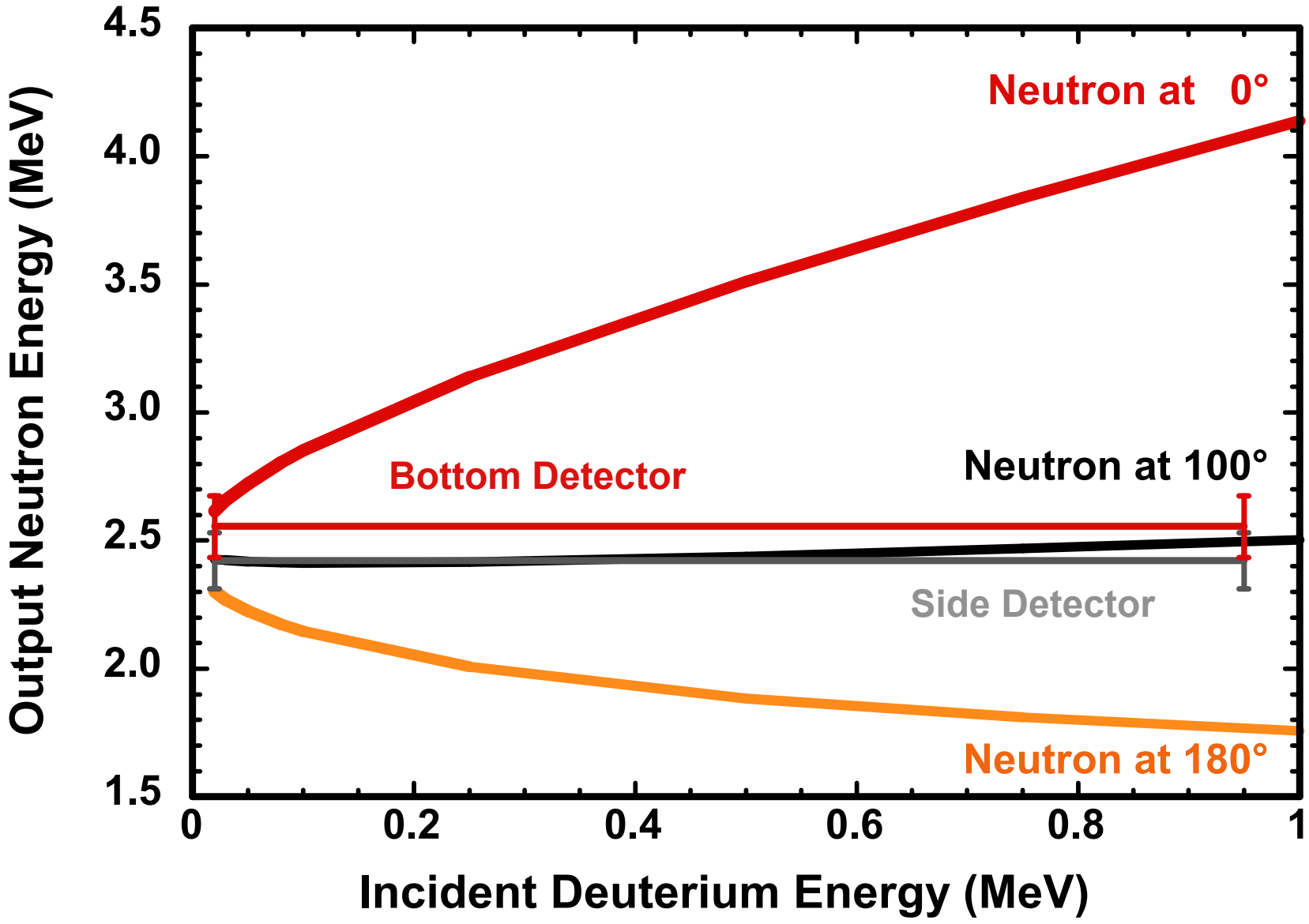

Position versus neutron arrival time

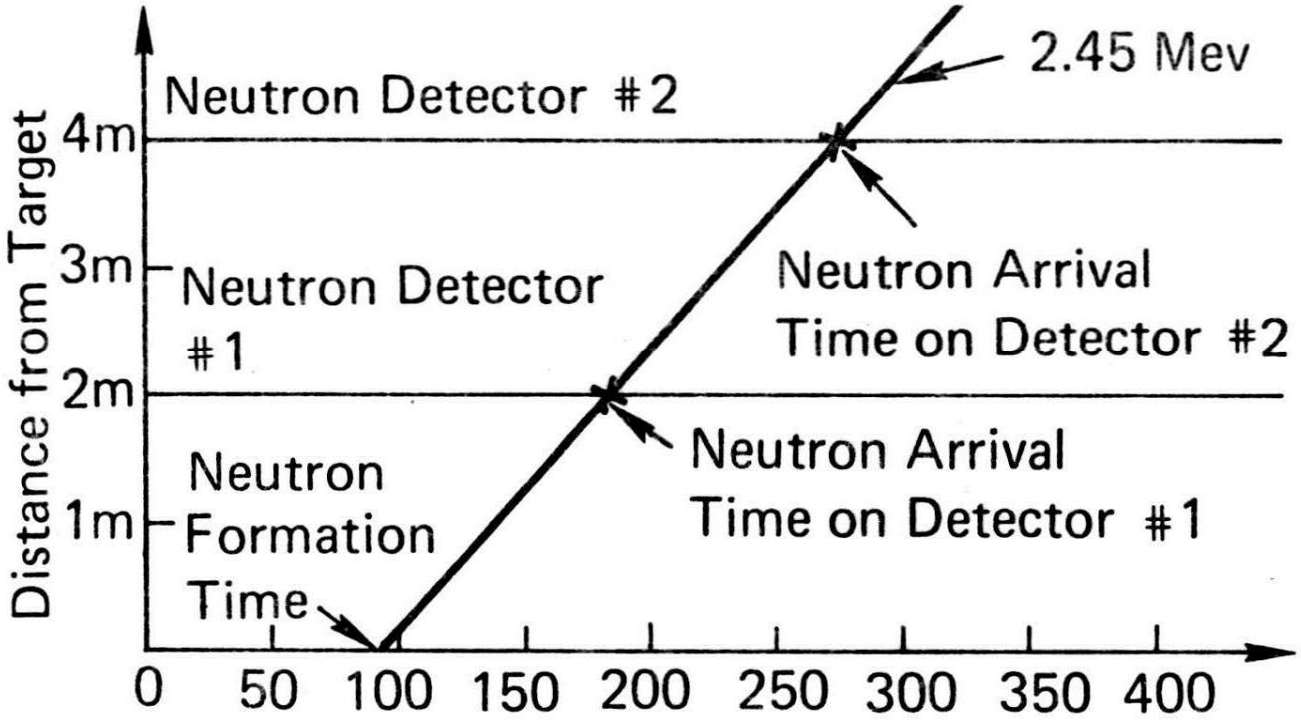

- **Neutron arrival time is determined from the sharp leading edge of the scintillator photomultiplier pulse**
- **The slope of the line connecting the neutron arrival determines the velocity or energy of the neutrons and the intercept of this line at the time axis determines the neutron formation time**

ICF ion temperatures are commonly determined using neutron time-of-flight (nToF) techniques

The energy spread of an instantaneous point source of fusion neutrons appears as a temporal spread at a distant detector

$$\Delta E = c_1\sqrt{kT_i} \qquad t_0 = \frac{d}{v_n} \qquad \Delta t = \frac{\Delta E\, t_0}{2E_0}$$

Ion temperature is related to ^2t by:

$$kT_i = \left(\frac{2\,\Delta t\, E_0}{c_1 t_0}\right)^2 \qquad \frac{\sigma_{kT_i}}{kT_i} = \frac{2\,\sigma_{\Delta t}}{\Delta t}$$

Neutron energy spectrum from a Maxwellian plasma may be used to measure ion temperature

$$N(E_n) \sim \exp\left[-(E_n - \langle E_n \rangle)^2 / (11298\ \theta_i)\right]$$

$$\Delta E = 177 \sqrt{\theta_i}$$

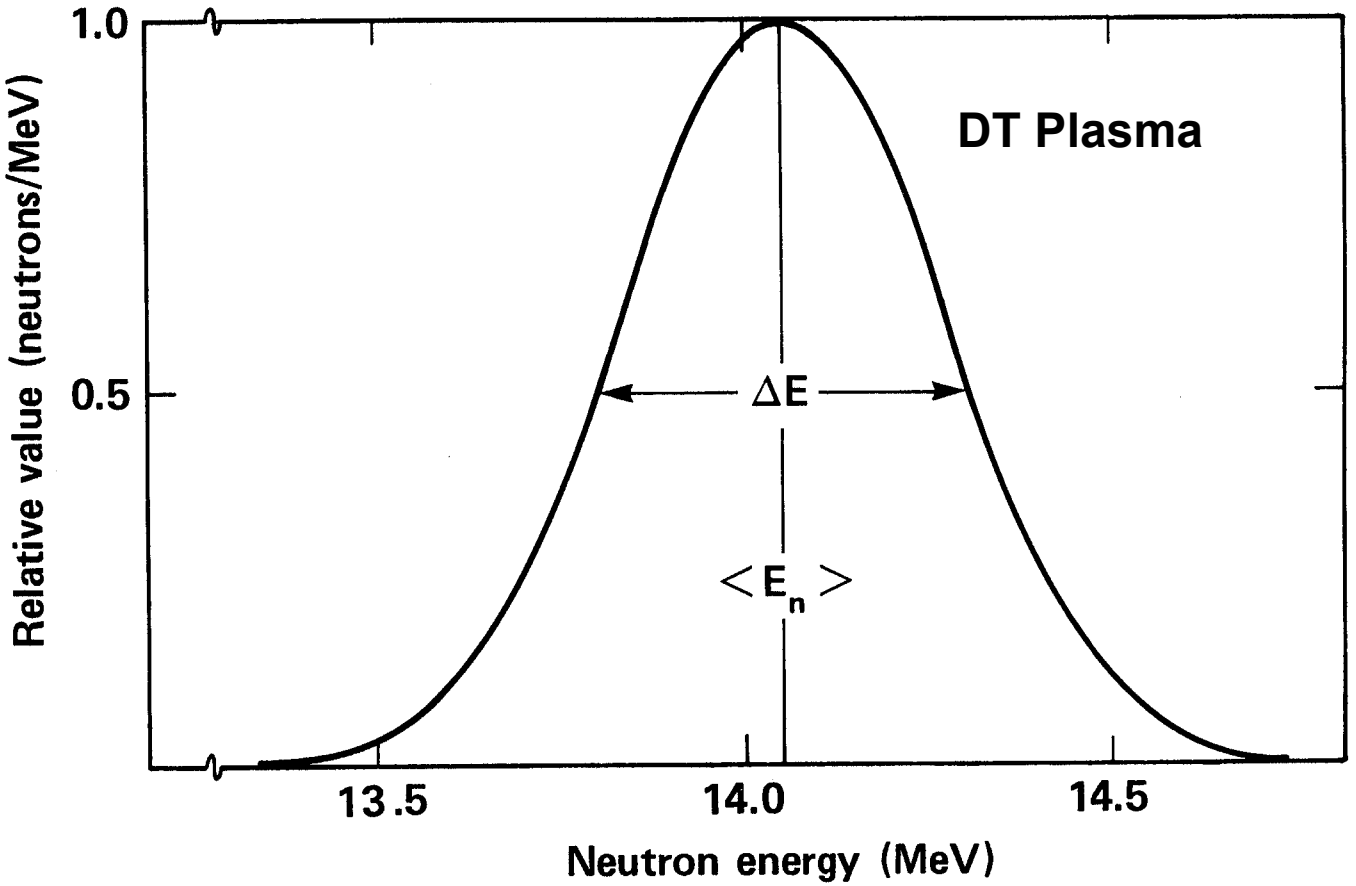

Ramon J. Leeper, 6/18/07

Scintillator photomultiplier combination (PMT) plus lead shielding

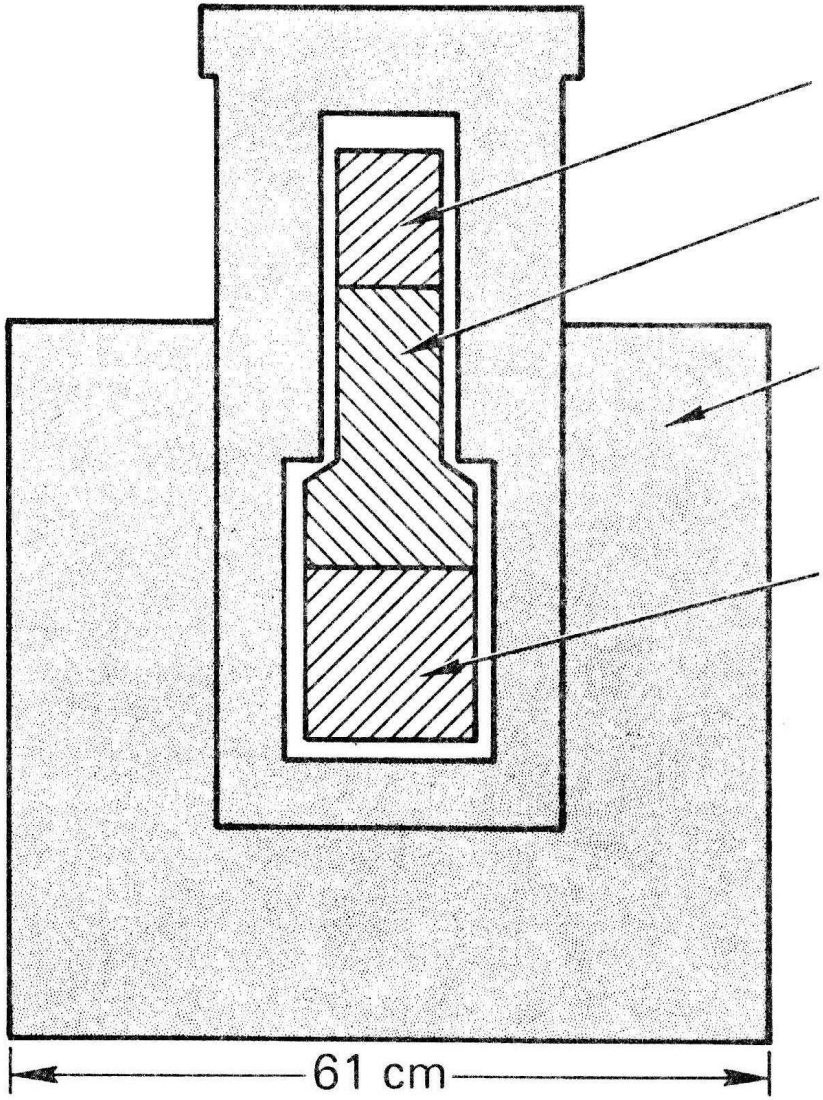

Photomultiplier Tube Base

Photomultiplier Tube

Lead Shielding (20.3 cm)

Scintillator

- Typical hard x-ray bremsstrahlung backgrounds in Z class pulsed power system are of order 10^9-10^{10} Rad/s
- Scintillator photomultiplier sensitivity in experiments designed to detect 10^{10} neutrons/4π is of order 0.1 amp/(Rad/s)
- Typical PMT linearity is 0.5-1.0 amps
- To prevent PMT saturation, detector shielding must provide attenuation factor of order 10^8 to 10^9

A heavy Pb shield (9000 lbs.) and collimator is required for neutron time-of-flight measurements on Z

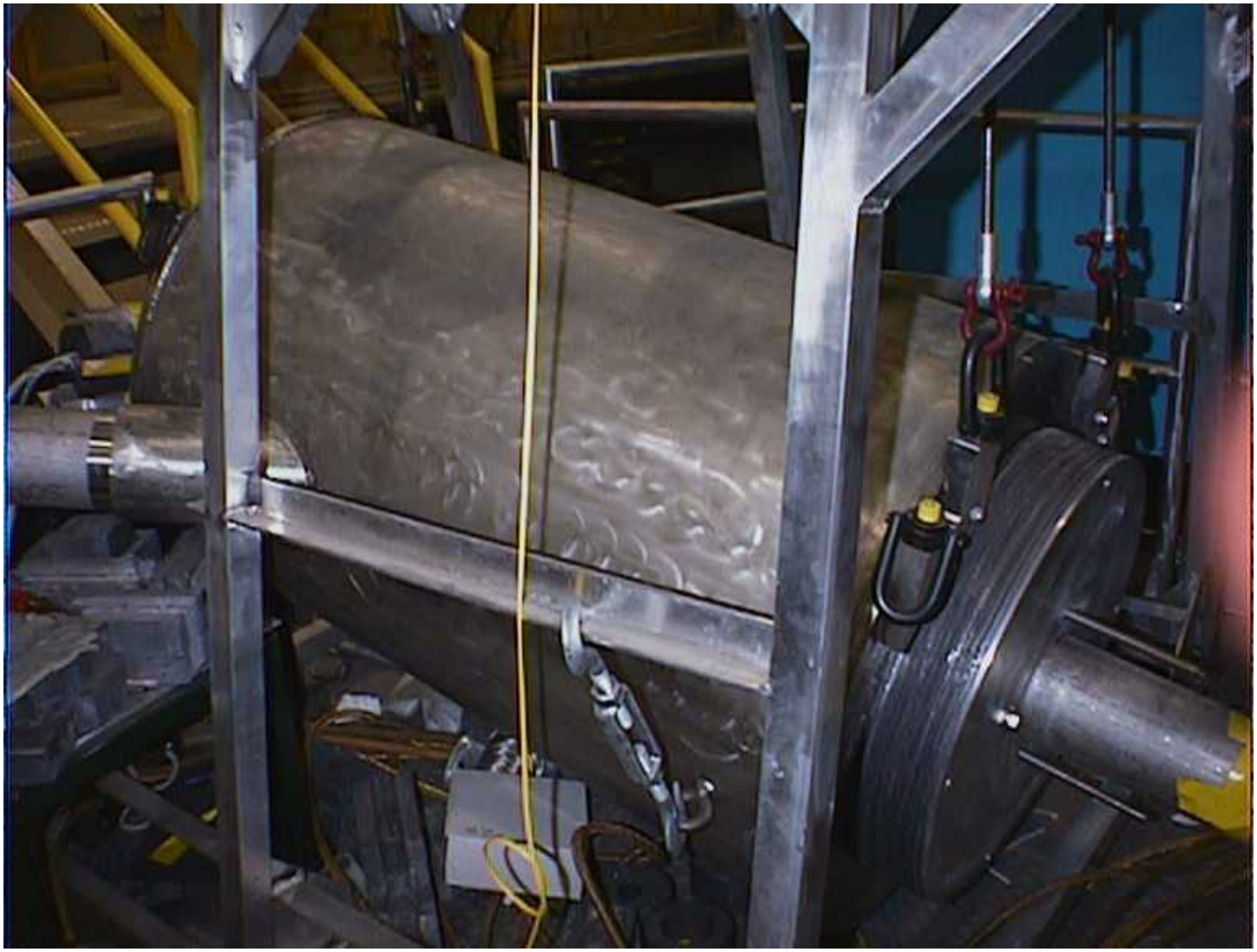

Ramon J. Leeper, 6/18/07

The thermonuclear neutron signature through heavily shielded scintillator photomultipliers was measured using a specially developed 3 ns neutron source (DD or DT)

DD neutron pulse
1.9 cm Pb

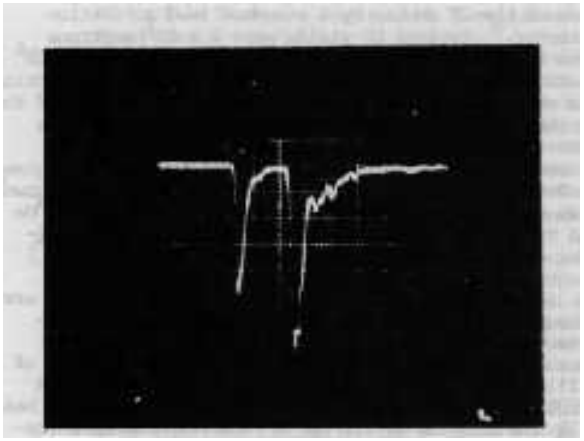

DD neutron pulse
10.2 cm Pb

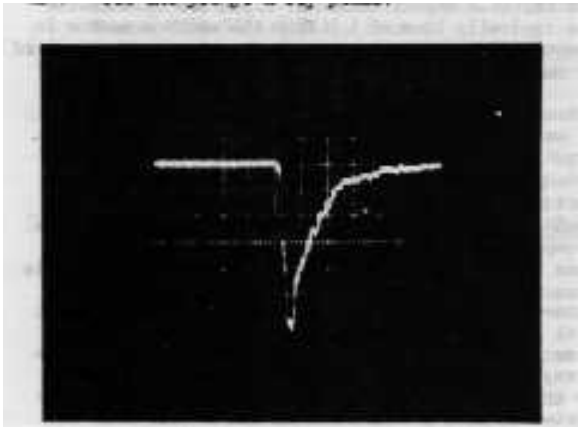

DD neutron pulse
20.3 cm Pb

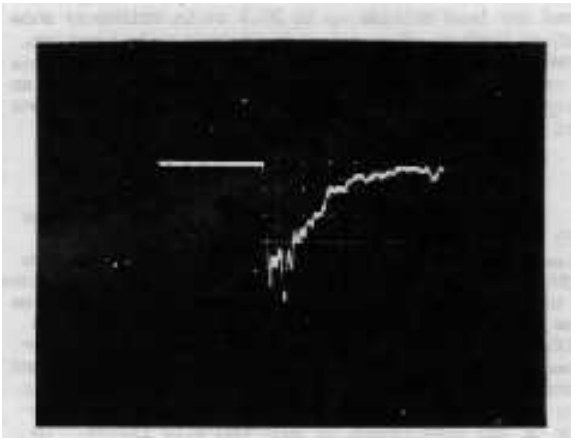

DT neutron pulse
1.9 cm Pb

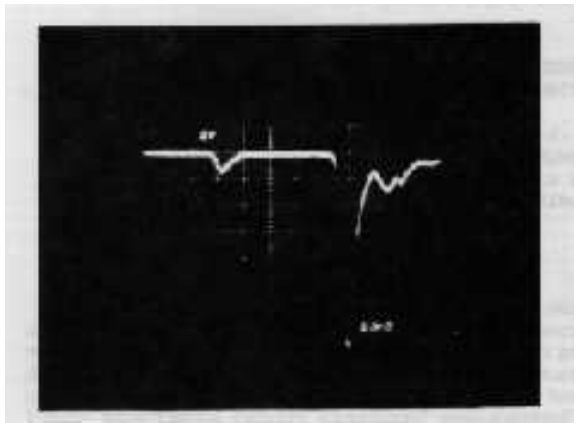

DT neutron pulse
10.2 cm Pb

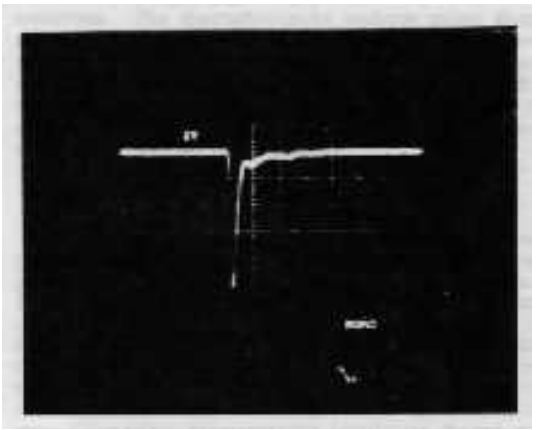

DT neutron pulse
20.3 cm Pb

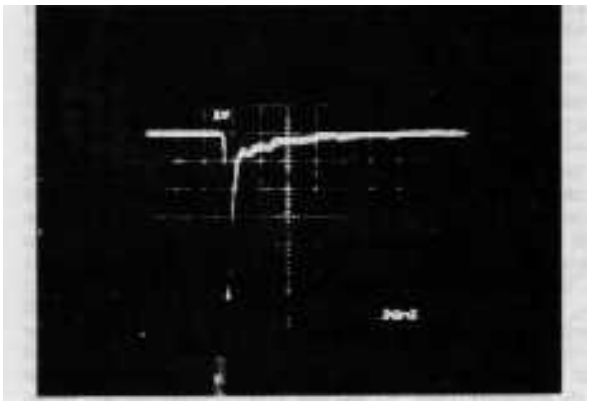

R. J. Leeper and J. Chang, IEEE Trans. Nucl. Sci. NS-29, 798 (1982).

Model diagram used in Monte Carlo calculations of a 20 m line-of-sight with varying placements of Pb

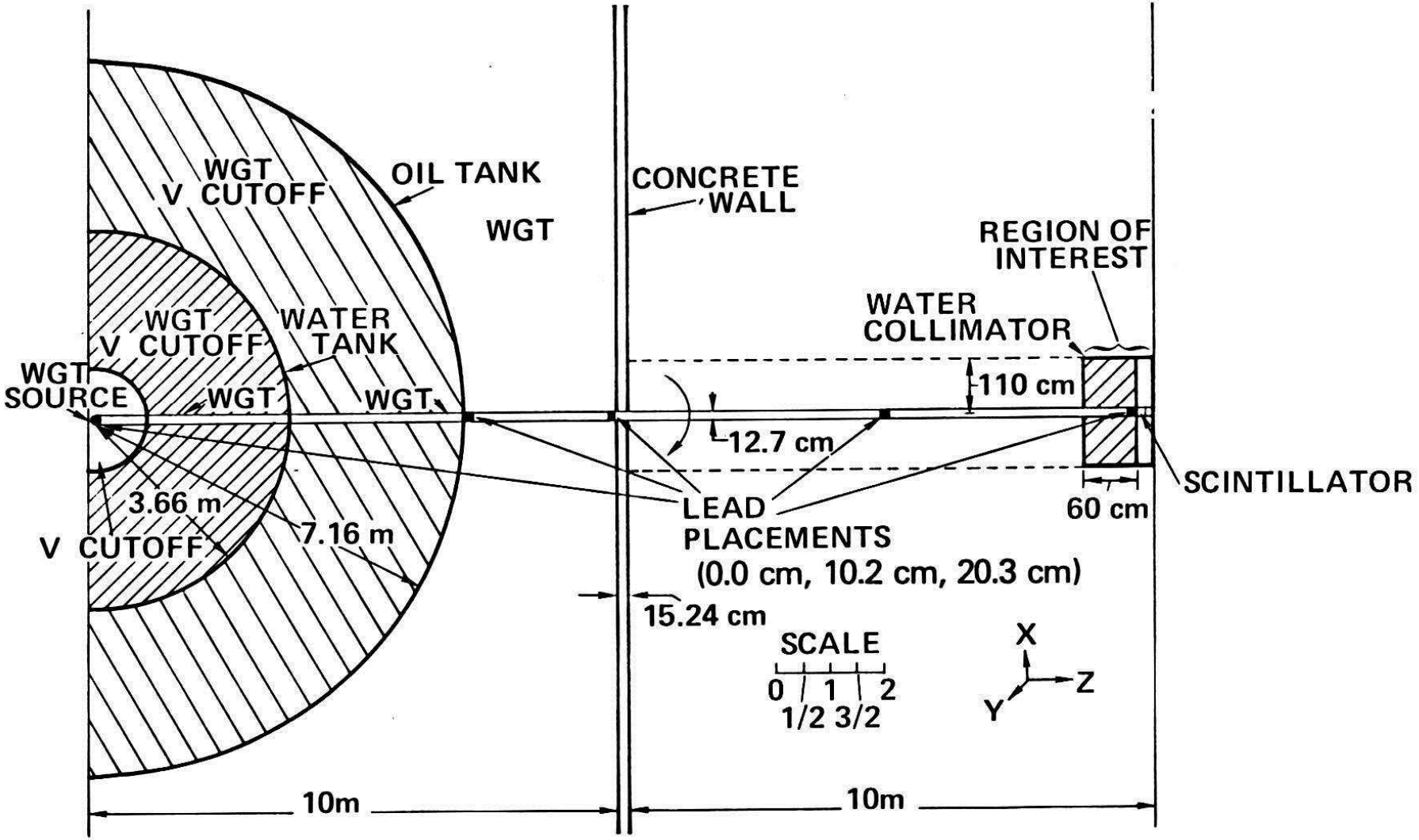

Ramon J. Leeper, 6/18/07

Scintillator energy deposition with lead filter 730 cm from source

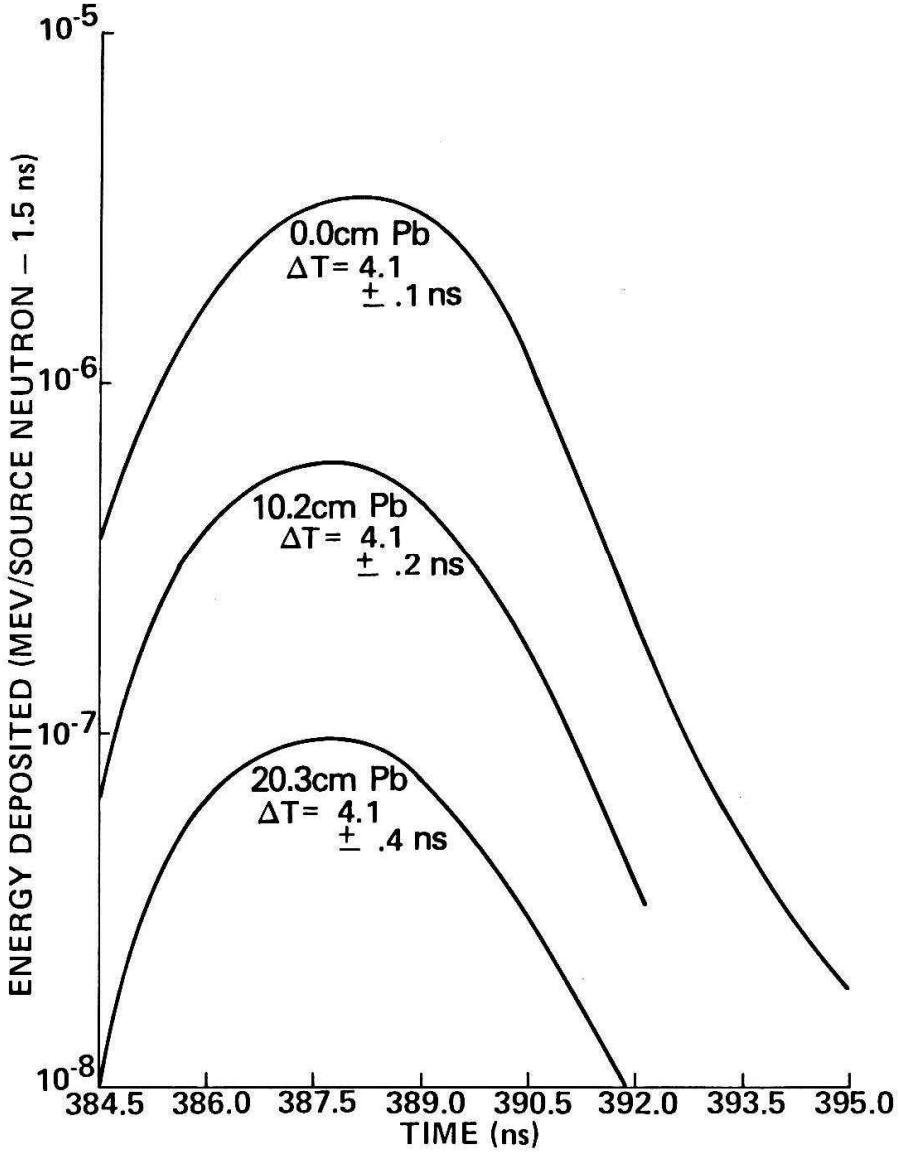

Ramon J. Leeper, 6/18/07

Scintillator energy deposition with lead filter 980 cm from source

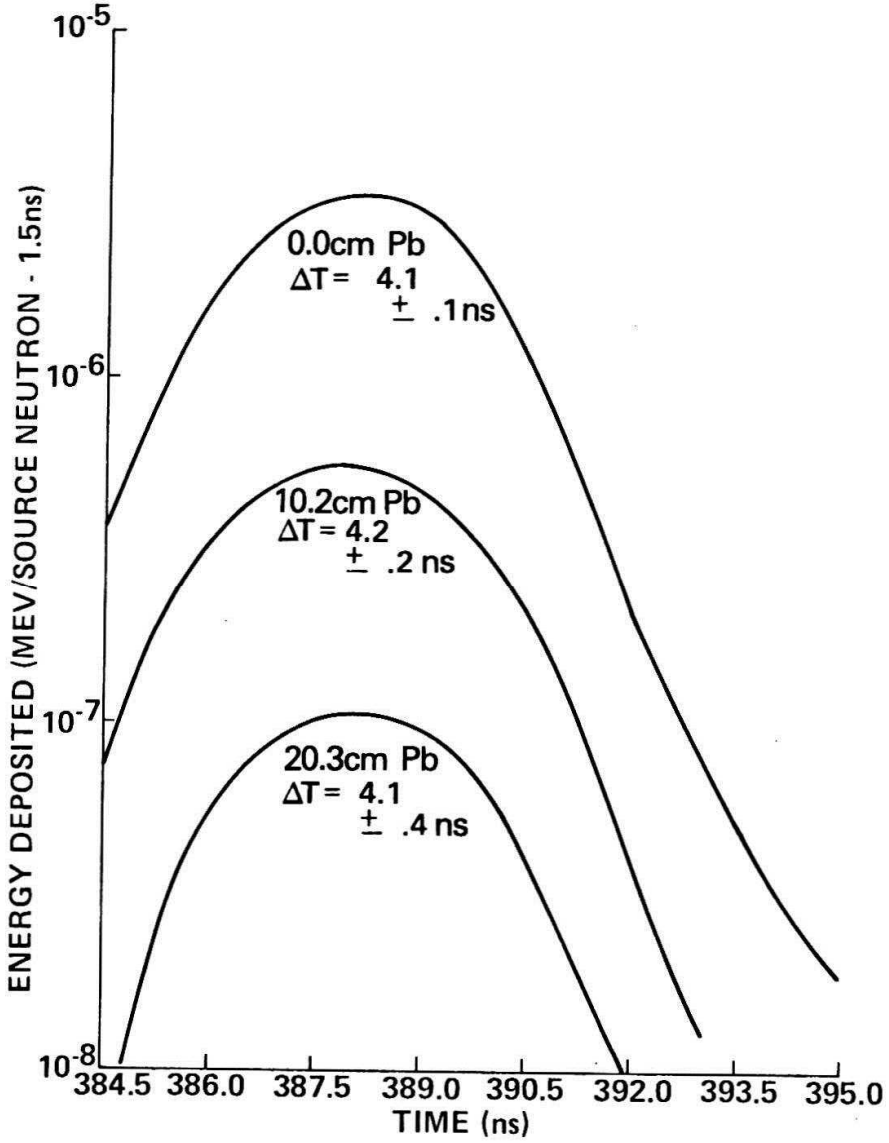

Scintillator energy deposition with lead filter 1980 cm from source

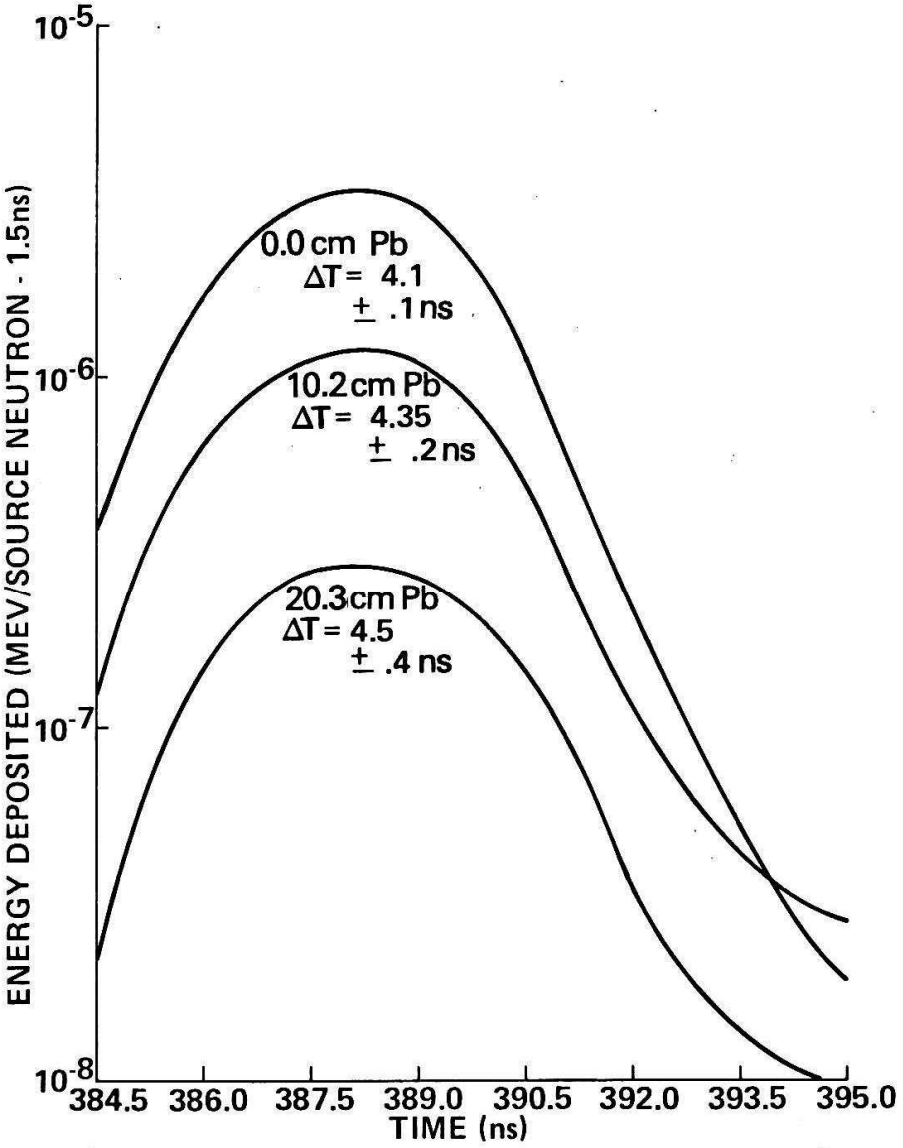

Ramon J. Leeper, 6/18/07

Scintillator energy deposition with extra lead shielding surrounding detector with no water collimator present

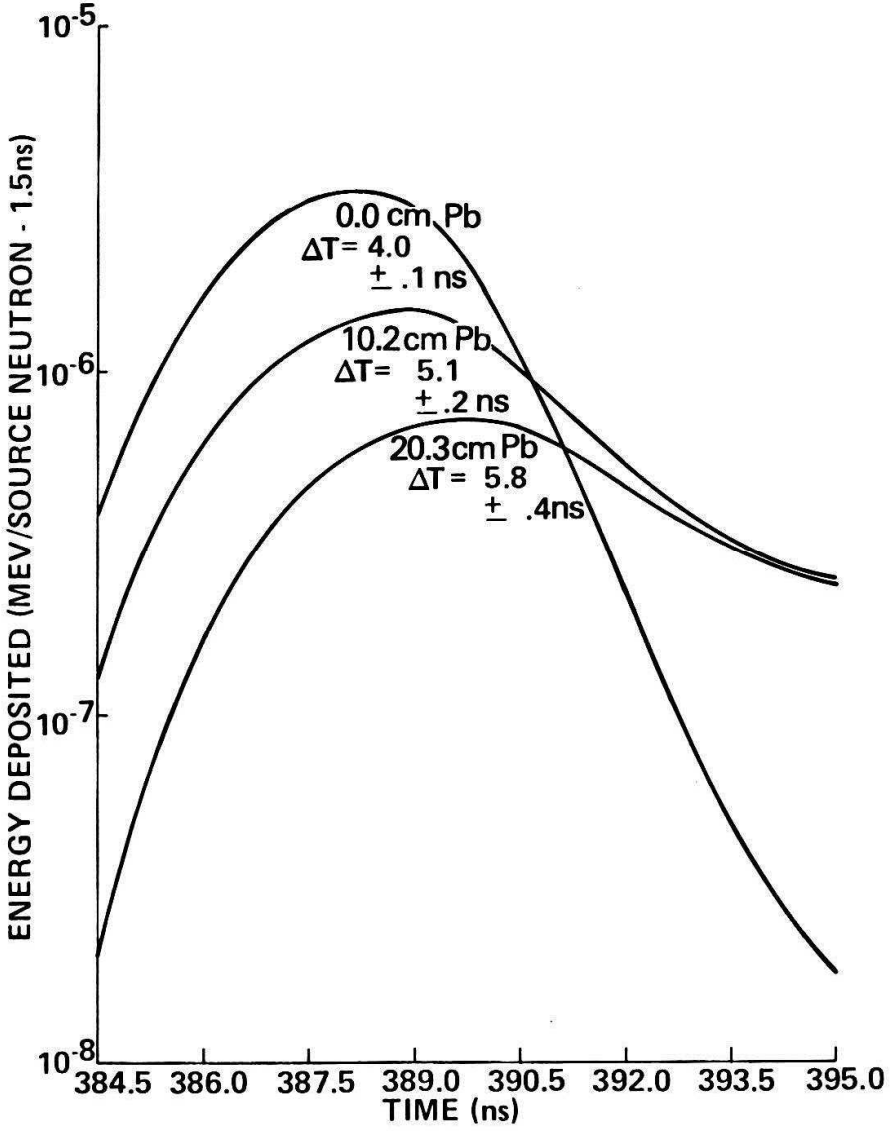

Ramon J. Leeper, 6/18/07

The neutron energy and yield are consistent with thermonuclear production

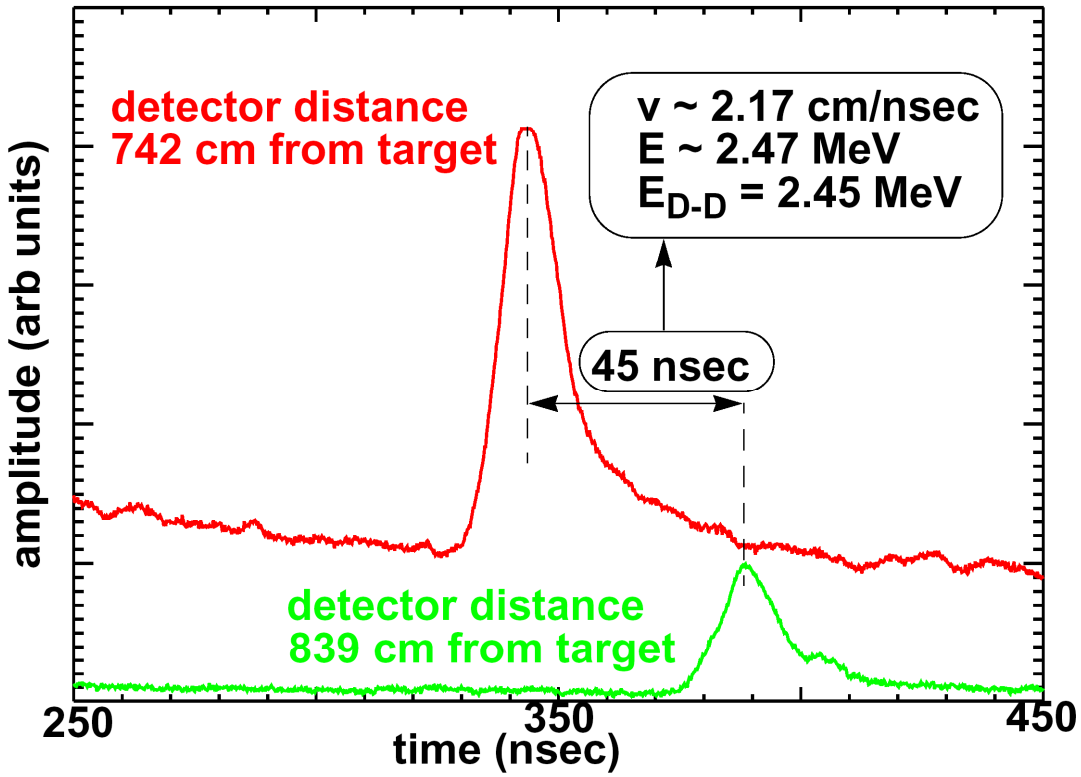

data is from z1031
50 μm CH wall,
2 mm diameter
24 atm D2 + 0.085 atm Ar

side-on detectors

- Measured neutron energy from two side-on detectors for z1031 was 2.47 ± 0.12 MeV
- Measured neutron energy from two bottom detectors for z1031 was 2.56 ± 0.13 MeV
- Neutron yield (Shot z1031) of (2.6 ± 1.3) x10^{10} measured with In activation is consistent with calculated mass averaged T_i yield of ~2x10^{10}; 1-D predicted clean yield was ~ 2x10^{11}

Neutron time-of-flight signal dramatically decreases when Xe fill gas is added to "null" the production of thermonuclear neutrons

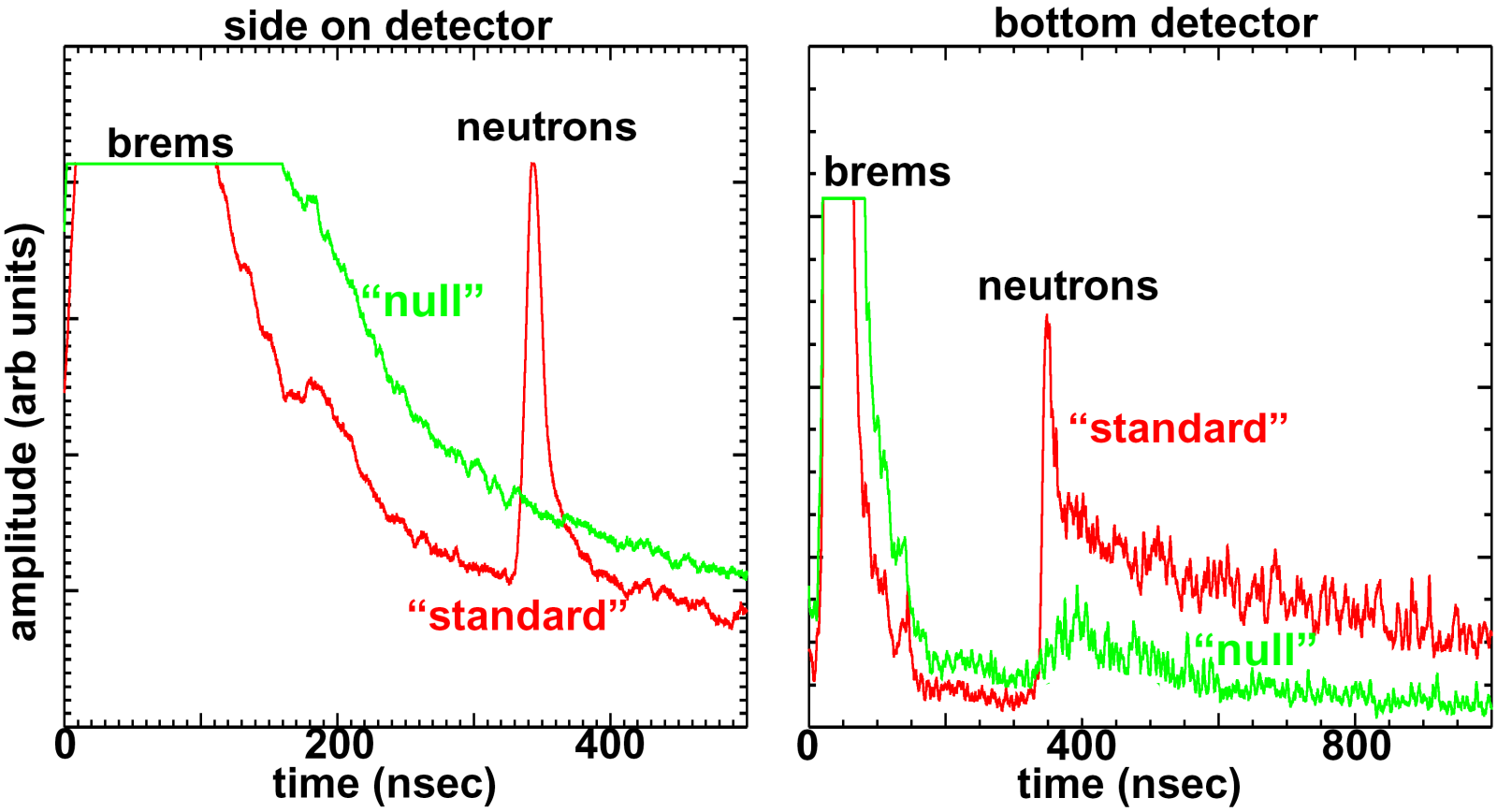

z1031"standard" fill(24 atm D2 + 0.085 atm Ar)
z1032"standard" fill + 0.6 atm Xe

- On "null shots," neutron yield measured by Be activation decreased by more than an order of magnitude

The evidence of thermonuclear neutron production in Z dynamic hohlraum experiments

- On "null shots" doped with 0.6 atm Xe gas, the fast neutron time-of-flight signal is substantially reduced on both side-on and bottom detectors in agreement with expectations from calculations
- On "null shots", the neutron yield decreased by more than an order of magnitude as measured by the Be activation detector in agreement with an expected decrease by a factor of ~ 20 from calculations
  - Any neutron yield from beam target interactions is at the level of the "null shots"
- On "null shots", Ar spectroscopy lines are not detected indicating a plasma of a much lower temperature in agreement with calculations that predict an electron temperature of 450 eV
- Measured neutron energy (Shot z1031) from side-on detectors was 2.47 ± 0.12 MeV and from the bottom detectors was 2.56 ± 0.13 MeV
  - If beam target interactions were responsible for the production of these neutrons, one would expect a shift in the neutron energy along the direction of the beam due to reaction kinematics
- The neutron yield (Shot z1031) measured by averaging the In activation detectors was $(2.6 \pm 1.3) \times 10^{10}$ to be compared to the calculated 1D clean yield of 2×10^{11}; 2D effects are expected to decrease this calculated yield by a factor of ~ 3-10

Fusion reaction rate provides information about plasma conditions in an ICF target

Burn history is an observable quantity

- **Depends on target hydrodynamics**
- **Related to plasma conditions**
- **Sensitive indicator of modeling accuracy**

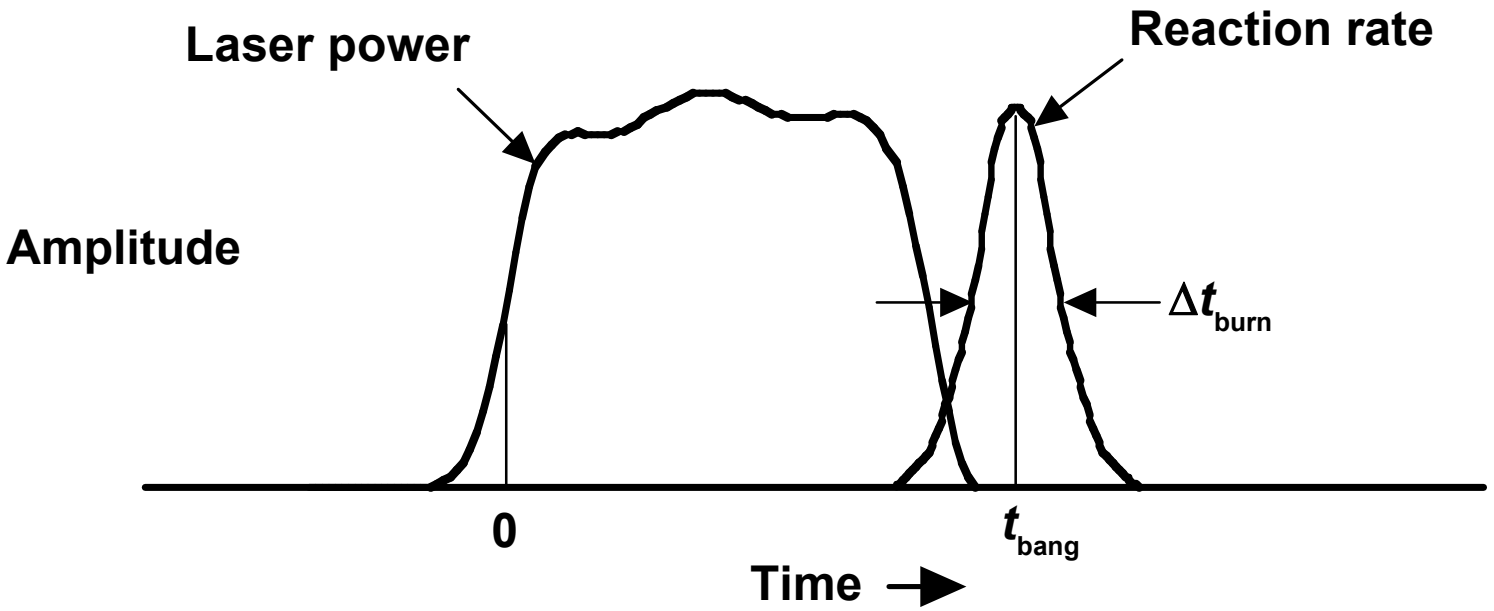

Burn history measurements can use either fusion neutrons or fusion γ rays

Reactions of interest

D + D $\rightarrow$ ^{3}He + n (2.45 MeV)
$\rightarrow$ T + p

D + T $\rightarrow$ ^{4}He + n (14.03 MeV)
$\rightarrow$ ^{5}He + γ (16.7 MeV)

Burn history characteristics

- Burn duration: 50 - 300 ps
- Required resolution: ~25 ps

Problems

- Neutrons - Doppler induced temporal dispersion
- γ rays - low branching ratio (5×10^{-5})

Reaction rate measurements will be difficult with direct neutrons

- **Required resolution: ~25 ps**

1. Doppler broadening limits resolution.

$\Delta t = 1.22\sqrt{T} \times d$ **(DT neutrons)**

Δt = time spread (ps)
T = ion temperature (keV)
d = target-to-detector distance (cm)

2. Laser energy sets minimum allowable distance, *d*.

Low power NIF	Full power NIF
d = 50 cm	d = 5 m
T = 1 - 4 keV	T = 1 - 4 keV
Δt = 61 - 122 ps	Δt = 610 - 1220 ps

Burn history can be measured from the 16.7 MeV gamma produced in the reaction D + T ⟶ ^{5}He + γ reaction

LANL Cherenkov Detector Design

J. M. Mack, S. E. Caldwell, S. C. Evans, T. J. Sedillo, D. C. Wilson, C. J. Horsfield, R. L. Griffith, and R. A. Lerche, Rev. Sci. Instrum. 77, 10E728 (2006)

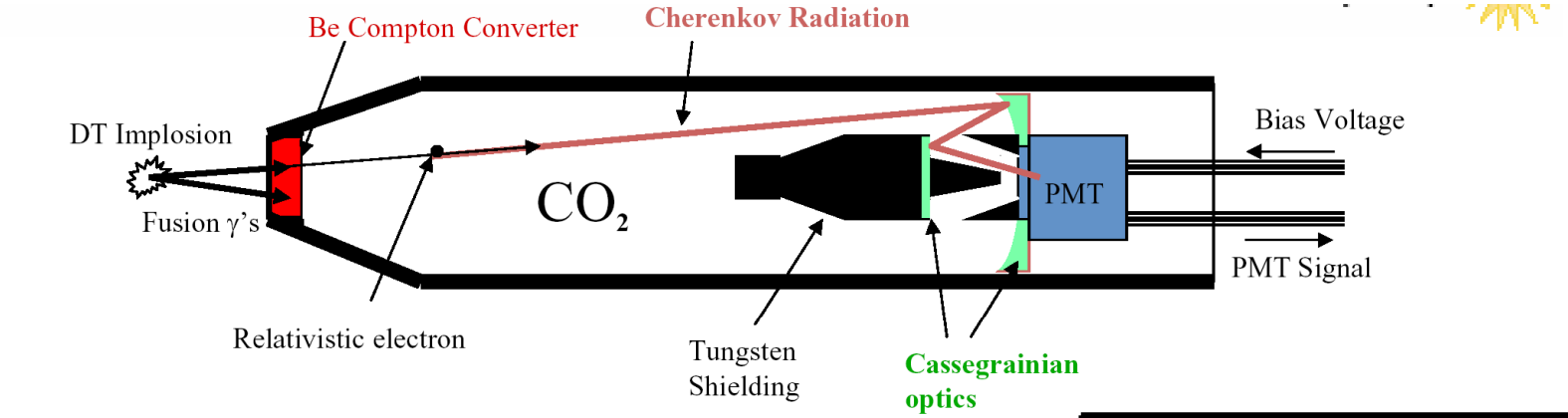

D+T → n+α, branching ratio ~1
D+T → n+α+γ(16.75 MeV), branching ratio ~1e-4

Gas Press (psia)	Energy Threshold (MeV)
30	12
100	6.3

- Why use Gammas?
  - No Doppler Spreading → High Bandwidth measurement at large Standoff!
    - Neutron Spreading: for Ti=10 keV, Δt≈40 ps at 10 cm (Omega), Δt≈2 ns at 5 m (NIF?)
  - Speed of Light Signal → easy to temporally discriminate γ signal from later signals
  - Energy Thresholding → distinguishes fusion γ's from secondary γ's

A schematic of the basic concept of a thin target proton recoil diagnostic for neutron spectral measurements is shown here

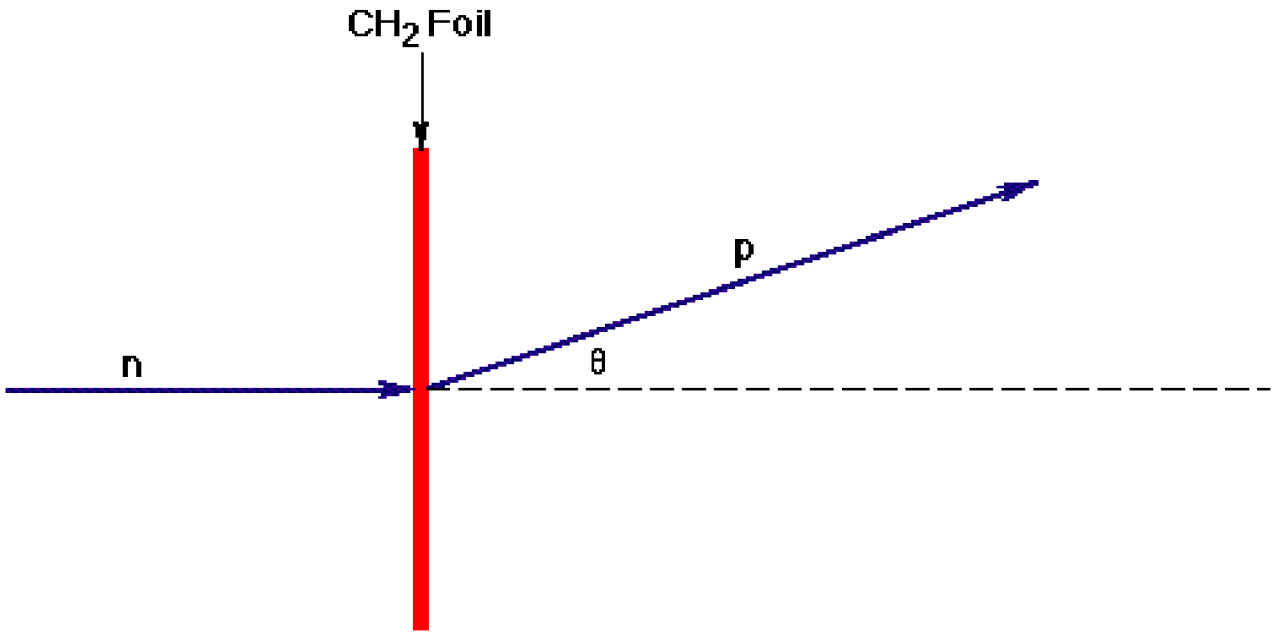

- Recoil protons from a thin (e. g., 10 mg/cm^2) CH_2 foil are detected at near forward angles
- Proton energy E_p at θ is related to the neutron E_n by $E_p(\theta)=E_n\cos^2(\theta)$
- At 14.1 MeV, the n-p cross-section $d\sigma/d\Omega$=233 mb/sr and is known to better than 2 %
- Proposed by Kallne and Enge for tokamak neutron measurements (J. Kallne and H. Enge, Nucl. Instrum. Meth. A311, 595 (1992))

Proton recoil spectrograph has been designed to measure the neutron energy spectrum on NIF ignition experiments by MIT/LLE/LLNL/SNL

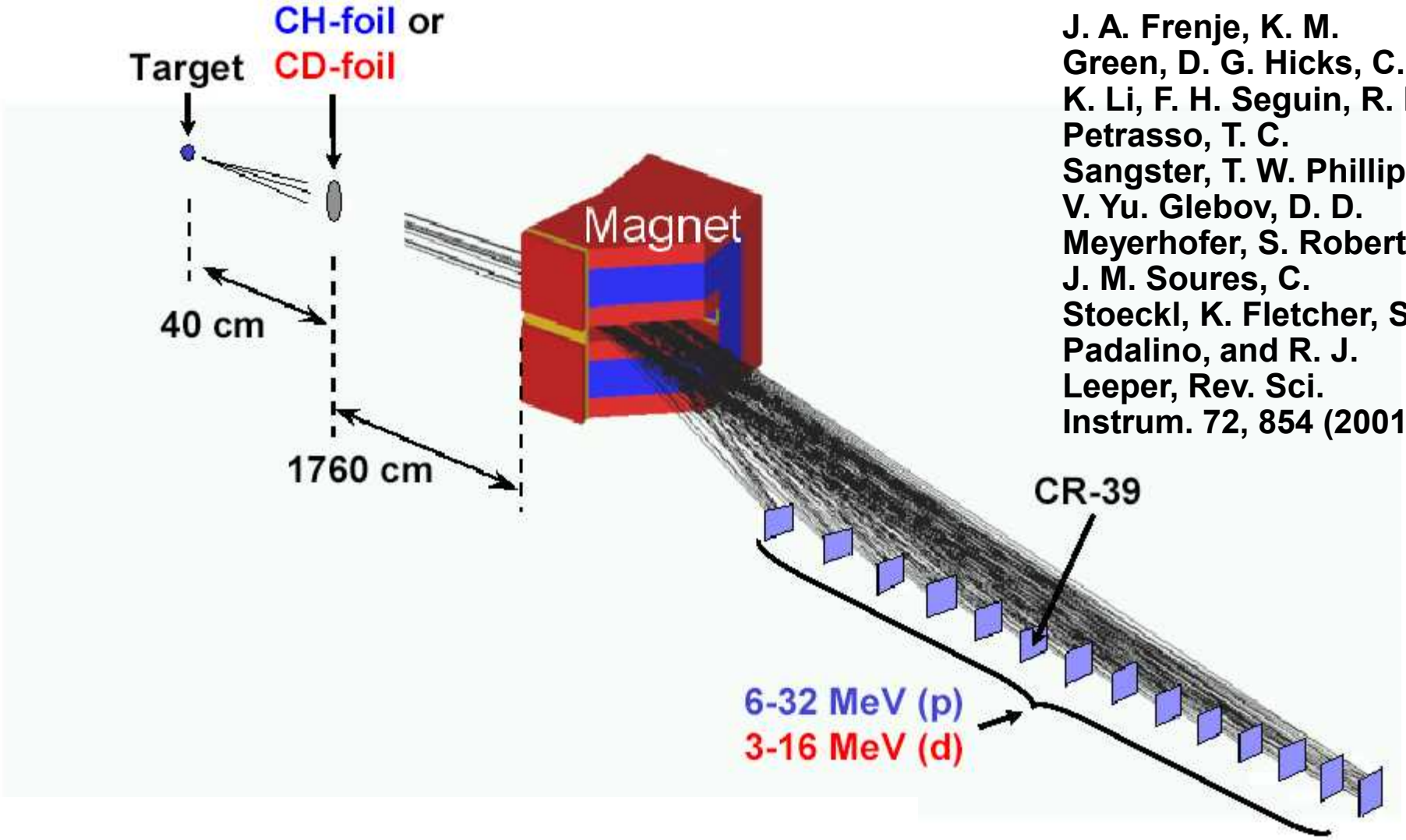

J. A. Frenje, K. M. Green, D. G. Hicks, C. K. Li, F. H. Seguin, R. D. Petrasso, T. C. Sangster, T. W. Phillips, V. Yu. Glebov, D. D. Meyerhofer, S. Roberts, J. M. Soures, C. Stoeckl, K. Fletcher, S. Padalino, and R. J. Leeper, Rev. Sci. Instrum. 72, 854 (2001).

A n-p recoil magnetic spectrograph could provide the following information

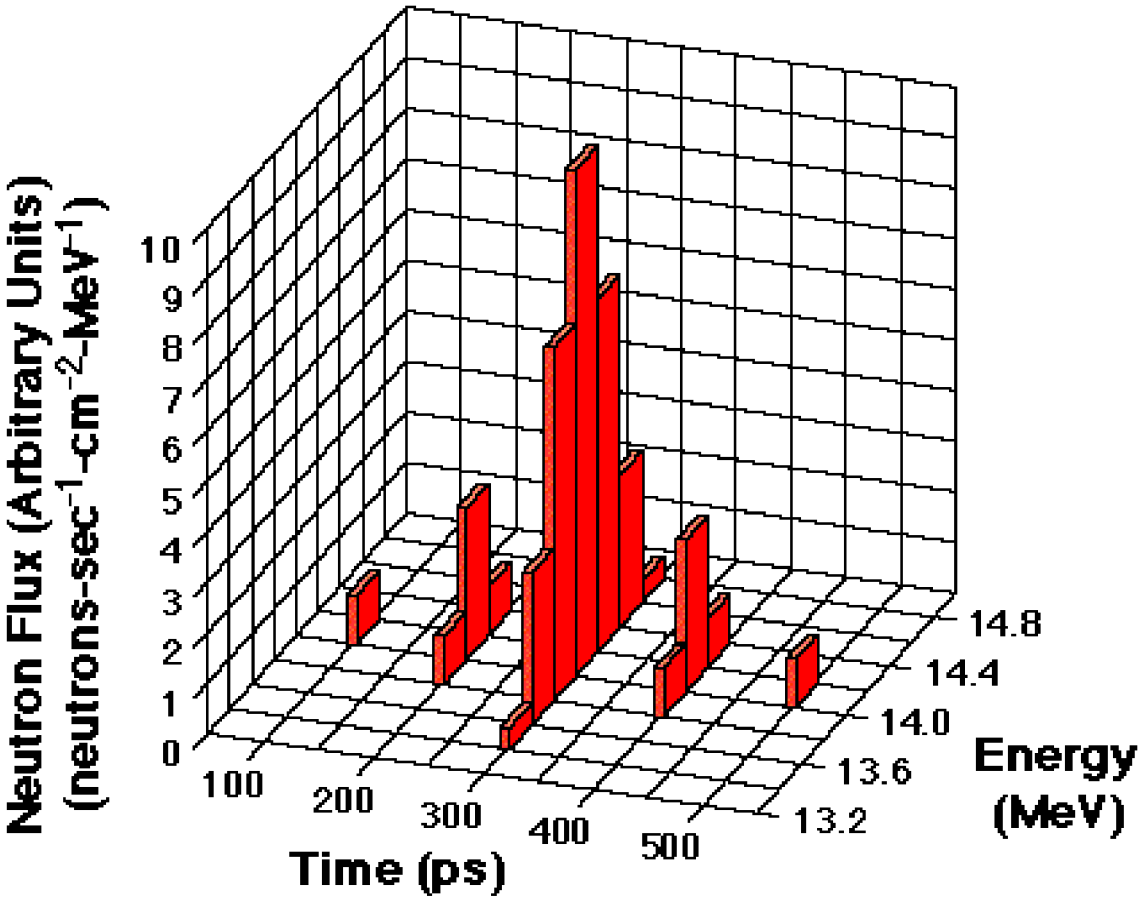

- Neutron energy $\Delta E(t)$ is a measure of the time-dependent ion temperature
- With standoff, the burn-history can be reconstructed by tracing each energy bin backward in time to the target -- as limited by the energy resolution of the instrument

In summary, high energy density physics measurements require extensive diagnostic suites

- X-ray fluence and flux diagnostics
- X-ray imaging diagnostics
- X-ray backlighting diagnostics
- Time-integrated and time resolved spectroscopy diagnostics
- Shock physics based diagnostics
- Neutron detector systems